

SPECTRAL CHARACTERISTICS OF WIND WAVES
IN THE EASTERN BLACK SEA

A THESIS SUBMITTED TO
THE GRADUATE SCHOOL OF NATURAL AND APPLIED SCIENCES
OF
MIDDLE EAST TECHNICAL UNIVERSITY

BY

NIHAL YILMAZ

IN PARTIAL FULFILLMENT OF THE REQUIREMENTS
FOR
THE DEGREE OF DOCTOR OF PHILOSOPHY
IN
CIVIL ENGINEERING

JULY 2007

Approval of the Graduate School of the Natural and Applied Sciences

Prof. Dr. Canan Özgen
Director

I certify that this thesis satisfies all the requirements as a thesis for the degree of Doctor of Philosophy.

Prof. Dr. Güney Özcebe
Head of Department

This is to certify that we have read this thesis and that in our opinion it is fully adequate, in scope and quality, as a thesis for the degree of Doctor of Philosophy.

Prof. Dr. Erdal Özhan
Supervisor

Examining Committee Members

| | | |
|---------------------------|-------------------|-------|
| Prof. Dr. Ayşen Ergin | (METU, CE) | _____ |
| Prof. Dr. Erdal Özhan | (METU, CE) | _____ |
| Prof. Dr. Melih Yanmaz | (METU, CE) | _____ |
| Prof.Dr. Selçuk Soyupak | (Atılım Unv., CE) | _____ |
| Assoc.Prof.Dr. Lale Balas | (Gazi Unv., CE) | _____ |

I hereby declare that all information in this document has been obtained and presented in accordance with academic rules and ethical conduct. I also declare that, as required by these rules and conduct, I have fully cited and referenced all material and results that are not original to this work.

Name, Last name : Nihal Yılmaz

Signature :

ABSTRACT

SPECTRAL CHARACTERISTICS OF WIND WAVES IN THE EASTERN BLACK SEA

Yılmaz, Nihal

Ph.D., Department of Civil Engineering

Supervisor: Prof. Dr. Erdal Özhan

July 2007, 108 pages

Wind waves are highly complex, random phenomena. One way to describe the irregular nature of the sea surface is the use of wave energy spectrum. Spectral information for wind waves in the Black Sea is extremely limited. Knowledge on spectral characteristics of wind waves would contribute to scientific, engineering and operational coastal and marine activities in the Black Sea. The aim of the present thesis is to investigate characteristics of wind wave spectra for the Eastern Black Sea. This would allow detailed understanding of the nature of the waves occurring in this enclosed basin. Long-term wave measurements obtained by directional buoys deployed offshore at Sinop, Hopa and Gelendzhik were utilized as the three sets of wave data. Records were analyzed to identify them as uni-modal or multi-modal spectra, and occurrences of spectral peaks were computed. Single peaked spectra were studied as belonging to fully arisen or developing sea

states. Model parameters of JONSWAP and PM spectra were estimated for the observed spectra by using a least square error method. The records of developing seas were further analyzed to select the ones belonging to stable wind conditions. Fetch dependencies of non-dimensional spectral variables, mean parameters of JONSWAP model spectrum and the envelop of dimensionless spectra were investigated for this data sub-set.

Keywords: Eastern Black Sea, Wind-wave spectrum, JONSWAP spectrum, Multi-modal spectrum, Spectral analysis

ÖZ

DOĞU KARADENİZ'DEKİ RÜZGAR DALGALARININ SPEKTRAL ÖZELLİKLERİ

Yılmaz, Nihal

Doktora, İnşaat Mühendisliği Bölümü

Tez Yöneticisi: Prof. Dr. Erdal Özhan

Temmuz 2007, 108 sayfa

Fırtınalarca deniz yüzeyinde yaratılan dalgaların çok karmaşık yapısı vardır. Rüzgar dalgalarının karmaşık yapısını açıklamaya yönelik yollardan birisi dalga enerji spektrumunu kullanmaktır. Kıyı mühendisliğinde pek çok kıyı ve deniz etkinliği için gereken rüzgar dalgalarının spectral özelliklerine ilişkin mevcut bilgi Karadeniz için son derece sınırlıdır. Bu çalışmanın amacı, Doğu Karadeniz için rüzgar dalgalarının spektrumu üzerine güvenilir bilgiler elde ederek bu kapalı denizde oluşan dalgaların yapısının anlaşılmasına katkı sağlamaktır. Çalışmada Sinop, Hopa ve Gelincik (Rusya) açıklarına yerleştirilen yönsel dalga ölçer şamandıralardan elde edilen oldukça uzun süreli derin deniz dalga ölçümleri kullanılmıştır. Dalga ölçümleri tek tepeli veya çok tepeli olarak tanımlanmış, ve oluşma yüzdeleri hesaplanmıştır. Tek tepeli spektruma sahip ölçümler tam gelişmiş veya gelişmekte olan deniz durumuna ait olarak ayrılmıştır. Gözlenen

spektrumlar için JONSWAP ve PM spektrumlarının model parametreleri en küçük kareler yöntemi ile tahmin edilmiştir. Gelişmekte olan deniz durumuna ait ölçümler, sabit rüzgar koşullarında oluşmuş olanlarını seçmek üzere ayrıca incelenmiştir. Bu veri alt seti için, boyutsuz spektral değişkenlerin kabarma uzunluğu ile değişimi, JONSWAP model spektrumunun ortalama parametreleri ve boyutsuz spektrumlar kümesi elde edilmiştir.

Anahtar Kelimeler: Doğu Karadeniz, Rüzgar dalgası spektrumu, JONSWAP spektrumu, Çok tepeli spektrum, Spektral analiz

To My Family
of which I am very proud to be a part!

Parçası olmaktan gurur duyduğum
Aileme!

ACKNOWLEDGMENTS

The author would like to express her deepest gratitude to her supervisor, Prof. Dr. Erdal Özhan for his patient guidance, advice, criticism, encouragements and insight throughout the study. The author feels very fortunate to get the chance of being his last PhD student.

The author would also like to acknowledge Prof. Dr. Ayşen Ergin and Assoc. Prof. Dr. Lale Balas for serving on her doctoral committee. Their comments and suggestions, and especially their invaluable moral support are highly appreciated.

Special thanks are to Dr. Saleh Abdalla who has given his time and support even from thousands of kms away whenever the author has needed throughout her graduate education.

Thanks are extended to all of the staff in Coastal and Harbor Engineering Laboratory of METU, and in Engineering Faculty of Muğla University for their encouragement and friendship.

Finally, the author would like to present her sincere thanks to her parents, Mehmet and Nahide Yılmaz for their love and care, and for their continuous encouragement and endless support throughout her educational life.

TABLE OF CONTENTS

| | |
|---|------|
| ABSTRACT..... | iv |
| ÖZ..... | vi |
| DEDICATION..... | viii |
| ACKNOWLEDGMENTS..... | ix |
| TABLE OF CONTENTS..... | x |
| LIST OF TABLES..... | xiii |
| LIST OF FIGURES..... | xv |
| CHAPTER | |
| 1. INTRODUCTION..... | 1 |
| 1.1 General Description..... | 1 |
| 1.2 Scope of the Work..... | 3 |
| 2. LITERATURE REVIEW..... | 5 |
| 2.1 Wind Waves..... | 5 |
| 2.1.1 Evolution of Wind Waves..... | 6 |
| 2.2 Irregular Waves..... | 8 |
| 2.2.1 Random Nature of Wind Waves..... | 9 |
| 2.2.2 Concept of Spectral Analysis..... | 11 |
| 2.3 Wind Wave Spectrum..... | 16 |

| | | |
|---------|---|----|
| 2.3.1 | Spectral Shape and Parametric Model Spectrum..... | 17 |
| 2.4 | Multi-Peaked Spectra..... | 27 |
| 2.4.1 | Probability of Occurrence of Multi-Peaked Spectra..... | 29 |
| 2.4.2 | Identification of Multi-Peaked Spectra..... | 31 |
| 2.5 | Methods for Spectral Fitting..... | 34 |
| 2.6 | Fetch Dependencies of Spectral Parameters..... | 39 |
| 3. | SPECTRAL ANALYSIS OF THE WAVE DATA AT SINOP, HOPA AND GELENDZHIK..... | 44 |
| 3.1 | Data Source..... | 44 |
| 3.1.1 | NATO TU-WAVES Project..... | 44 |
| 3.1.2 | Wave Measurements..... | 45 |
| 3.1.3 | ECMWF Analysis Wind Fields..... | 48 |
| 3.2 | Arrangement of the Data for Analysis..... | 50 |
| 3.2.1 | Classification According to Significant Wave Height...50 | |
| 3.2.2 | Classification According to the Number of Spectral Peaks..... | 51 |
| 3.2.2.1 | Identification of Multi-modal Spectra..... | 51 |
| 3.3 | Fitting JONSWAP Spectrum to Single Peak Spectra..... | 61 |
| 3.4 | Fetch Dependencies of the JONSWAP Spectrum Parameters at Sinop, Hopa and Gelendzhik..... | 69 |
| 4. | SUMMARY AND CONCLUSIONS..... | 89 |
| | REFERENCES..... | 93 |

APPENDICES

| | |
|--------------------------------------|-----|
| A. CONTENT OF THE SPECTRA FILES..... | 99 |
| B. NUMBER OF SEASONAL DATA..... | 101 |
| C. MESH OVER THE BLACK SEA..... | 104 |
| VITA..... | 108 |

LIST OF TABLES

TABLES

| | |
|---|----|
| Table 2.1 Estimates of constants A, a, B, b, C, c in Equation 2.45. | 40 |
| Table 3.1 Number of measured spectra in each significant wave height range..... | 51 |
| Table 3.2 Occurrence of spectral peaks at Sinop (all data)..... | 53 |
| Table 3.3 Occurrence of spectral peaks at Hopa (all data)..... | 53 |
| Table 3.4 Occurrence of spectral peaks at Gelendzhik (all data)..... | 54 |
| Table 3.5 Comparison of the three stations in case of peak numbers for the overall measurements with Hs greater than or equal to 1.0..... | 55 |
| Table 3.6 Seasonal probability of occurrence of multi-peaked spectra for overall data with significant wave height greater and equal to 0.5 m at Sinop..... | 58 |
| Table 3.7 Seasonal probability of occurrence of multi-peaked spectra for overall data with significant wave height greater and equal to 1.0 m at Sinop..... | 58 |
| Table 3.8 Seasonal probability of occurrence of multi-peaked spectra for overall data with significant wave height greater and equal to 0.5 m at Hopa..... | 59 |
| Table 3.9 Seasonal probability of occurrence of multi-peaked spectra for overall data with significant wave height greater and equal to 1.0 m at Hopa..... | 59 |
| Table 3.10 Seasonal probability of occurrence of multi-peaked spectra for overall data with significant wave height greater and equal to 0.5 m at Gelendzhik..... | 60 |

| | |
|---|-----|
| Table 3.11 Seasonal probability of occurrence of multi-peaked spectra for overall data with significant wave height greater and equal to 1.0 m at Gelendzhik..... | 60 |
| Table 3.12 JONSWAP Spectrum parameters determined by using four methods at each sea state for the measurements at Sinop..... | 62 |
| Table 3.13 Parameters of JONSWAP spectrum obtained from the modified fitting method of Acar at Sinop..... | 66 |
| Table 3.14 Parameters of JONSWAP spectrum obtained from the modified fitting method of Acar at Hopa..... | 66 |
| Table 3.15 Parameters of JONSWAP spectrum obtained from the modified fitting method of Acar at Gelendzhik..... | 67 |
| Table 3.16 Parameters of PM spectrum..... | 68 |
| Table 3.17 Mean parameters of JONSWAP spectrum recomputed for the data set identified as belonging to developing sea of stable wind conditions at Sinop, Hopa and Gelendzhik..... | 86 |
| Table B1 Number of Winter measurements in each significant wave height range..... | 101 |
| Table B2 Number of Spring measurements in each significant wave height range..... | 102 |
| Table B3 Number of Summer measurements in each significant wave height range..... | 102 |
| Table B4 Number of Autumn measurements in each significant wave height range..... | 103 |

LIST OF FIGURES

FIGURES

| | |
|---|----|
| Figure 2.1 Evolution of wind waves growth..... | 7 |
| Figure 2.2 A typical measured frequency spectrum..... | 13 |
| Figure 2.3 Comparison of the PM and JONSWAP spectra..... | 22 |
| Figure 2.4 Dependence of dimensionless variance \tilde{E} on dimensionless fetch \tilde{X} | 41 |
| Figure 2.5 Dependence of dimensionless peak frequency \tilde{f}_m on dimensionless fetch \tilde{X} | 42 |
| Figure 2.6 Dependence of dimensionless variance \tilde{E} on dimensionless peak frequency \tilde{f}_m | 42 |
| Figure 3.1 The Black Sea wave gauging network..... | 46 |
| Figure 3.2 Annual wind and wave roses at Sinop..... | 56 |
| Figure 3.3 Annual wind and wave roses at Hopa..... | 56 |
| Figure 3.4 Annual wind and wave roses at Gelendzhik..... | 57 |
| Figure 3.5 An example of observed and fitted spectrum (11141928.SPT, Sinop at 1994)..... | 64 |
| Figure 3.6 Relations between the dimensionless fetch and energy obtained for four alternatives at Sinop..... | 73 |
| Figure 3.7 Relations between the dimensionless fetch and peak frequency obtained for four alternatives at Sinop..... | 73 |

| | |
|---|----|
| Figure 3.8 Relations between the dimensionless peak frequency and energy obtained for four alternatives at Sinop..... | 74 |
| Figure 3.9 Relations between the dimensionless fetch and energy obtained for four alternatives at Hopa..... | 74 |
| Figure 3.10 Relations between the dimensionless fetch and peak frequency obtained for four alternatives at Hopa..... | 75 |
| Figure 3.11 Relations between the dimensionless peak frequency and energy obtained for four alternatives at Hopa..... | 75 |
| Figure 3.12 Relations between the dimensionless fetch and energy obtained for four alternatives at Gelendzhik..... | 76 |
| Figure 3.13 Relations between the dimensionless fetch and peak frequency obtained for four alternatives at Gelendzhik..... | 76 |
| Figure 3.14 Relations between the dimensionless peak frequency and energy obtained for four alternatives at Gelendzhik..... | 77 |
| Figure 3.15 Relations between dimensionless fetch and energy obtained for 22.5° angle and the larger area around the stations..... | 80 |
| Figure 3.16 Relations between dimensionless fetch and peak frequency obtained for 22.5° angle and the larger area around the stations..... | 80 |
| Figure 3.17 Relations between dimensionless peak frequency and energy obtained for 22.5° angle and the larger area around the stations..... | 81 |
| Figure 3.18 Relations between dimensionless spectral parameters and dimensionless fetch at Sinop..... | 82 |
| Figure 3.19 Relations between dimensionless spectral parameters and dimensionless fetch at Hopa..... | 83 |
| Figure 3.20 Relations between dimensionless spectral parameters and dimensionless fetch at Gelendzhik..... | 84 |
| Figure 3.21 Cluster of dimensionless spectra together with the mean JONSWAP spectrum (red line) at Sinop..... | 87 |

| | |
|---|-----|
| Figure 3.22 Cluster of dimensionless spectra together with the mean JONSWAP spectrum (red line) at Hopa..... | 87 |
| Figure 3.23 Cluster of dimensionless spectra together with the mean JONSWAP spectrum (red line) at Gelendzhik..... | 88 |
| Figure 3.24 Non-dimensional mean JONSWAP spectra at Sinop, Hopa and Gelendzhik..... | 88 |
| Figure C1 Location of Sinop on the mesh and alignments of directions considered in the analysis..... | 105 |
| Figure C2 Location of Hopa on the mesh and alignments of directions considered in the analysis..... | 106 |
| Figure C3 Location of Gelendzhik on the mesh and alignments of directions considered in the analysis..... | 107 |

CHAPTER 1

INTRODUCTION

1.1 General Description

In the coastal engineering profession, wind-waves are the most important phenomenon to be considered among the environmental conditions affecting maritime structures and other marine and coastal activities. However, wind waves have very complex natures. Looking out at the sea, one never sees a constant progression of identical waves. Instead, the sea surface is composed of waves of varying heights and periods moving in different directions. Wind waves are highly irregular with respect to their direction, amplitude and frequency, and moreover, the irregularity is of random nature. Therefore, the shape of sea surface in the presence of wind waves cannot be deterministically described.

Once the fundamental randomness of the sea surface is recognized, it becomes necessary to treat the characteristics of the sea surface in appropriate ways. There are two approaches for describing the irregular nature of wind waves in a storm. One of them is to use the statistical probability distributions of individual wave characteristics. The other way is to use the wave energy spectrum.

For the study of wave characteristics and for the design of marine structures and vessels, the spectral description of the sea states is an important input. For example, the spectral information is required in the estimation of induced loads on marine structures and the response of floating bodies to the wave action.

The spectrum measured in a particular point of the ocean is generally considered as the sum of wave systems generated by events separated either in space, in time, or both. Although the wave spectrum is quite complex, there is a remarkable similarity of its shape in different locations under an enormous variety of wind speeds, spanning from small waves in lakes up to storm waves generated by hurricanes. It is widely accepted that it has some general fundamental properties.

Several studies have been carried out for proper description and parameterization of wind wave spectrum over the last 50 years. A series of empirical expressions have been developed, which can be fitted to the spectrum of the sea surface elevation. These are called parametric spectrum models. PM model for “Fully Developed Sea” and JONSWAP model for fetch limited “Developing Sea” are the widely accepted and used models all around the world for decades.

It should be noted that the earlier proposed parametric spectral models, including the PM and JONSWAP, account only for wind-driven seas, which are locally generated. For this reason these spectra have uni-modal, or single-peaked shapes. However, it is well known that not all sea states have single peaked spectra. It has been demonstrated that in many occasions, the sea states are the result of the combination of more than one wave system. In such a case, the frequency spectrum exhibits two or more peaks. It is

important to identify the multi modal spectra from the observed spectra and to analyze the two groups separately. It has been reported that bimodal sea states can have a significant impact on the design and operability of fixed and floating offshore platforms. Engineering design and planning calculations involving such sea states should be based on an accurate spectral description. There are a few models proposed for this purpose, and almost all are based on modifications of PM or JONSWAP spectrum or a combination of these two models for separate components.

1.2 Scope of the Work

In the Black Sea, spectral information for wind waves is extremely limited. Knowledge on spectral characteristics of wind waves would contribute to scientific, engineering and operational coastal and marine activities in the Black Sea. Thus, the aim of the present thesis was set as to produce accurate information on wind wave spectrum for the Black Sea, that would allow detailed understanding of the nature of the waves occurring in the Black Sea.

For investigating wind-wave spectra over the eastern Black Sea basin, long-term wave measurements obtained by directional buoys deployed offshore at Sinop and Hopa in Turkey and Gelendzhik in Russia were used. These measurements were carried out in the scope of the NATO TU-WAVES project, an extensive research effort during 1994-2001 which was financially supported by NATO Science for Stability Programme-Phase III. Thousands of frequency spectra of wind waves recorded at Sinop, Hopa and Gelendzhik were analyzed to identify them as uni-modal or multi-modal spectra, and later as fully developed or developing sea records. The criteria

to be satisfied for these identifications were developed. The method used was based on the frequency spectra alone. The single-peaked spectra were compared with JONSWAP and PM model spectra for developing and fully developed sea states respectively. Model parameters were estimated for the observed spectra by using a least square error method. Averages of the spectral parameters were computed for different sea states and for the overall data. Then, the records which were identified as belonging to developing seas were further analyzed by using rather rigid criteria for determining the records belonging to stable wind conditions. Fetch dependencies of non-dimensional spectral variables, mean parameters of JONSWAP model spectrum and the envelop of dimensionless spectra were investigated for this data sub-set.

The second chapter of the thesis describes the available information on the characteristics of wind waves and concept of wave spectrum together with a few existing model wave spectra. Methods in order to identify multi-modal spectra and methods for fitting model spectra to observed spectra are reviewed in this chapter. Lastly, the concept of fetch dependencies of non-dimensional spectral parameters is presented.

The third chapter gives information about wave measurements at Sinop, Hopa and Gelendzhik. The methods of analysis used in the thesis are described in line with the theoretical background. The results obtained in this thesis are provided in this chapter.

The fourth chapter provides a summary and the conclusions of this study.

CHAPTER 2

LITERATURE REVIEW

2.1 Wind Waves

Waves are generated by forces that disturb a body of water. They can result from a wide range of forces like the gravitational pull of the sun and the moon, underwater earthquakes and landslides, the movements of boats and swimmers. However, the vast majority of sea waves are generated by wind. As the wind blows across a smooth water surface, air molecules push against the water. This friction between the air and water creates tiny ridges or ripples on the ocean surface. As the wind continues to blow, these ripples increase in size, eventually growing into waves that may reach several meters in height.

Three factors determine how large wind-generated waves can grow; wind speed, wind duration and fetch, which is the distance over which the wind blows without a change in direction. The faster the wind, the longer it blows, and the longer the fetch, the larger the waves that are generated. However, the growth of waves is not indefinite. After a certain point, the energy imparted to the water by wind is dissipated by wave breaking. When this occurs and the waves can no longer grow, the sea state is said to be “fully developed”.

When waves are being generated by strong winds in a storm, the sea surface generally looks very chaotic, with lots of short, steep waves of varying heights. In calm areas far from strong winds, ocean waves often have quite different features, forming long, rolling peaks of uniform shape. For this reason, physical oceanographers differentiate between two types of surface waves: seas and swells. Seas refer to short-period waves that are still being created by winds or are very close to the area in which they were generated. Swells refer to waves that have moved out of the generating area, far from the influence of the winds that caused them. In general, seas are short-crested and irregular, and their surface appears much more disturbed than for swells. Swells, on the other hand, have smooth, well-defined crests and relatively longer periods.

2.1.1 Evolution of Wind Waves

After the onset of wind over a calm sea, evolution of individual wave components may go through five main stages; the linear growth, the exponential growth, the non-linear growth, wave breaking (white capping) and quasi-equilibrium stages as schematically shown in Figure 2.1 (Abdalla, 1991).

Firstly, the small pressure fluctuations associated with turbulence in the airflow above the water induce small perturbations on the sea surface and support a subsequent linear growth as the wavelets move in resonance with the pressure fluctuations. This mechanism is called Philips resonance (Philips, 1957).

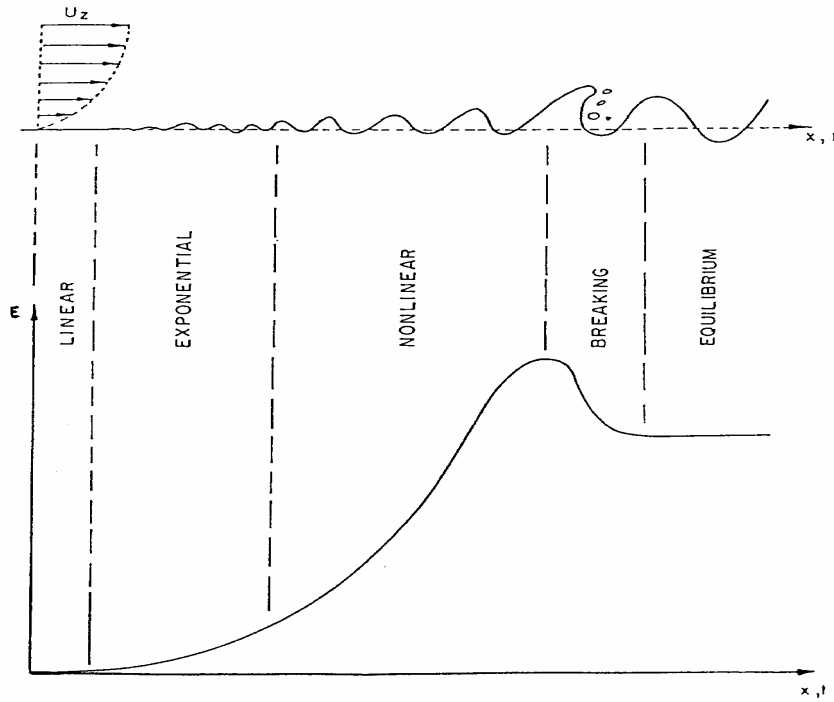


Figure 2.1 Evolution of wind waves growth (Abdalla, 1991)

Most of the development commences when the wavelets grow to a sufficient size to start affecting the flow of air above them. The waves which are already formed affect the mean shear flow in the air above them, causing the airflow sucking at the crests and pushing on the troughs. This interaction of air and sea leads to an exponential increase in wave energy, depending on the existing state of the sea (Miles, 1957). The period when wave growth is at linear and exponential rate is called initial stage. (WMO, 1988)

At the third stage, as the average wave slope gets larger, the non-linear wave-wave interactions become dominant and they try to give the spectrum the self-similar shape. During this stage, which is called the developing sea stage, the major wind input is transferred to wave components with frequencies slightly higher than the dominant spectral frequency (peak frequency). The process of non-linear wave-wave interactions then act as a

pump that sucks the wave energy from these wave components and transfers it to both lower and higher frequencies. The energy transferred to lower frequencies is retained while that to higher frequencies is usually dissipated through wave breaking and turbulence. As a result, the spectrum grows in magnitude and shifts its peak towards lower frequencies under the action of the same wind field. This situation was clarified during the JONSWAP experiment by Hasselmann et al. (1973). The mechanism of non-linear interactions plays a role maintaining the self-similar spectral shape by eliminating any instability which may be formed in the spectrum. (Abdalla, 1991)

As the waves continue to grow, they become steep and unstable. Consequently, they break and white caps are formed on the sea surface. Finally, when all these processes acting over, all the wave components balance each other with a null resultant effect, the wave spectrum attains a quasi equilibrium state. This last stage is called the fully arisen sea state. (Arıkan, 1998)

2.2 Irregular Waves

In order to understand the motion and behavior of waves, it helps to start with simple waves, which can be described in simple mathematical terms. Sinusoidal or monochromatic waves are examples of simple waves. Their surface profile can be described by a single sine or cosine function. Simple waves like these are readily measured and analyzed, since all of their basic characteristics remain constant. Their motion and behavior can be fully described when the wave length, height, period and depth are known. However, simple waves may be generated in laboratories but rare in nature.

In nature, wind waves are very complex. Looking out at the sea, one never sees a constant progression of identical waves. Instead, the sea surface is composed of waves of varying heights and periods moving in differing directions. When the wind blows and the waves grow in response, the seas tend to be confused: a wide range of heights and periods is observed. Therefore with their perfect regularity, simple waves do not accurately depict the random nature of ocean waves.

Once the fundamental randomness of the sea surface is recognized, it becomes necessary to treat the characteristics of the sea surface in statistical and/or spectral terms. The ocean surface is often considered as the combination of many wave components. These individual components may be generated by winds in different regions of the ocean and may propagate to the point of observation, forming complex waves. If a recorder were to measure waves at a fixed location of the ocean, record of the wave surface would be rather irregular and random, a non-repeating wave profile would be seen. Although individual waves can be identified, there is significant variability in height and period from wave to wave. Consequently, definitions of wave characteristics, height, period, etc., must be statistical or probabilistic and simply indicate the severity of wave conditions. (CEM, 2006)

2.2.1 Random Nature of Wind Waves

The random nature of wind waves is usually described as a stationary Gaussian process, which means that the instantaneous surface elevations follow the Gaussian distribution and the ensemble averages do not change

with respect to time and space. The probability density function of the Gaussian distribution for surface elevations is written as,

$$p(\eta) = \frac{1}{\sqrt{2\pi}\sigma} \exp\{-\eta^2 / 2\sigma^2\} \quad (2.1)$$

where,

η : Instantaneous surface elevations

$\sigma^2 = \overline{\eta^2}$: Variance of the surface elevations, η

The Gaussian distribution has the following properties:

$$\overline{\eta} = \int_{-\infty}^{+\infty} \eta p(\eta) d\eta = 0 \quad (2.2)$$

$$\sigma^2 = \overline{\eta^2} = \int_{-\infty}^{+\infty} (\eta - \overline{\eta})^2 p(\eta) d\eta \quad (2.3)$$

The Gaussian distribution is symmetrical about $\eta = 0$ (i.e. Skewness=0).

For the sea waves, it is a matter of discussion if they are truly a stationary Gaussian process. They show some deviations from the Gaussian distribution. However, it is accepted that the deviation is small and the theory of a stationary Gaussian process is frequently used. The basic models that have been developed are based on this assumption. (Acar, 1983)

An important result of this assumption is that the wind waves can be resolved as a sum of infinite number of sinusoidal waves with infinitesimal amplitudes and random phases. This is expressed as follows:

$$\eta(t) = \sum_{n=1}^{\infty} a_n \sin(2\pi f_n t + \phi_n) \quad (2.4)$$

where;

$\eta(t)$: Surface elevation at time, t at a fixed point

a_n : The amplitude of the n^{th} sinusoidal component

f_n : The frequency of the n^{th} sinusoidal component

ϕ_n : Phase angle of the n^{th} sinusoidal component

2.2.2 Concept of Spectral Analysis

Two main approaches exist for treating complex waves: spectral analysis and wave-by-wave (wave train) analysis. The more powerful and popular of these two approaches is the spectral analysis. The spectral modeling of the sea states is the basic description of the probabilistic nature of the sea surface elevation. It is based on the assumption that the sea surface elevation can be modeled as an ergodic, and thus stationary, Gaussian stochastic process (Guedes Soares and Nolasco, 1992).

Spectral analysis assumes that the sea state can be considered as a combination or superposition of a large number of regular sinusoidal wave components with different frequencies, heights, and directions as given in Equation 2.5. This equation is similar to Equation 2.4. The only difference is that the latter is the sum of a finite number (N) of the wave components.

$$\eta(t) = \sum_{n=1}^N a_n \sin(2\pi f_n t + \phi_n) \quad (2.5)$$

Mathematically, spectral analysis is based on the Fourier Transform of the sea surface. The Fourier Transform allows any continuous, zero-mean signal - like time-series record of the sea surface elevation - to be transformed into a summation of simple sine waves. These sine waves are the components of the sea state, each with a distinct height, frequency, and direction. In other words, the spectral analysis method determines the distribution of wave energy for each wave frequency by converting the time series of the wave record into a wave spectrum. This is essentially a transformation from the time-domain to the frequency-domain, and is accomplished most conveniently using a mathematical tool known as the Fast Fourier Transform (FFT) (CEM, 2006).

As the result of Fourier analysis, the squares of amplitudes, a_n^2 of wave components can be obtained. When these values are multiplied by 1/2 and plotted against frequency, the graph represents the energy of wave components at each frequency.

Following relation exists between a_n^2 and $S(f_n)$, which is the energy density of the wave component with frequency f_n in the frequency interval Δf_n :

$$S(f_n) \Delta f_n = 1/2 a_n^2 \quad (2.6)$$

$S(f)$ versus f graph is called the wave frequency spectrum.

From Equations (2.5) and (2.6), the following relation can be obtained:

$$\overline{\eta^2} = \sum_{n=1}^N S(f_n) \Delta f_n \quad (2.7)$$

Equation (2.7) implies that the area under the spectral curve gives the variance of water surface fluctuations.

Wave spectrum is usually given as a continuous curve connecting the discrete points found from Fourier analysis. A typical measured wave frequency spectrum is shown in Figure 2.2.

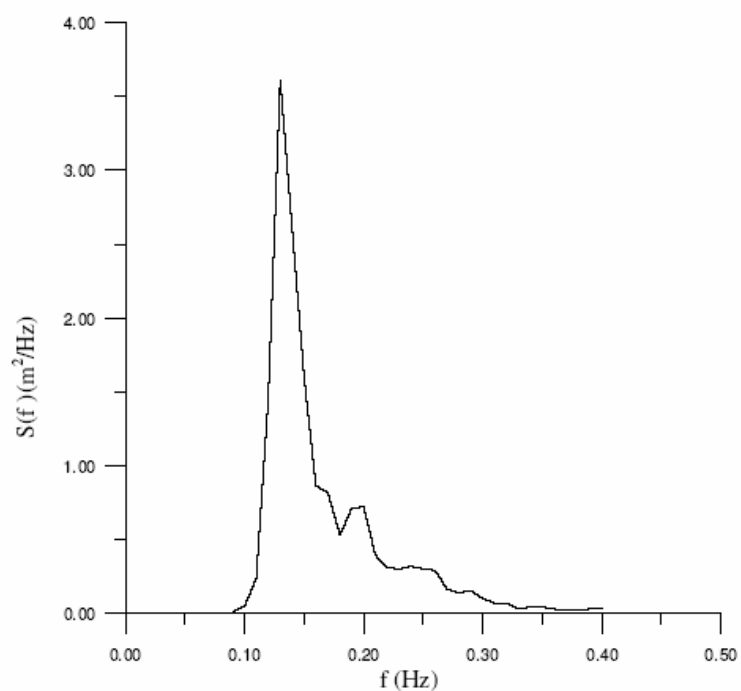


Figure 2.2 A typical measured frequency spectrum

A wave spectrum can reveal a great deal information about a wave sample and ocean conditions. The general shape of the plotted spectrum reveals for example whether sea or swell predominate, the number of distinct swells present, etc. During strong wind events, the spectrum tends to have a broad central peak. For swell that has propagated a long distance from the source

of generation, on the other hand, waves tend to have a single sharp, low-frequency (long period) peak.

Several characteristic parameters to describe the sea state can be defined in terms of the moments of the wave spectrum. In general, the n^{th} moment of the spectrum is given by:

$$m_n = \int_0^{\infty} f^n S(f) df \quad (2.8)$$

In this formula, $S(f)df$ represents the energy contained in the frequency interval between $f-df/2$ and $f+df/2$.

The zeroth moment of the spectrum, m_0 , gives the total area under the spectral curve and represents the total energy of the waves in the wave record.

The commonly used spectral wave height parameter, H_{m0} , is related to m_0 as:

$$H_{m0} = 4 \sqrt{m_0} \quad (2.9)$$

There exist two approximate spectral wave period parameters for estimating the average wave period. They are given in terms of the moments of spectrum as:

$$T_{01} = m_0 / m_1 \quad (2.10)$$

$$T_{02} = \sqrt{m_0 / m_2} \quad (2.11)$$

The width of the wave spectrum, i.e. spectral width, is used as a measure of irregularity of the sea state. Its definition is given as:

$$\varepsilon = \sqrt{1 - \frac{m_2^2}{m_0 m_4}} \quad (2.12)$$

The spectral width parameter ε varies theoretically between $\varepsilon = 0$ (very narrow spectrum, regular waves) and $\varepsilon = 1$ (broad spectrum, white noise).

A more robust definition of the spectral width parameter is given as:

$$\nu = \sqrt{\frac{m_0 m_2}{m_1^2} - 1} \quad (2.13)$$

In the range of sufficiently small values of ν , it is nearly equal to 1/2 of the spectral width parameter ε defined by Equation 2.12. Therefore, the values of ν changes between $\nu=0$ and $\nu=0.5$.

Over five decades, Fourier spectrum analysis has been the standard procedure used by atmospheric and oceanic scientists as well as coastal and marine engineers to analyze and predict wind-generated ocean waves. The long lasting usefulness of wind wave spectrum analysis is clearly not accidental but well warranted. Some of the notable successes of wave spectrum analysis are:

- The wave spectrum provides an appropriate representation of energy distribution at the ocean or lake surface.
- The wave spectrum encompasses all the Fourier components of a spatially homogeneous and temporally stationary wave field.

- Most of the common measures of wind wave characteristics are conveniently related to the moments of a wave frequency spectrum.
- The concept of wave spectrum has also contributed significantly to progress in numerical modeling for wind wave predictions. (Liu, 2000)

2.3 Wind Wave Spectrum

The wave spectrum describes how the wave energy spreads over the range of frequency and that of direction. The distribution of wave energy over the frequency is represented by the frequency spectrum $S(f)$, while the energy spreading over the direction is described with the directional spreading function $G(\theta|f)$. Thus, the directional wave spectrum $S(f,\theta)$ is expressed as:

$$S(f,\theta) = S(f) G(\theta|f) \quad (2.14)$$

where θ is the angle from the principal direction of wave propagation. The function $G(\theta|f)$ has been found to vary with wave frequency. Therefore, it contains the frequency variable f . The directional spreading function carries no dimensions and is normalized as:

$$\int_{-\pi}^{\pi} G(\theta | f) d\theta = 1 \quad (2.15)$$

Thus the frequency spectrum $S(f)$ gives the absolute value of the wave energy density, while the function $G(\theta|f)$ represents the relative magnitude of directional spreading of wave energy (Goda, 2000).

For the functional form of $G(\theta|f)$, several proposed formulas are available. Since directional spectrum is not studied in this thesis, these results are not given here. The comparative review of Goda (1999) on the functional forms of directional wave spectrum is recommended by the author for more information.

The present study focused on the frequency spectrum (one-dimensional). Therefore, throughout the thesis, the term wave spectrum is used to indicate the frequency spectrum, unless otherwise stated.

2.3.1 Spectral Shape and Parametric Model Spectrum

Detailed knowledge of the shape of the ocean wave spectrum and its growth is important information for offshore engineering applications. The spectrum measured in a particular point of the ocean is the sum of wave systems generated by events separated either in space, in time, or both. Although it is quite complex, under certain wind conditions the spectrum does have a specific shape. A series of empirical expressions have been found which can be fitted to the spectrum of the sea surface elevation. These are called parametric spectrum models, and are useful for routine engineering applications. (CEM, 2006)

The detailed processes that govern the shape and evolution of wind waves are still not completely understood. It is however common knowledge that the growth of waves in deep water is a function of three dynamic processes called the source terms, that is, the input of kinetic energy by the wind (S_{in}), energy dissipation due to wave breaking (S_{ds}), and nonlinear wave-wave interaction (S_{nl}) (Violante-Carvalho et al., 2004). The nonlinear interactions

play a very important role in the shape stabilization of the wave spectrum $S(f)$, forcing its high-frequency portion beyond the peak frequency to decay in a manner inversely proportional to frequency to a power 'n' in the form $S(f) \propto f^{-n}$ (Violante-Carvalho et al., 2002).

In a pioneering paper, Phillips (1958) suggested that in the portion of higher energy within the equilibrium range (in the band of frequencies from $1.5f_p$ to $3.0f_p$ where f_p is the peak frequency), the spectrum is a function of f^{-5} decay expressed as:

$$S(f) = 0.0081g^2(2\pi)^{-4}f^{-5} \quad (2.16)$$

where g is the gravitational acceleration.

Phillips' work was based on dimensional considerations and on the fact that due to the wave steepness, the high-frequency part of the spectrum is limited by wave breaking. Energy inputted by wind in these frequencies is lost by wave breaking, and hence Equation 2.16 describes the high-frequency part of the wave spectrum (Violante-Carvalho et al., 2002). The Phillips' spectral model received considerable support from analyses of experimental data published during the 1960s and the early 1970s (Rodriguez and Guedes Soares, 1999).

Phillips' equation for the equilibrium range of the spectrum became the basis of most subsequent developments. The characteristics of the frequency spectra of sea waves have been fairly well established through analyses of a large number of wave records taken in various waters of the world (Goda, 2000). There exist several model frequency spectra, proposed to represent the energy distribution of a wave field, which are based on one or more

parameters such as wind speed, significant wave height, wave period, shape factors, etc.

Some well-known models of frequency spectra are those of Neumann (1953), Darbyshire (1955), Bretschneider (1962), Pierson-Moskowitz (PM) (1964) and JONSWAP (1973). Especially, PM and JONSWAP spectra have been widely accepted and used all over the world. The three relatively more recent model spectra, which have been proposed at the first half of 1980s, are Wallops, TMA and Donelan spectra. Some details of PM, JONSWAP, Wallops and Donelan spectra, which are all for single-peaked spectra, are given in the following paragraphs.

Pierson-Moskowitz (PM) spectrum:

After several models were proposed based on different considerations in the 1950s, the one that has been generally accepted to describe fully developed wind-driven wave systems was introduced by Pierson and Moskowitz (1964) from analysis of measurements in the North Atlantic. They added an exponential term to Phillips' expression (Equation 2.16) to generate a low-frequency spectral face. The original form of their model spectrum is given as:

$$S(f) = 8.10 \times 10^{-3} g^2 (2\pi)^{-4} f^{-5} \exp(-0.74(g/2\pi f U_w)^4) \quad (2.17)$$

where U_w is the wind speed at the elevation 19.5 m above the sea surface.

In a general form, PM spectrum can be written as:

$$S(f) = 8.10 \times 10^{-3} g^2 (2\pi)^{-4} f^{-5} \exp\left(-\frac{5}{4} \left(\frac{f}{f_p}\right)^{-4}\right) \quad (2.18)$$

where f_p is the peak frequency (the frequency at the maximum spectral density of the spectrum).

In 1970, Mitsuyasu reformulated the PM spectrum with the significant wave height, $H_{1/3}$ and the significant wave period, $T_{1/3}$ by adjusting the coefficient values so that the theoretical relations between the wave spectrum and wave height and period statistics could be satisfied.

$$S(f) = 0.257 H_{1/3}^2 T_{1/3}^{-4} f^{-5} \exp(-1.03 (T_{1/3} f)^{-4}) \quad (2.19)$$

The functional form of Equation 2.19 is called as the *Bretschneider-Mitsuyasu spectrum* because of the initial contribution by Bretschneider in 1959. The spectral peak period T_p (the inverse of the peak frequency f_p) was correlated to $T_{1/3}$ as $T_p = 1.05 T_{1/3}$ by Mitsuyasu based on his field data (Goda, 2000).

JONSWAP spectrum:

PM spectrum describes the waves developed with no limitations in fetch and wind duration which are called as fully developed. However, these waves are not very common in nature, as they require a steady wind blowing for a long period over a large area. In younger seas and for shorter fetches as they may occur in coastal waters, the wave system may not have time enough to

fully develop. The spectrum in this case is more peaked and has, in general, higher peak frequencies. As the sea state develops, the nonlinear wave-wave interactions move the peak toward lower frequencies and make it flatter, converging to the Pierson-Moskowitz model (Guedes Soares, 2003). This feature has been demonstrated by a wave observation program named the Joint North Sea Wave Project (JONSWAP), which produced a model widely used since then to describe developing sea states. The proposed spectral form is known as the JONSWAP spectrum (Hasselmann et al. (1973)) that described fetch-limited waves very well by using five parameters (f_p , α , γ , σ_a and σ_b) (Violante-Carvalho et al., 2002).

$$S(f) = \alpha g^2 (2\pi)^{-4} f^{-5} \exp\left[-\frac{5}{4}\left(\frac{f}{f_p}\right)^{-4}\right] \gamma^{\exp\left[\frac{(f-f_p)^2}{2\sigma^2 f_p^2}\right]} \quad (2.20)$$

where

$$\sigma = \begin{cases} \sigma_a & \text{for } f \leq f_p \\ \sigma_b & \text{for } f > f_p \end{cases}$$

As it is seen from Equations 2.18 and 2.20, the JONSWAP spectrum is based on the PM spectrum with an enhancement factor γ added to control the sharpness of the spectral peak (Figure 2.3). This enhancement is only significant in the region near the spectral peak. Widths of the peak region at the left and right-side are represented, respectively, by σ_a and σ_b . At higher frequencies, the decay is inversely proportional to frequency to the fifth power, as suggested by Phillips. However, the high-frequency scale parameter α is not constant as initially proposed by Phillips to be equal to 0.0081. Hasselmann et al. (1973) found a relationship between α and fetch

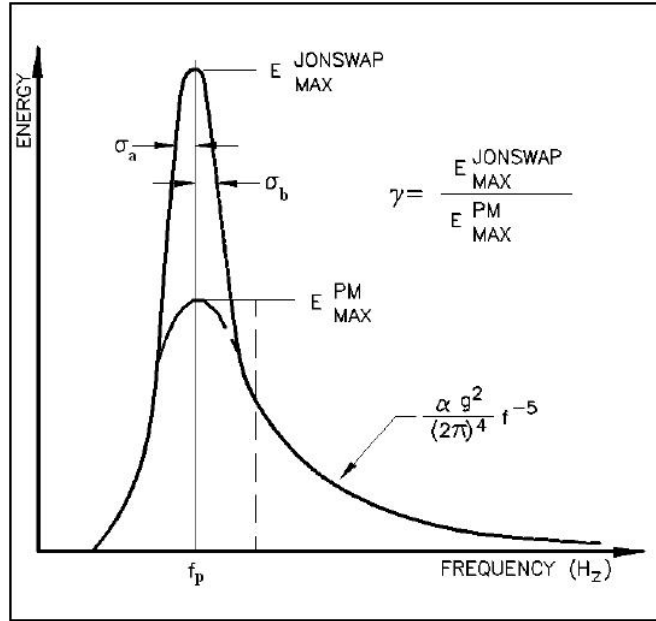


Figure 2.3 Comparison of the PM and JONSWAP spectra (CEM, 2006)

length which confirmed the suggestion of Longuet-Higgins (1969) that α decreases with increasing fetch F .

$$\alpha = 0.076 \left(\frac{gF}{U_{10}^2} \right)^{-0.22} \quad (2.21)$$

where U_{10} is the wind speed at 10 m height.

Besides they found that peak frequency f_p is also related to fetch.

$$f_p = 3.5 \left(\frac{g^2 F}{U_{10}^3} \right)^{-0.33} \quad (2.22)$$

They found no correlation of γ , σ_a and σ_b with fetch and proposed mean values for their representation as $\gamma=3.3$ (found to vary between 1 and 7), $\sigma_a=0.07$ and $\sigma_b=0.09$.

Goda in 1988 converted the JONSWAP spectrum to be expressed in terms of the significant wave height and peak wave period:

$$S(f) = \beta_J H_{1/3}^2 T_p^{-4} f^{-5} \exp[-1.25(T_p f)^{-4}] \gamma^{\exp[-(T_p f - 1)^2 / 2\sigma^2]} \quad (2.23)$$

where,

$$\beta_J \cong \frac{0.06238}{0.230 + 0.0336\gamma - 0.185(1.9 + \gamma)^{-1}} [1.094 - 0.01915 \ln \gamma] \quad (2.24)$$

$$T_{1/3} \cong \left[1 - 0.132(\gamma + 0.2)^{-0.559} \right] T_p \quad (2.25)$$

$$\bar{T} \cong \left[1 - 0.532(\gamma + 2.5)^{-0.569} \right] T_p \quad (2.26)$$

$$\sigma = \begin{cases} 0.07 : f \leq f_p \\ 0.09 : f > f_p \end{cases} \quad (2.27)$$

JONSWAP group reported that the value of γ ranged between 1 and 7 with the mean of 3.3. However, the empirical Equations 2.23 to 2.27 were derived by Goda for the range of $\gamma = 1$ to 20. The numerical simulation of wave profiles was carried out by the Monte Carlo technique with the sampling time interval of $\Delta t = T_p/12$ or $f_{\max} = 6f_p$, and two thousands wave profiles were simulated for each spectral condition (Goda, 1999).

The above spectral forms are characterized by the high frequency tail proportional to f^{-5} , which is based on the theoretical examination by Phillips

of the equilibrium range of wave spectrum due to the wave breaking phenomenon. However, several laboratory and full scale measurements have shown that the tail is closer to -4 than to -5. For example, Toba (1973) argued that the form f^{-4} is more appropriate for wind waves after his empirical study. Moreover, wave spectra in relatively shallow water often exhibit the energy density decrease slower than f^{-5} , sometimes proportional to f^{-3} (Goda, 1999). This change is attributed to the effect of water depth on the shape of wave spectrum and to the interaction between spectral components. Bouws et al. (1984) proposed a variation to the JONSWAP energy spectrum for representing wave spectra at finite-depth water. This spectrum, which is the product of JONSWAP and the Kitaigorodskii depth function accounting for the influence of the water depth, is called the *TMA spectrum* after the names of three sources of data used in its development (Texel, Marsen, and Arsloe) (CEM, 2006).

It is reported by Goda that the *Wallops spectrum* proposed by Huang et al. in 1981 is useful for generalization of various spectral forms. Wallops spectrum was rewritten by Goda in 1988 in terms of the parameters of wave height and period as in the following:

$$S(f) = \beta_w H_{1/3}^2 T_p^{1-m} f^{-m} \exp[-m/4(T_p f)^{-4}] \quad (2.28)$$

where,

$$\beta_w \cong \frac{0.06238 m^{(m-1)/4}}{4^{(m-5)/4} \Gamma[(m-1)/4]} \left[1 + 0.7458(m+2)^{-1.057} \right] \quad (2.29)$$

$$T_{1/3} \cong \left[1 - 0.283(m-1.5)^{-0.684} \right] T_p \quad (2.30)$$

$$\bar{T} \cong \left[1 - 1.295(m-0.5)^{-1.072} \right] T_p \quad (2.31)$$

where Γ denotes the Gamma function. The JONSWAP spectrum with $\gamma = 1$ (Equation 2.23) produces the spectral form similar to the Wallops spectrum with $m = 5$ (Goda, 1999).

Another spectral form is proposed by Donelan et al. (1985) based on detailed field measurements in Lake Ontario. It is a modified version of the JONSWAP spectrum with a f^{-4} frequency tail.

$$S(f) = \alpha_d g^2 (2\pi)^{-4} f_p^{-1} f^{-4} \exp\left[\left(\frac{f}{f_p}\right)^{-4}\right] \gamma_d \exp\left[\frac{(f-f_p)^2}{2\sigma^2 f_p^2}\right] \quad (2.32)$$

Unlike Hasselmann et al. (1973) who presented spectral parameters dependent on fetch, Donelan et al. (1985) parameterized them in terms of the reciprocal wave age U_c / c_p , where U_c is the component of the wind in the wave direction and c_p is the celerity at the peak frequency. For the high-frequency scale parameter, they proposed,

$$\alpha_d = 0.006 (U_c / c_p)^{0.55} \quad ; \quad 0.83 < U_c / c_p < 5 \quad (2.33)$$

They suggested that, in contrast to Hasselmann et al. (1973), γ_d and σ also depend on wave age,

$$\gamma_d = \begin{cases} 1.7 & , \quad 0.83 < U_c / c_p < 1 \\ 1.7 + 6.0 \log(U_c / c_p) & , \quad 1 \leq U_c / c_p < 5 \end{cases} \quad (2.34)$$

$$\sigma = 0.08 \left[1 + 4 / (U_c / c_p)^3 \right], \quad 0.83 < U_c / c_p < 5 \quad (2.35)$$

The exponent n of the high-frequency tail that best describes the spectrum decay $S(f) \propto f^{-n}$ is still an open question. In many studies (Toba 1973, Donelan et al. 1985, Liu 1989, Young 1998, Rodriguez and Guedes Soares 1999, Violante-Carvalho et al. 2004), the value of n varied between -3.5 and -5. Rodriguez et al. (1999), following considerations of Kitaigorodskii (1983), point out the existence of a transitional frequency at which the decay changes from f^{-4} to an f^{-5} tail. These works raise the question of whether there is a universal high-frequency decay in the form $S(f) \propto f^{-n}$, but also give strong evidence that n lies between -4 and -5 (Violante-Carvalho et al. 2002).

For swell systems, it is more complicated to describe them since a single self-similar form does not exist as in the case of wind-driven sea states (Guedes Soares, 2003). The spectrum of swell is transformed from that of wind waves through its propagation over a long distance after the waves leave the storm area. During the swell propagation, since the low frequency wave components propagate faster than the high frequency components, the swell observed at a fixed station has a spectrum restricted to a narrow frequency range. Thus, the swell spectrum exhibits a peak much sharper than that of wind waves (Goda, 2000).

According to the analysis of swell which was generated off New Zealand and propagated over a distance of some 9000 km to the Pacific coast of Costa Rica still maintaining a significant wave height of about 3 m, Goda (1983) found that the swell spectral peaks were equivalent to the JONSWAP spectra (Equation 2.23) with $\gamma = 8 \sim 9$, and to the Wallops spectra (Equation 2.28) with $m = 8 \sim 10$, on the average. Thus, the swell spectrum for engineering applications may be approximated by the JONSWAP spectra

with the peak enhancement factor being chosen between $\gamma = 3 \sim 10$, depending on the distance traveled. (Goda, 2000)

2.4 Multi-Peaked Spectra

As summarized in the previous section, several studies have sought to properly describe and parameterize the wave spectrum over the last 50 years, and several standard spectral models have been proposed. Almost all of these produced spectral models describe only the wind sea part of the spectrum that is generated by local wind, hence, they are uni-modal (Violante-Carvalho et al., 2002). However, actual wave spectra usually exhibit some deviations from these standard forms, in particular, when swell coexists with wind waves resulting in a mixed wave system. In this case, spectrum exhibits a secondary peak at the frequency corresponding to the representative period of swell or wind waves, depending on their relative magnitudes (Goda, 2000). If the peak frequencies of the spectra are relatively close, the spectrum of the mixed sea state may still look single peaked although the directional spectrum may indicate that two wave systems come from the same or from different directions. When the peak frequencies are well separated, the spectrum has distinct double peak and none of the spectral models can describe them (Guedes Soares, 2003).

One of the first models proposed to describe double-peaked spectra was proposed by Strekalov and Massel in 1971, who suggested that it would be obtained by one high frequency spectrum describing the wind driven component and a Gaussian shaped model describing the swell system. Ochi and Hubble in 1976 proposed another form by combining a JONSWAP and

a PM spectrum describing two individual wave systems. (Ewans et al., 2006)

Guedes Soares (1984) proposed a model that represents both sea components by JONSWAP spectra of different peak frequencies. While the choice of the model for the wind sea component is obvious, the choice to model the swell component was made because the JONSWAP model is able to fit very peaked spectra which would be appropriate for the narrow swell spectral component as shown by Goda (1983).

Torsethaugen (1993) adopted also the two JONSWAP models to describe the two-peaked spectra but instead of using average JONSWAP parameters as done by Guedes Soares (1984), he used more adjustable parameters of the JONSWAP model. As a result, while the model of Guedes Soares is described by 4 parameters, the Torsethaugen model uses 7 parameters. (Guedes Soares, 2003)

More recently, two more studies (Moon and Oh (1998) and Violante-Carvalho et al. (2002)) attempted to fit empirically bi-modal spectra. Both use a similar approach. They assume the spectrum as the sum of a high-frequency and a low-frequency component yielding, $S(f)=S_{hf} + S_{lf}$. They first adjust the high-frequency part. Then after subtracting the adjusted high-frequency spectrum from the measured spectrum, they continue with adjusting the remaining low frequency part. The difference between these two studies is due to the model spectrum applied. While Moon and Oh (1998) method base on TMA spectrum, Violante-Carvalho et al. (2002) use JONSWAP spectrum.

2.4.1 Probability of Occurrence of Multi-Peaked Spectra

Frequently, sea states are the result of the presence of various wave systems. In particular, local wind waves often develop in the presence of some background low frequency swell coming from distant storms. As a consequence, the measured wave spectra have an additional low frequency peak due to swell reaching from storms in remote areas (Guedes Soares, 1984).

It is cited by Rodriguez and Guedes Soares (1999) that Thompson analyzed wave records from nine locations along United States Atlantic, Pacific, Gulf and Great Lakes coasts in 1980. He observed that multi-peaked spectra are common at all locations. In 1981, Cummings et al. using hindcast data from the North Atlantic determined that 25% of the spectra were double-peaked. From the analysis of measured data of the same area, Aranuvachapun reported in 1987 that 24% of the spectra were double peaked. (Rodriguez and Guedes Soares, 1999)

Guedes Soares (1991) used measured data from the open North Sea and North Atlantic to examine the probability of occurrence of double peaked spectra and observed that the global percentage of occurrence of spectra with bimodal structure is about 20–25%, in both areas. Guedes Soares and Nolasco (1992) obtained a range of 23–26% for data of a coastal site off Portugal.

Moon and Oh (1998) found that 25% from 17,750 wave spectra observed over seas around Korea are double peaked.

Two separate studies in Brazil reported higher probability of occurrence of multi-modal spectra. The study of Araujo et al. (2003) presented that assessment of a one-year waverider time series at Santa Catarina Island neighborhood in Southern Brazil reveals 31% of two-peaked spectra for the whole year. The other study was carried out by Violante-Carvalho who presented a comprehensive description of the wave climate in Campos Basin, off Rio de Janeiro. In this study, analysis of 5807 wave spectra from a period of 26 months indicated that about 25% of the spectra were uni-modal, whereas the vast majority presented two or more peaks (Violante-Carvalho et al., 2002).

From these results, it is clear that combined wind-wave and swell systems can occur with relatively high frequency all around the world both in the open ocean and in coastal sites. Furthermore, sometimes three or more peaks can be detected in a spectrum. It is important to know the probability of occurrence of spectra with more than one peak at a given location. Bimodal sea states can have a significant impact on the design and operation of fixed and floating offshore platforms. Engineering design and planning calculations involving such sea states should be based on an accurate spectral description (Ewans et al., 2006). It has been shown by Guedes Soares and Nolasco (1992) and Guedes Soares and Henriques (1996) that the longterm joint distribution of significant wave height and mean period and the marginal distribution of significant wave height are different for sea states with one single wave system and for multiple sea states.

2.4.2 Identification of Multi-Peaked Spectra

Starting from the spectral estimates obtained from the analysis of wave records, the first step for its characterization is to identify the type of spectra, whether it is a single peaked or a multi-peaked spectra. In practice, due to random fluctuations of the spectral ordinates estimated from a finite length wave record, it is a difficult task to decide if a spectral peak is true maximum or a noise. In other words, sometimes it is difficult to identify if the peaks in the spectrum correspond to the coexistence of different wave systems or if they are the result of the irregularity of the spectral estimates. In many situations, the decision is clear by visual inspection and no other formal criterion is needed. However, a precise criterion is often required to separate consistently the spectra as uni-modal, bi-modal, and so on, mainly if this task is to be made automatically through a computer algorithm. (Rodriguez and Guedes Soares, 1999)

The identification of a combined sea state can be made through the directional spectrum, and of the previous history of waves and wind. Several methods for the partitioning of the directional spectrum have been proposed following the original work by Gerling in 1992 (later modified by Hasselmann et al. in 1996, Violante-Carvalho et al., 2004). However, usually the information yielded directly by the buoys in the routine data collection systems is the frequency spectrum which is collected and analyzed in an automatic way. This situation gives a special importance to the existence of a criterion of automatic detection of peaks based on information about the spectral ordinates alone. Therefore, several works have attempted to address the problem of partitioning of the frequency wave spectrum and have suggested various criteria to detect peaks in estimated wave spectra.

One of the first efforts on the subject was the study of Houmb and Due in 1978 (Rodriguez and Guedes Soares, 1999; Moon and Oh, 1998). Their criteria to accept spectral peaks as true maximum or not require that number of degrees of freedom of spectral estimates must be at least 16 and the minimum difference in frequency between two peaks must be at least 6.4 times the bandwidth of the estimates. In addition, they require that the lower 90% confidence limits of the two peaks should represent a higher variance density than the trough between them.

More recently, Guedes Soares and Nolasco (1992) discussed various criteria for identifying two-peaked spectra. They considered five different tests using different combinations of these criteria to verify their effect. Fourth and fifth tests are based on the concept of confidence intervals.

In estimating a spectrum from a record of sea surface elevation, the spectral ordinates are random variables distributed according to a chi-square distribution. Thus, depending on the number of degrees of freedom in the estimation procedure, and on the confidence level, it is possible to establish confidence intervals for the estimated spectral ordinates. The confidence bounds for the spectral estimates with v degrees of freedom are given by;

$$\left(\frac{v}{\chi_{v;\alpha/2}^2} \right) \hat{S}(f) \leq S(f) \leq \left(\frac{v}{\chi_{v;1-\alpha/2}^2} \right) \hat{S}(f) \quad (2.36)$$

where α is the confidence level, $\chi_{v;\alpha/2}^2$ and $\chi_{v;1-\alpha/2}^2$ denote the 100($\alpha/2$)th and 100(1- $\alpha/2$)th percentiles for a chi-squared random variable with v

degrees of freedom, respectively, and $\hat{S}(f)$ is an estimation of the true value of $S(f)$. (Rodriguez and Guedes Soares, 1999)

In this context, the fourth test of Guedes Soares and Nolasco (1992) imposes as the necessary condition for a spectrum to be two-peaked, the lower limit of the 90% confidence level interval of the largest peak be higher than the upper limit of the interval of the adjacent minimum. The fifth test imposes the condition that the minimum between the two peaks should be below the lower limit of the confidence interval of the smaller of the two peaks. These two conditions are based on the idea that for a peak to correspond to a wave system, its maximum and minimum value must lie outside the confidence interval, which indicates the accepted variability of the spectral estimates.

Since the estimates of the spectral ordinates are often contaminated by some noise level, one additional condition was added for a peak to correspond to an accountable wave system. The peak must be larger than 15% of the dominant peak. The value of 15% that was adopted by those authors is largely arbitrary and based on judgment, which resulted from the analysis of many measured spectra with some variations of that threshold level.

Similar criteria were used in several works to identify multimodal spectra. For instance, Moon and Oh (1998) used the following three conditions in order to classify spectra with two peaks for their study in which they presented a newly developed TMA spectrum called “double-peaked TMA spectrum”:

- 1) Maximum energy density of second TMA spectra should be greater than a third of first TMA spectra;

- 2) Distance between frequencies of two spectral peaks should be more than 0.05 Hz;
- 3) The trough between the two spectral peaks should have an ordinate smaller than the lower 90% confidence limit of each peak as suggested by Houmb and Due (1978).

Violante-Carvalho et al. (2002) and Violante-Carvalho et al. (2004) adopted three conditions that must be all satisfied for the selection of the spectral peaks:

- 1) Each peak must be separated by twice the frequency resolution (0.03 Hz) from adjacent peaks (which is reported as a rather arbitrary value but which yielded satisfactory results in their study);
- 2) The ratio between the two spectra must be less than 15 to eliminate peaks that are below a background noise;
- 3) Two peaks are accepted if the ordinate of lower limit of the 90 percent confidence interval of the greater peak is higher than the ordinate of the upper limit of the 90 percent confidence interval of the trough between the peaks, which basically means that the valley between the peaks has to be sufficiently low.

2.5 Methods for Spectral Fitting

Several methods for fitting the observed spectra to a parametric model spectrum are based on the principle of minimizing the least square error between measured and fitted spectra as discussed in the following paragraphs.

Method used by Acar (1983):

For the observed spectra, JONSWAP spectrum parameters, α , γ , f_p are estimated by using a least square error analysis. The parameter values resulting in the smallest sum of square errors are found by changing the values of these parameters by small increments in the extent of their possible ranges and by numerically computing the sum of squared errors. Using trial values α , γ , f_p the spectral values of JONSWAP are calculated at the middle of each frequency band. Then the sum of the squared errors are computed from:

$$\text{Error: } \Sigma \{S(f) - S_J(f)\}^2 \quad (2.37)$$

where $S_J(f)$ is the theoretical value obtained from the JONSWAP spectrum.

In the above procedure, the trial values of α , γ , f_p are not chosen arbitrarily.

Initial values are taken as:

$$\alpha_{in} = 0.0002$$

$$\gamma_{in} = 1.00$$

$$f_{pin} = f_p$$

where f_p denotes the peak frequency of the calculated spectrum.

In the first run, initial values are changed one by one with small increments, $\Delta\alpha_1 = 0.0003$, $\Delta\gamma_1 = 0.25$, $\Delta f_{p1} = \Delta f/10$ Hz to cover their possible ranges. The

later trial values of the parameters can be written as:

$$\begin{aligned} \alpha_i &= \alpha_{in} + i \times \Delta\alpha_1 & i=0, 1, \dots, 60 \\ \gamma_j &= \gamma_{in} + j \times \Delta\gamma_1 & j=0, 1, \dots, 24 \\ f_{pk} &= f_{pin} + (k - 5) \Delta f_{p1} & k=0, 1, \dots, 10 \end{aligned} \quad (2.38)$$

As it is seen, the following ranges for α , γ and f_p are covered :

$$0.0002 < \alpha < 0.0200$$

$$1.00 < \gamma < 7.00$$

$$f_{pin} - 0.5 \Delta f < f_p < f_{pin} + 0.5 \Delta f$$

The combination of α_i , γ_j , f_{pk} which gives the minimum error are detected as the first estimates (α_1 , γ_1 , f_{p1}).

Using first estimates as the initial values, the more accurate estimates are searched by changing the values of the parameters with smaller increments:

$$\begin{aligned} \alpha_i &= \alpha_1 + (i-3) \times \Delta\alpha_1/6 \\ \gamma_i &= \gamma_1 + (i-3) \times \Delta\gamma_1/6 \\ f_{pi} &= f_{p1} + (i-3) \times \Delta f_{p1}/6 \end{aligned} \quad i=0, 1, \dots, 6 \quad (2.39)$$

In this second run, the ranges for α , γ , f_p covers all the way between the smaller and the higher adjacent values around the first estimates.

The procedure is repeated 3 times to obtain final estimates of α , γ , f_p .

Method used by Moon and Oh (1998):

Four steps were used by Moon and Oh (1998) in the following order in order to determine the parameters of the TMA spectrum.

- 1) Peak frequency f_p is determined as the frequency corresponding to the maximum spectral density,
- 2) α is determined by following equation over the range $1.35 f_p$ to $2.0 f_p$,

$$\alpha = \frac{\sum_{N_{1.35f_m}}^{N_{2.0f_m}} S(f_i)/C(f_i)}{N_{2.0f_m} - N_{1.35f_m} + 1} \quad (2.40)$$

where,

$$C(f) = \frac{g^2 f^{-5}}{(2\pi)^4} \exp\left[-\frac{5}{4} \left(\frac{f}{f_p}\right)^{-4}\right] \quad (2.41)$$

$S(f)$ = Energy of observed spectrum

$N_{2.0f_m} - N_{1.35f_m} + 1$ = Total frequency number of range $1.35f_p$ to $2.0 f_p$.

3) Peak enhancement factor γ is determined from the ratio of peak maximum energy of the observed spectrum to one of the PM spectrum with the same values of f_p and α .

$$\gamma = \frac{S_{MAX}(f_p)}{S_{MAX}^{PM}(f_p)} \quad (2.42)$$

4) Finally sigma is determined by changing it from 0.01 to 1 and finding the value which gives the least square difference between the observed and the theoretical spectra.

Method used by Violante-Carvalho et al. (2002):

Violante-Carvalho et al. (2002) considered the f^{-5} tail of the JONSWAP spectrum as variable, n considering the question marks related with its actual value and employed the following model which is based on JONSWAP spectrum. When n equals to -5, the equation reduces to the JONSWAP spectrum.

$$S(f) = (2\pi)\alpha g^2 (2\pi f)^{-n} \exp\left[-\frac{5}{4}\left(\frac{f}{f_p}\right)^{-4}\right] \gamma^{\exp[-(f-f_p)^2/2\sigma^2 f_p^2]} \quad (2.43)$$

In the fitting process, the exponent n is determined by logarithmic regression of the points greater than $2.0f_p$. To obtain α the value of γ is set to 1 in Equation 2.43, because its effect at frequencies higher than $f/f_p > 1.37$ is accepted as negligible. The value of α is obtained by iterating from 0.0001 to 0.1 in order to minimize the total square error for the range between 1.37 and 2 times the peak frequency. Once f_p , n , and α are known, γ is the last parameter to define the spectrum $S(f)$. γ is chosen as the value that produces the least-square error between measured and fitted spectra.

Method used by Feld and Mørk (2004):

They applied the following steps to fit the JONSWAP spectrum:

- 1) To identify the peak frequency, f_p , a parabola is fitted to the highest spectral density estimate and one point either side as in the Gunther method, (the method is referenced to be described in Tucker and Pitt (2001) by the authors).
- 2) Phillips' constant α is calculated by assuming that the spectrum in the range $1.35f_p$ to $2.00f_p$ can be approximated by a PM spectrum (again, as referenced to the Gunther method).
- 3) The remaining JONSWAP parameters, γ , σ_a and σ_b are then calculated by using a least squares fit to the single-peaked spectrum. If γ is calculated to

be less than 1, then a PM spectrum is assumed. In these circumstances, f_p and α are fitted by a least squares approach.

4) A normalized rms error and a bias are calculated to assess the goodness of fit. These parameters are used as a means of selecting reliable spectral fits for the quantitative comparison between measured and model data.

2.6 Fetch Dependencies of Spectral Parameters

The concept that fetch limited growth could be represented in terms of the non-dimensional variables combining energy, frequency and fetch was first proposed by Kitaigorodskii in 1962 (Young and Verhagen, 1996). Kitaigorodskii's similarity law has been traditionally used as an effective tool to express the wave growth under the condition of a steady wind blowing over a fetch limited by a straight shoreline orthogonal to the wind direction (Kahma and Calhoun, 1992).

Following Hasselmann et al. (1973), it is generally assumed that any particular spectral parameter follows a relationship of the form:

$$P = p\tilde{X}^n \quad (2.44)$$

where P is the spectral parameter ($\alpha, f_m, \gamma, \sigma_a, \sigma_b$), $\tilde{X} = gX/U^2$ is the non-dimensional fetch (X is fetch length and U is wind speed) and p and n are constants to be determined. A linear regression analysis of $\log_{10}(P)$ versus $\log_{10}(\tilde{X})$ is usually carried out to determine the values of the constants p and n . (Ewans and Kibblewhite, 1990)

As the result of their field observations or laboratory experiments, several studies in literature has described the variation of Phillips' constant α ,

dimensionless peak frequency $\tilde{f}_m = Uf_m / g$, where f_m is the peak frequency, and dimensionless variance (also referred to as the dimensionless energy) $\tilde{E} = Eg^2 / U^4$ with dimensionless fetch.

Shokurov and Efimov (1999) tabulated some of these previous results together with the results of their study (Table 2.1) for the following relations:

$$\tilde{E} = A\tilde{X}^a, \tilde{f}_m = B\tilde{X}^b, \tilde{E} = C\tilde{f}_m^c \quad (2.45)$$

Table 2.1 Estimates of constants A, a, B, b, C, c in Equation 2.45. (Shokurov and Efimov, 1999)

| Authors | A*10 ⁻⁷ | a | B | b | C*10 ⁻⁶ | c |
|---|--------------------|------|------|--------|--------------------|-------|
| JONSWAP, Hasselmann et al. (1973) | 1.6 | 1 | 3.50 | -0.33 | 5.1 | -3.33 |
| Davidan in 1980 | 4.44 | 0.84 | 2.55 | -0.28 | 6.84 | -2.94 |
| Kahma (1981) | 3.6 | 1 | 3.18 | -0.33 | 11.6 | -3.00 |
| Donelan et al. (1985) | | | 1.85 | -0.23 | 5.74 | -3.3 |
| Dobson et al. in 1989 | 8.73 | 0.79 | 1.7 | -0.24 | 5.03 | -3.3 |
| Wen et al. in 1989 | 16.6 | 0.70 | 1.66 | -0.23 | 7.69 | -3.03 |
| Evans and Kibblewhite (1990) | 2.59 | 0.87 | 2.98 | -0.30 | 6.22 | -2.91 |
| Efimov et al. in 1986, Babanin and Soloviev in 1998 | 4.41 | 0.89 | 2.41 | -0.275 | 8.30 | -3.01 |
| Theory, Zakharov and Zaslavskii in 1983 | 40.8 | 4/7 | 1.46 | -3/14 | 11.2 | -8/3 |
| Shokurov and Efimov (1999) | 1.84 | 1.00 | 2.94 | -0.30 | 6.51 | -3.30 |

Discrepancies among the studies can be observed from the table. In order to provide a visual representation, the earlier results are also shown graphically in Figures 2.4, 2.5 and 2.6. The differences between the regression equations given to describe the wave growth are evident from these figures. The most striking difference is observed for the growth relation of energy deduced from Bothnian Sea data (Kahma, 1981) which indicates almost double the energy compared to the JONSWAP result.

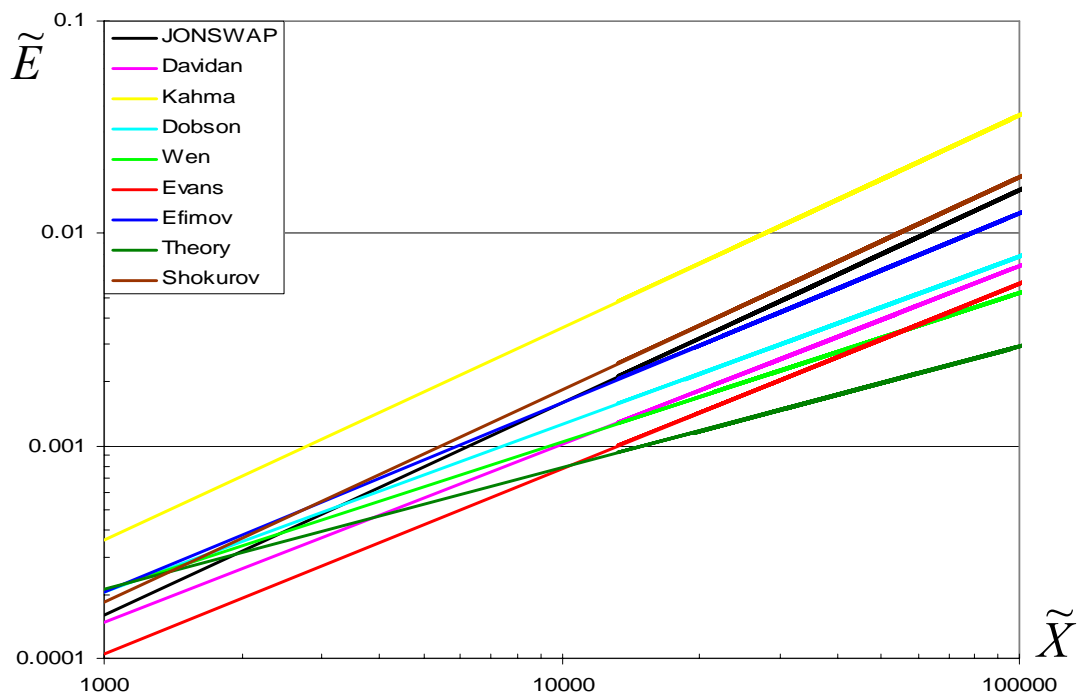


Figure 2.4 Dependence of dimensionless variance \tilde{E} on dimensionless fetch \tilde{X}

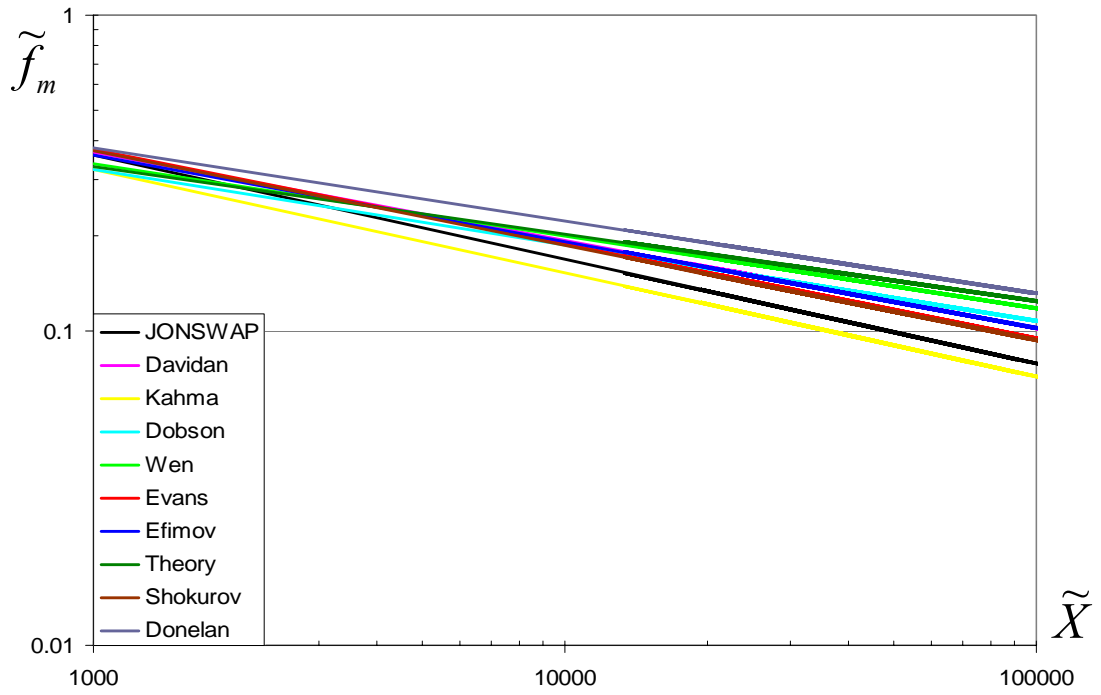


Figure 2.5 Dependence of dimensionless peak frequency \tilde{f}_m on dimensionless fetch \tilde{X}

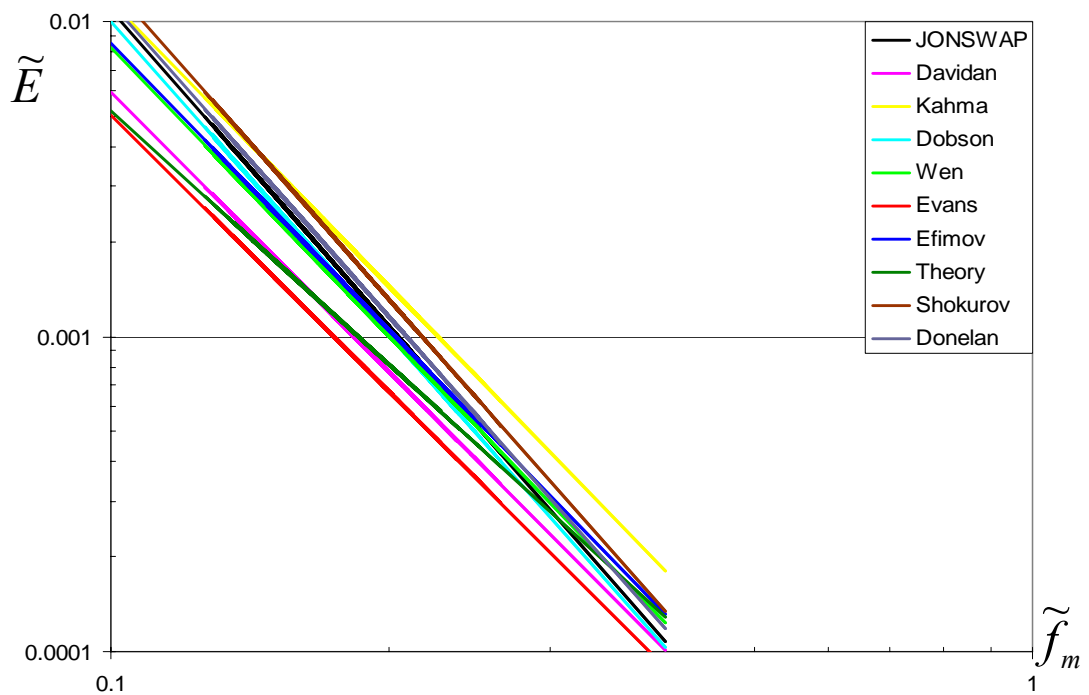


Figure 2.6 Dependence of dimensionless variance \tilde{E} on dimensionless peak frequency \tilde{f}_m

As mentioned earlier, one of the primary assumptions in fetch limited growth studies is that the wind speed is constant over the fetch, so-called the ideal condition of wave generation. However, during field experiments the actual conditions are seldom ideal and even in the most stable meteorological conditions this assumption is not fully satisfied. This is one of the reasons for discrepancies between the various data sets and scatter within specific data sets. Attempts to explain these discrepancies have identified two factors which underline the importance of detailed information on the wind field; the influence of stratification of atmospheric boundary layer and possible nonhomogeneity of wind along fetch from the shore to the measurement point.

CHAPTER 3

SPECTRAL ANALYSIS OF THE WAVE DATA AT SINOP, HOPA AND GELENDZHIK

3.1 Data Source

3.1.1 NATO TU-WAVES Project

Obtaining information on wind-wave characteristics of the Turkish coast, which is in excess of 8300 km and extends along the Black Sea, the Aegean Sea, the Mediterranean, and the inland Sea of Marmara, is essential to use the coastal area of the country efficiently. Reliable wind-wave data did not exist for the Turkish coastline until a few years ago. In order to fill this gap, an extensive project, called NATO TU-WAVES Project was planned and executed in the leadership of Coastal and Harbor Engineering Laboratory of Middle East Technical University (METU-KLARE) with partial financial support from the NATO Science for Stability (SfS) Programme Phase III. Three national organizations; Department of Navigation, Hydrography and Oceanography of the Turkish Navy (TN-DNHO), General Directorate of State Meteorological Services (SMS), and Railway, Harbor and Airport Construction General Directorate of Ministry of Transport (MT-RHAC GD), were the other collaborators in the project.

The Black Sea wind-wave climate was the international dimension of the project. This outreach component was handled in collaboration with eight institutes from four Black Sea riparian countries: Institute of Oceanology, Varna, Bulgaria; the National Institute of Meteorology and Hydrology, Bucharest, and the Romanian Marine Research Institute, Constantza, Romania; Arctic and Antarctic Research Institute, St. Petersburg, Moscow State Technological University, Moscow, and the P.P. Shirshov Institute of Oceanology, Gelendzhik, and State Oceanographical Institute, St. Petersburg, Russia; and Marine Hydrophysical Institute, Sevastopol, Ukraine.

NATO TU-WAVES Project was a major project that aimed to find out the wind and wave climate affecting the Turkish coast as well as the Black Sea basin. The project involved systematic wave measurements, wave modeling and wave climate computations. The main objectives of this project were:

- to obtain detailed knowledge on wind waves and to establish a reliable data bank,
- to implement an advanced (third generation) wave model for the seas surrounding Turkey,
- to construct a wave atlas for the Turkish coast and the Black Sea basin in order to provide statistical information on sea state parameters.

3.1.2 Wave Measurements

Obtaining reliable wave measurements was needed to achieve the objectives of the NATO TU-WAVES Project. For this purpose, Black Sea wave gauging network of six stations at Sinop and Hopa of Turkey, Gelendzhik of

Russia, Katziveli and Karkinitzskaya Platforms of Ukraine, and Gloria Platform of Romania were set-up. The network consisted of three directional wave buoys (Sinop, Hopa, Gelendzhik) and three non-directional wave gauges (Katziveli, Katziveli, Gloria) as shown in Figure 3.1.

Proper locations of gauging stations were selected by considering several criteria to cover most of the possible wave regimes affecting the Black Sea coasts. Wave measurements started at various dates at each station and lasted for various periods of time ranging from few months to few years. The data collected at the gauging stations were gathered at the project center which was located at METU-KLARE.

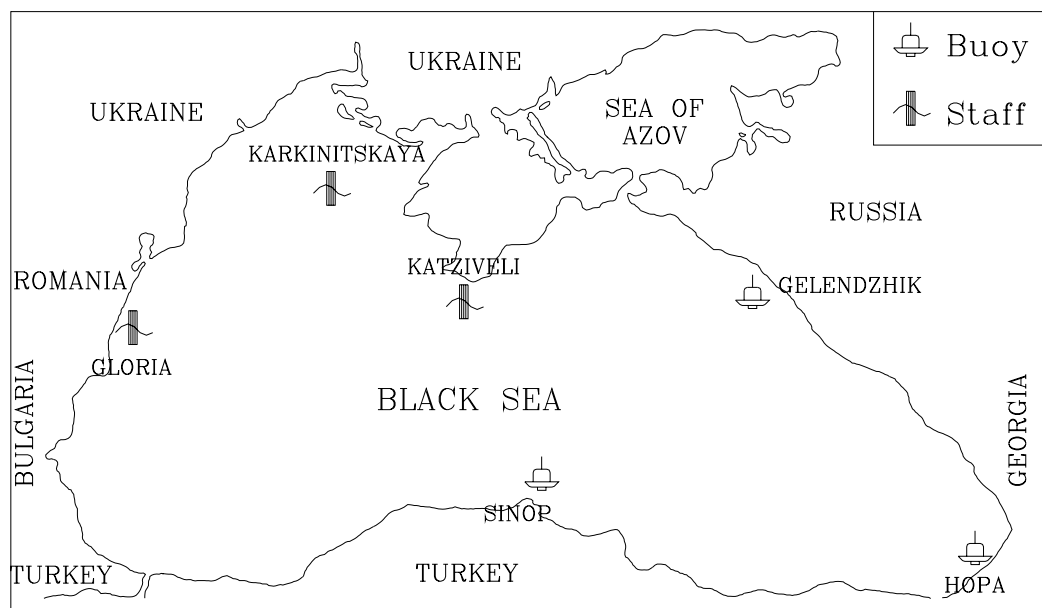


Figure 3.1 The Black Sea wave gauging network

For this study, wave records collected from the three directional wave buoys at Sinop, Hopa and Gelendzhik were utilized. Since this type of devices are deployed far away from the shore, they are vulnerable to dangers like ship collision, mooring failure and being lost during severe storms. Unfortunately, it had also been the case at these stations, and none of these buoys are in operation at the moment. However, there are still considerable length of data recorded to study the spectral characteristics in the mentioned stations; Sinop (about 8 months), Hopa (about 41 months) and Gelendzhik (about 52 months).

The buoys used to collect the directional wave data were of Directional Waverider type of Datawell. It is a 0.90 m diameter spherical buoy which measures sea surface elevation and direction. The buoy contains a heave-pitch-roll sensor, three-axis fluxgate compass, two fixed x and y accelerometers, and a microprocessor. The accelerations measured in the x and y directions of the moving buoy reference frame are used to calculate the accelerations along the fixed north and west axes. All three accelerations (vertical, north and west) are then digitally integrated to displacements and filtered to a high frequency cut-off (0.6 Hz). Finally, Fast Fourier Transform (FFT) is performed every 30 minutes. Raw data are compressed to motion vertical, motion north and motion west. Some spectral parameters like spectral energy density, main direction, directional spread, skewness, curtosis, and some other sea-state parameters like H_{m0} (significant wave height calculated from wave spectrum) and T_z (mean wave period) are computed on-board and called as processed data. The buoy transmits both raw and processed data. The buoy measures individual wave heights up to 40 m (with a resolution of 1 cm) and periods between 1.6 s - 30 s. Directional resolution is 1.50 and the frequency resolution is 0.005 Hz for frequencies less than 0.1 Hz, and 0.01 Hz otherwise. The standard buoy also

measures sea surface water temperature in the range -5°C to $+45^{\circ}\text{C}$. Because the directional waverider buoy measures the horizontal motions instead of wave slopes, the measurements are not affected by the roll motions of the buoy. This also justifies the small size of the buoy. On the other hand, the current velocities over 2.5 m/s could cause some distortions on the buoy measurements. (Özhan et al., 1995)

Buoys were deployed at the depths of 100 m, 100 m and 85 m at Sinop, Hopa and Gelendzhik, respectively to record deep water waves. The data are automatically assembled and processed by means of a spectral analysis system provided by Datawell, which estimates the directional properties of the wave field. The results of this analysis are saved in a Datawell pre-defined “SPT” file (Appendix A), which contains the energy density, mean direction and directional spreading for each frequency band from which other general parameters can be calculated. The file also contains significant wave height ($4\sqrt{m_0}$), and mean period ($\sqrt{m_0/m_2}$) of the record. These SPT files are the main data source of this study.

3.1.3 ECMWF Analysis Wind Fields

ECMWF (European Centre for Medium-Range Weather Forecasts) runs a global operational meteorological model since early 1980’s. Surface wind velocities (U10) are among the several meteorological parameters computed by the model. The model provides both objective analysis fields by assimilating available observations and daily forecasts. The forecasting system has undergone several modifications and enhancements over the years. The system predictions, especially the analysis fields, are of acceptable quality for wave prediction only since September 1991 when the

model was upgraded to what was called T213 spectral model, with a nominal horizontal resolution of about 80 km and vertical resolution of 31 levels. The wind fields of the model during 1987-1991 were of lower quality basically due to the coarse resolutions. The current operational atmospheric model of ECMWF is called T_L799L91, and has a horizontal resolution of about 25 km and a vertical resolution of 91 levels.

During NATO TU-WAVES Project, after a survey for the available wind sources for the Black Sea and the other seas surrounding Turkey, it was concluded that, in general, the ECMWF analysis wind fields since September 1991 were of acceptable quality for wave prediction in the considered seas. Therefore, for computing the corresponding wave fields, and for obtaining the long-term (operational) wind and wave statistics part of the Project, ECMWF analysis wind fields with 6 hours interval and 0.5°x0.5° spatial resolution for a period of 8 years between 01 September 1991 and 31 July 1999, which were the output of the T213 model were utilized.

It was documented by previous studies and also verified by TU-WAVES Project that wind speeds were underestimated by the ECMWF T213 atmospheric model. This behavior was investigated and found to be mainly due to the treatment of the land-boundary in the ECMWF meteorological model. The model generally produced low speeds at a certain proportion especially for enclosed basins. Consequently, the predicted wind fields were modified (Yilmaz 2000; Yilmaz, Ozhan and Abdalla 2003). The modification was mainly to increase the wind speeds by a certain percentage over the whole basin, and to stretch the wind field to get rid of the land boundary error. This enhancement provided wave predictions that showed much better agreement with wave measurements. Thus, these enhanced

(calibrated) ECMWF wind fields were used for wave computations and for wind and wave statistics in NATO TU-WAVES Project.

3.2 Arrangement of the Data for Analysis

3.2.1 Classification According to Significant Wave Height

There are 3417, 13222 and 14264 numbers of spectra files, obtained from Datawell directional waverider buoys, at Sinop, Hopa and Gelendzhik, respectively. For easier examination of these numerous measurement files, they were grouped according to the significant wave heights for the sea states with limits of 0.5 m, 1.0 m, 2.0 m, 3.0 m, 4.0 m and 5.0 m at each station. Results of this classification are given in Table 3.1. Sea states corresponding to significant wave heights less than 0.5 m were considered as calm, and were not analyzed.

During the wind wave climate studies of TU-WAVES Project, it was found that intensity of waves at Sinop was higher than at Hopa and Gelendzhik. However, it is seen in Table 3.1 that there is no record with significant wave height greater than or equal to 4 m at Sinop. This situation is the result of shorter measurements and the smaller number of storms recorded at this station.

In order to observe the seasonal variability, the data were classified according to the seasons also. In Appendix B, Tables B1 to B4 give the seasonal classification of the spectra.

Table 3.1 Number of measured spectra in each significant wave height range.

| | SINOP | HOPA | GELENDZHIK |
|------------------------------------|-------|-------|------------|
| $H_s \geq 6.0$ m. | 0 | 0 | 5 |
| $5.0 \text{ m.} \leq H_s < 6.0$ m. | 0 | 1 | 9 |
| $4.0 \text{ m.} \leq H_s < 5.0$ m. | 3 | 12 | 57 |
| $3.0 \text{ m.} \leq H_s < 4.0$ m. | 40 | 80 | 261 |
| $2.0 \text{ m.} \leq H_s < 3.0$ m. | 194 | 501 | 1340 |
| $1.0 \text{ m.} \leq H_s < 2.0$ m. | 892 | 1858 | 3368 |
| $0.5 \text{ m.} \leq H_s < 1.0$ m. | 1321 | 3086 | 3244 |
| $H_s < 0.5$ m. | 963 | 7684 | 5976 |
| TOTAL # | 3413 | 13222 | 14260 |

3.2.2 Classification According to the Number of Spectral Peaks

3.2.2.1 Identification of Multi-modal Spectra

Criteria that have been used in the literature to identify the spectra as uni-modal or multi-modal by considering the frequency spectra alone were discussed in Chapter 2. These criteria were applied to the available data. A detailed visual observation was carried out in order to set the required conditions that would be utilized in this study to identify the spectral peaks. The effect of each condition in identifying the spectral peaks was observed.

Finally, three conditions were determined to impose in order to identify the peaks for belonging to separate wave systems:

- 1) Minimum distance between frequencies of the peaks should be 0.03 Hz. This value is determined as the best one after several trials from 0.02 Hz. to 0.05 Hz. and comparisons with visual inspections.
- 2) For the other maxima to be considered as a spectral peak, they must have ordinates larger or equal to 15% of the largest one. The value of 15% was chosen considering the recommendation of Guedes Soares and Nolasco (1992). After a few trials and comparisons with visual inspections, this criterion was found to be a reasonable one. This requirement eliminates peaks that are below a background noise.
- 3) The ordinate of the trough between the two peaks must be lower than the lower limit of the 90-percent confidence interval of the smaller of the two peaks.

A computer program was prepared in Visual FORTRAN programming language considering the above conditions adopted to classify the files as having single peak, two peaks, three peaks or more peaks. Tables 3.2 to 3.4 give the results of this program for Sinop, Hopa and Gelendzhik, respectively.

One observes from these tables the decreasing percentage of occurrence of the multi-peaked spectra with increasing significant wave height. At Sinop and Gelendzhik, the percentage of occurrence of the double-peaked spectra decreases from about 30% in the lowest wave group to about 15% for the waves with significant wave height greater than 2.0 meters. Similarly, it decreases from 26% to 6% at Hopa.

Table 3.2 Occurrence of spectral peaks at Sinop (all data)

| Hs (m) | 1 peak | 2 peaks | 3 peaks | 4 or more | num. obs. | % obs. |
|----------------------|-----------------|-----------------|-----------------|---------------|-----------|--------|
| $H_s \geq 3.0$ | 37 (86.05%) | 6 (13.95%) | - | - | 43 | 1.76 |
| $3.0 > H_s \geq 2.0$ | 160 (82.47%) | 32 (16.49%) | 2 (1.03%) | - | 194 | 7.92 |
| $2.0 > H_s \geq 1.0$ | 570 (63.90%) | 265 (29.71%) | 50 (5.61%) | 7 (0.78%) | 892 | 36.41 |
| $1.0 > H_s \geq 0.5$ | 665 (50.34%) | 408 (30.89%) | 193 (14.61%) | 55 (4.16%) | 1321 | 53.92 |
| num.obs. | 1432 | 711 | 245 | 62 | 2450 | |
| % obs. | 58.45 | 29.02 | 10.00 | 2.53 | | 100 |

Table 3.3 Occurrence of spectral peaks at Hopa (all data)

| Hs (m) | 1 peak | 2 peaks | 3 peaks | 4 or more | num. obs. | % obs. |
|----------------------|------------------|-----------------|----------------|---------------|-----------|--------|
| $H_s \geq 3.0$ | 92 (98.92%) | 1 (1.08%) | - | - | 93 | 1.68 |
| $3.0 > H_s \geq 2.0$ | 467 (93.21%) | 34 (6.79%) | - | - | 501 | 9.05 |
| $2.0 > H_s \geq 1.0$ | 1557 (83.80%) | 259 (13.94%) | 39 (2.10%) | 3 (0.16%) | 1858 | 33.55 |
| $1.0 > H_s \geq 0.5$ | 2012 (65.20%) | 811 (26.28%) | 209 (6.77%) | 54 (1.75%) | 3086 | 55.72 |
| num.obs. | 4128 | 1105 | 248 | 57 | 5538 | |
| % obs. | 74.54 | 19.95 | 4.48 | 1.03 | | 100 |

Table 3.4 Occurrence of spectral peaks at Gelendzhik (all data)

| Hs (m) | 1 peak | 2 peaks | 3 peaks | 4 or more | num. obs. | % obs. |
|----------------------|------------------|------------------|-----------------|----------------|-----------|--------|
| $H_s \geq 3.0$ | 322 (96.99%) | 10 (3.01%) | - | - | 332 | 4.00 |
| $3.0 > H_s \geq 2.0$ | 1106 (82.54%) | 216 (16.12%) | 18 (1.34%) | - | 1340 | 16.18 |
| $2.0 > H_s \geq 1.0$ | 2344 (69.60%) | 818 (24.29%) | 179 (5.31%) | 27 (0.80%) | 3368 | 40.66 |
| $1.0 > H_s \geq 0.5$ | 1408 (43.40%) | 1078 (33.23%) | 543 (16.74%) | 215 (6.63%) | 3244 | 39.16 |
| num.obs. | 5180 | 2122 | 740 | 242 | 8284 | |
| % obs. | 62.53 | 25.62 | 8.93 | 2.92 | | 100 |

Percentage of occurrence of the double-peaked spectra for the whole data is computed as 29%, 20% and 25% at Sinop, Hopa and Gelendzhik, respectively.

The last group of waves with significant wave heights less than 1.0 m and greater than 0.5 m is in fact a range that is not too important for engineering applications that require spectral information. Besides, as it is seen from the tables, this range is more variable than the others. At all three stations, percent occurrences of spectra with 3 or more peaks are rather high for this group of waves (19%, 9% and 23% at Sinop, Hopa and Gelendzhik respectively). Therefore, results of the analysis are given in two ways in this study. One is the average of whole data including these small waves and the other is the average obtained with discarding these waves. Thus, overall percentages for the occurrence of multi-peaked spectra for the data with significant wave heights greater and equal to 1.0 m were also computed as

given in Table 3.5. It is seen that when the sea state of small waves was excluded, overall percentages for the occurrence of the double-peaked spectra decrease from 29%, 20% and 25% to 26%, 12% and 20% at Sinop, Hopa and Gelendzhik, respectively.

Another clear result from analysis is that for all sea states and for the overall data, the occurrence of the multi-peaked spectra is higher at Sinop and Gelendzhik compared to Hopa. Actually, when the wind and wave regime of the Black Sea basin is considered, this is an expected result. The annual wind and wave roses of Sinop, Hopa and Gelendzhik obtained from the Wind and Deep Water Wave Atlas (2002), prepared as a product of NATO TU-WAVES Project, are given in Figures 3.2, 3.3 and 3.4. As it is seen in these figures, while Hopa has one clear dominant wave direction which is WNW, at Sinop there are three directions, WNW, NNE and W, which have almost equal probabilities as annual wave direction. Also at Gelendzhik, a similar variability in the wave direction is observed. While WSW is the dominant wave direction, SSE direction is also important at Gelendzhik.

Table 3.5 Comparison of the three stations in case of peak numbers for the overall measurements with H_s greater than or equal to 1.0 m.

| | tot. num. obs. | 1 peak num. obs. (%) | 2 peaks num. obs. (%) | 3 peaks num. obs. (%) | 4 or more num. obs. (%) |
|------------|----------------|----------------------|-----------------------|-----------------------|-------------------------|
| Sinop | 1129 | 767 (68.0) | 303 (26.8) | 52 (4.6) | 7 (0.6) |
| Hopa | 2452 | 2116 (86.3) | 294 (12.0) | 39 (1.6) | 3 (0.1) |
| Gelendzhik | 5040 | 3772 (74.8) | 1044 (20.7) | 197 (3.9) | 27 (0.5) |

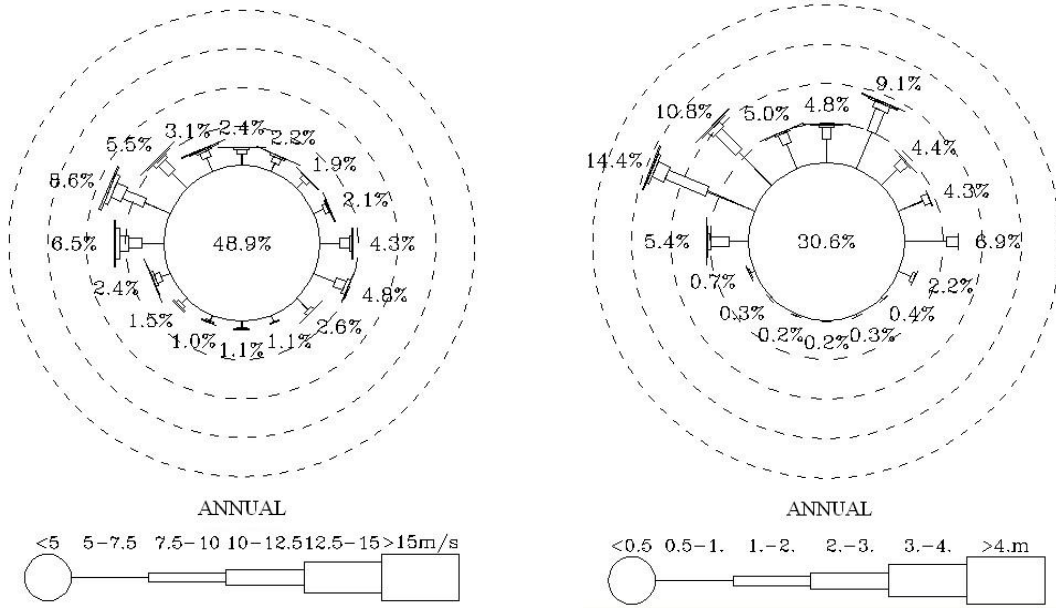


Figure 3.2 Annual wind and wave roses at Sinop.

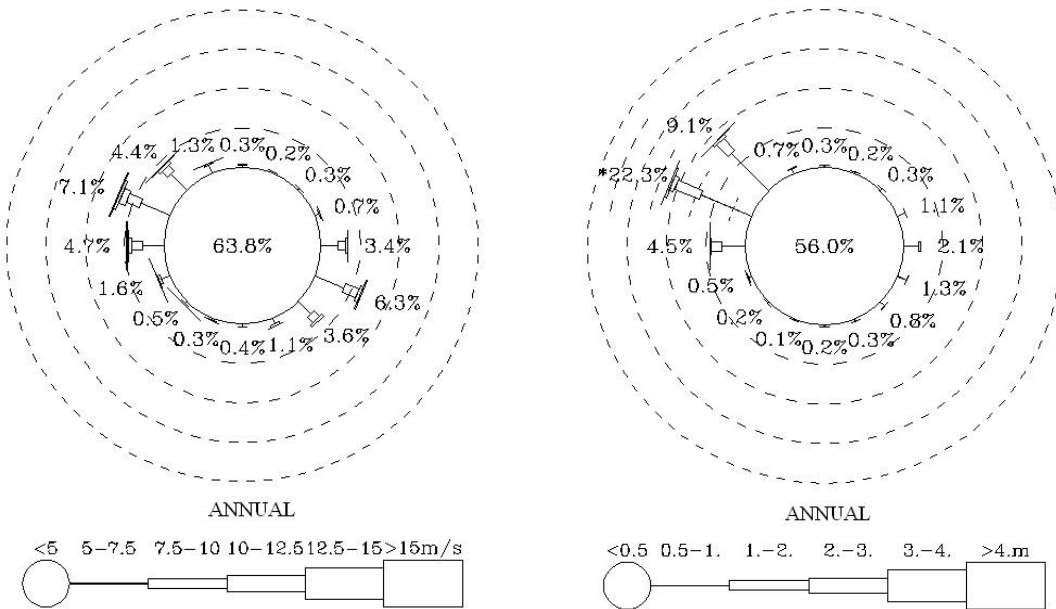


Figure 3.3 Annual wind and wave roses at Hopa.

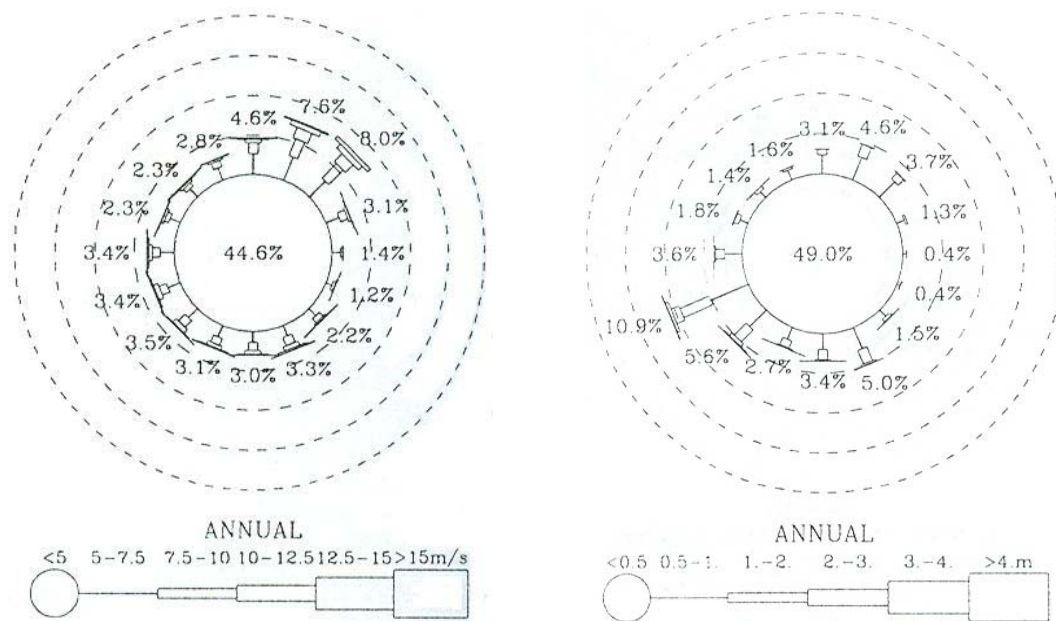


Figure 3.4 Annual wind and wave roses at Gelendzhik.

In order to investigate the seasonal variability of the multi-peaked spectra occurrences, the identification analysis were classified for each seasons. Tables 3.6 to 3.11 give the seasonal probabilities of spectra with different number of peaks for all data for records with significant wave height greater and equal to 1.0 m at Sinop, Hopa and Gelendzhik, respectively.

It is observed that there is no clear variability among the seasons in case of occurrence of multi-peaked spectra at all three stations. The percentages in all seasons are quite consistent with the annual probabilities at each location.

Table 3.6 Seasonal probability of occurrence of multi-peaked spectra for overall data with significant wave height greater and equal to 0.5 m at Sinop.

| Hs ≥ 0.5 m. | tot. num. obs. | 1 peak num. obs. (%) | 2 peaks num. obs. (%) | 3 peaks num. obs. (%) | 4 or more num. obs. (%) |
|--------------------|----------------|----------------------|-----------------------|-----------------------|-------------------------|
| Winter | 1125 | 690 (61.3) | 310 (27.6) | 96 (8.5) | 29 (2.6) |
| Spring | 974 | 510 (52.4) | 312 (32.0) | 121 (12.4) | 31 (3.2) |
| Summer | 130 | 81 (62.3) | 33 (25.4) | 14 (10.8) | 2 (1.5) |
| Autumn | 221 | 151 (68.3) | 56 (25.3) | 14 (6.3) | - |

Table 3.7 Seasonal probability of occurrence of multi-peaked spectra for overall data with significant wave height greater and equal to 1.0 m at Sinop.

| Hs ≥ 1.0 m. | tot. num. obs. | 1 peak num. obs. (%) | 2 peaks num. obs. (%) | 3 peaks num. obs. (%) | 4 or more num. obs. (%) |
|--------------------|----------------|----------------------|-----------------------|-----------------------|-------------------------|
| Winter | 515 | 342 (66.4) | 147 (28.5%) | 23 (4.5%) | 3 (0.6%) |
| Spring | 373 | 254 (68.1) | 98 (26.3%) | 17 (4.6%) | 4 (1.1%) |
| Summer | 76 | 54 (71.1%) | 17 (22.4%) | 5 (6.6%) | - |
| Autumn | 165 | 117 (70.9%) | 41 (24.9%) | 7 (4.2%) | - |

Table 3.8 Seasonal probability of occurrence of multi-peaked spectra for overall data with significant wave height greater and equal to 0.5 m at Hopa.

| H_s ≥ 0.5 m. | tot. num. obs. | 1 peak num. obs. (%) | 2 peaks num. obs. (%) | 3 peaks num. obs. (%) | 4 or more num. obs. (%) |
|-------------------------------|----------------|----------------------|-----------------------|-----------------------|-------------------------|
| Winter | 1590 | 1152 (72.5%) | 330 (20.8%) | 88 (5.5%) | 20 (1.3%) |
| Spring | 1276 | 922 (72.3%) | 290 (22.7%) | 51 (4.0%) | 13 (1.0%) |
| Summer | 1261 | 948 (75.2%) | 246 (19.5%) | 50 (4.0%) | 17 (1.3%) |
| Autumn | 1411 | 1106 (78.4%) | 239 (16.9%) | 59 (4.2%) | 7 (0.5%) |

Table 3.9 Seasonal probability of occurrence of multi-peaked spectra for overall data with significant wave height greater and equal to 1.0 m at Hopa.

| H_s ≥ 1.0 m. | tot. num. obs. | 1 peak num. obs. (%) | 2 peaks num. obs. (%) | 3 peaks num. obs. (%) | 4 or more num. obs. (%) |
|-------------------------------|----------------|----------------------|-----------------------|-----------------------|-------------------------|
| Winter | 813 | 717 (88.2%) | 87 (10.7%) | 8 (1.0%) | 1 (0.1%) |
| Spring | 494 | 413 (83.6%) | 70 (14.2%) | 10 (2.0%) | 1 (0.2%) |
| Summer | 376 | 327 (87.0%) | 43 (11.4%) | 5 (1.3%) | 1 (0.3%) |
| Autumn | 769 | 659 (85.7%) | 94 (12.2%) | 16 (2.1%) | - |

Table 3.10 Seasonal probability of occurrence of multi-peaked spectra for overall data with significant wave height greater and equal to 0.5 m at Gelendzhik.

| H_s ≥ 0.5 m. | tot. num. obs. | 1 peak num. obs. (%) | 2 peaks num. obs. (%) | 3 peaks num. obs. (%) | 4 or more num. obs. (%) |
|-------------------------------|----------------|----------------------|-----------------------|-----------------------|-------------------------|
| Winter | 2997 | 1921 (64.1%) | 755 (25.2%) | 237 (7.9%) | 84 (2.8%) |
| Spring | 1302 | 831 (63.8%) | 337 (25.9%) | 107 (8.2%) | 27 (2.1%) |
| Summer | 1544 | 852 (55.2%) | 465 (30.1%) | 173 (11.2%) | 54 (3.5%) |
| Autumn | 2441 | 1576 (64.6%) | 565 (23.1%) | 223 (9.1%) | 77 (3.2%) |

Table 3.11 Seasonal probability of occurrence of multi-peaked spectra for overall data with significant wave height greater and equal to 1.0 m at Gelendzhik.

| H_s ≥ 1.0 m. | tot. num. obs. | 1 peak num. obs. (%) | 2 peaks num. obs. (%) | 3 peaks num. obs. (%) | 4 or more num. obs. (%) |
|-------------------------------|----------------|----------------------|-----------------------|-----------------------|-------------------------|
| Winter | 2162 | 1593 (73.7%) | 472 (21.8%) | 84 (3.9%) | 13 (0.6%) |
| Spring | 816 | 623 (76.4%) | 167 (20.5%) | 22 (2.7%) | 4 (0.5%) |
| Summer | 579 | 417 (72.0%) | 131 (22.6%) | 26 (4.5%) | 5 (0.9%) |
| Autumn | 1483 | 1139 (76.8%) | 274 (18.5%) | 65 (4.4%) | 5 (0.3%) |

3.3 Fitting JONSWAP Spectrum to Single Peak Spectra

A number of methods used in the literature in fitting JONSWAP spectrum to observed spectra were described in Chapter 2. The methods used by Acar (1983), Moon and Oh (1998) and Violante-Carvalho et al. (2002) were compared in detail to determine the method that would be used in this study. In addition to these three methods, a modified version of Acar's method was formulated. In this modified form, α parameter is computed from the least square fit in the range of $1.35f_p$ and $2.0f_p$. In this range, peak enhancement factor γ is accepted as unity. These four methods were applied to estimate the spectrum parameters for the data which were identified as single-peaked after the analysis explained in the previous section.

In order to assess how well the fitting is, the scatter index, SI is defined as given below:

$$SI = \sqrt{\frac{\sum_{i=1}^N (S(f_i) - S_J(f_i))^2}{\sum_{i=1}^N S(f_i)^2}} \quad (3.1)$$

where $S(f_i)$ denotes observed spectra, and $S_J(f_i)$ denotes the JONSWAP model spectrum.

Mean values of the JONSWAP spectrum parameters calculated for each sea state by using four methods for fitting the spectra measured at Sinop are given in Table 3.12. Average SI values are also given as a measure for the level of fitting for each method. For indicating the variability of estimated parameters, standard deviations are also computed and given in the table.

Table 3.12 JONSWAP Spectrum parameters determined by using four methods at each sea state for the measurements at Sinop.

| | Alpha, α | | Gamma, γ | | Peak frequency, f_p (Hz) | | Scatter Index, SI | | |
|--------------------------|-----------------|------------|-----------------|------------|----------------------------|------------|-------------------|------------|--------|
| | mean | stand.dev. | mean | stand.dev. | mean | stand.dev. | mean | stand.dev. | |
| 0.5 m $\leq H_s < 1.0$ m | MOON | 0.00348 | 0.00345 | 2.79 | 1.36 | 0.194 | 0.038 | 0.0220 | 0.0252 |
| | CARVALHO | 0.00346 | 0.00338 | 2.68 | 1.66 | 0.194 | 0.038 | 0.0217 | 0.0280 |
| | ACAR | 0.00333 | 0.00295 | 2.54 | 1.13 | 0.193 | 0.037 | 0.0141 | 0.0152 |
| | ACAR-mod. | 0.00353 | 0.00329 | 2.50 | 1.12 | 0.194 | 0.037 | 0.0145 | 0.0152 |
| 1.0 m $\leq H_s < 2.0$ m | MOON | 0.00512 | 0.00298 | 2.37 | 1.07 | 0.161 | 0.028 | 0.0256 | 0.0326 |
| | CARVALHO | 0.00516 | 0.00296 | 2.27 | 1.23 | 0.161 | 0.028 | 0.0245 | 0.0319 |
| | ACAR | 0.00499 | 0.00296 | 2.36 | 1.02 | 0.161 | 0.025 | 0.0158 | 0.0196 |
| | ACAR-mod. | 0.00522 | 0.00296 | 2.30 | 0.97 | 0.161 | 0.026 | 0.0169 | 0.0227 |
| 2.0 m $\leq H_s < 3.0$ m | MOON | 0.00643 | 0.00267 | 1.97 | 0.71 | 0.126 | 0.015 | 0.0489 | 0.0412 |
| | CARVALHO | 0.00671 | 0.00303 | 1.80 | 0.81 | 0.126 | 0.015 | 0.0476 | 0.0391 |
| | ACAR | 0.00599 | 0.00322 | 2.34 | 0.90 | 0.127 | 0.013 | 0.0299 | 0.0258 |
| | ACAR-mod. | 0.00666 | 0.00315 | 2.13 | 0.83 | 0.127 | 0.013 | 0.0320 | 0.0277 |
| 3.0 m $\leq H_s$ | MOON | 0.00816 | 0.00234 | 2.51 | 0.83 | 0.118 | 0.011 | 0.0874 | 0.0535 |
| | CARVALHO | 0.00863 | 0.00269 | 2.34 | 0.99 | 0.118 | 0.011 | 0.0844 | 0.0505 |
| | ACAR | 0.00821 | 0.00309 | 2.87 | 1.04 | 0.119 | 0.009 | 0.0549 | 0.0332 |
| | ACAR-mod. | 0.00884 | 0.00298 | 2.67 | 0.89 | 0.120 | 0.009 | 0.0585 | 0.0380 |

It is observed that the method of Acar (1983) gives the least Scatter Index values among four methods for all sea states. Acar's modified method in the case of α computation, also have smaller SI values compared to the methods of Moon and Oh (1998) and Violante-Carvalho et al. (2002).

As a common initial step, Moon and Oh (1998) and Violante-Carvalho et al. (2002) accept the frequency corresponding to the maximum spectral density of the measured spectrum as the peak frequency of the model spectrum. They use this frequency to compute the other parameters α and γ . Acar (1983) also begins with the frequency of the maximum spectral density. However, he changes this initial value by small increments as he does for the other parameters, α and γ to obtain the set of data giving the least square error between the measured and modeled spectra. Therefore, the peak frequency of the model spectrum is found as the result of this iterative solution.

It is clear that accepting the frequency of the maximum spectral density as the peak frequency of the model spectrum decreases the quality of fitting especially whenever there is another high spectral density at the frequency next to the peak frequency. Figure 3.5 shows such a case. It is seen that the fitting is better for the method of Acar (1983), compared to the methods of Moon and Oh (1998) and Violante-Carvalho et al. (2002).

Considering the smaller SI values, it was decided to use the modified Acar's method in determining the parameters of the JONSWAP spectrum. Thus, JONSWAP parameters were estimated at three stations by using the FORTRAN program written for this purpose. It is well known that when γ equals to unity, JONSWAP spectrum reduces to PM spectrum. Therefore,

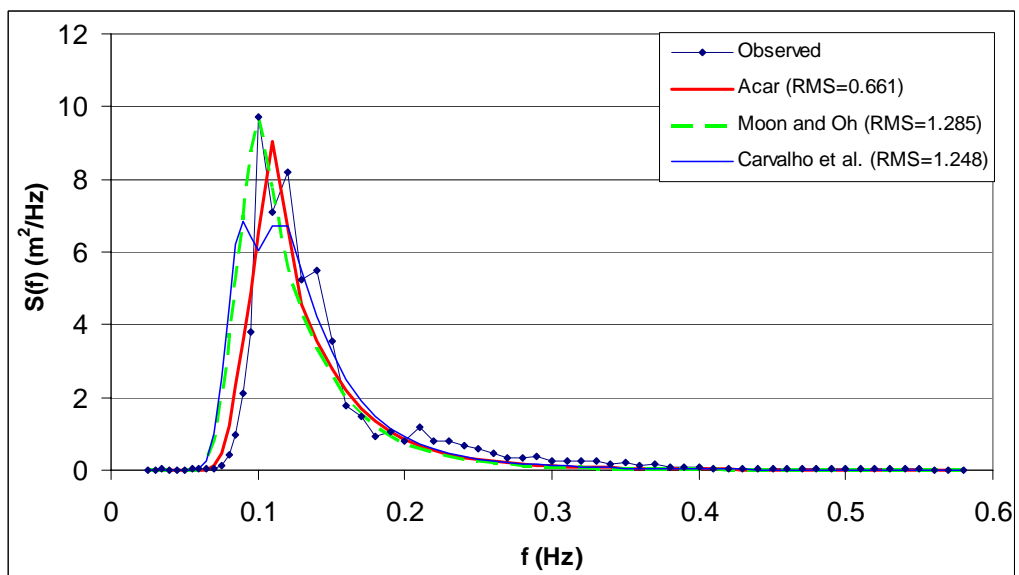
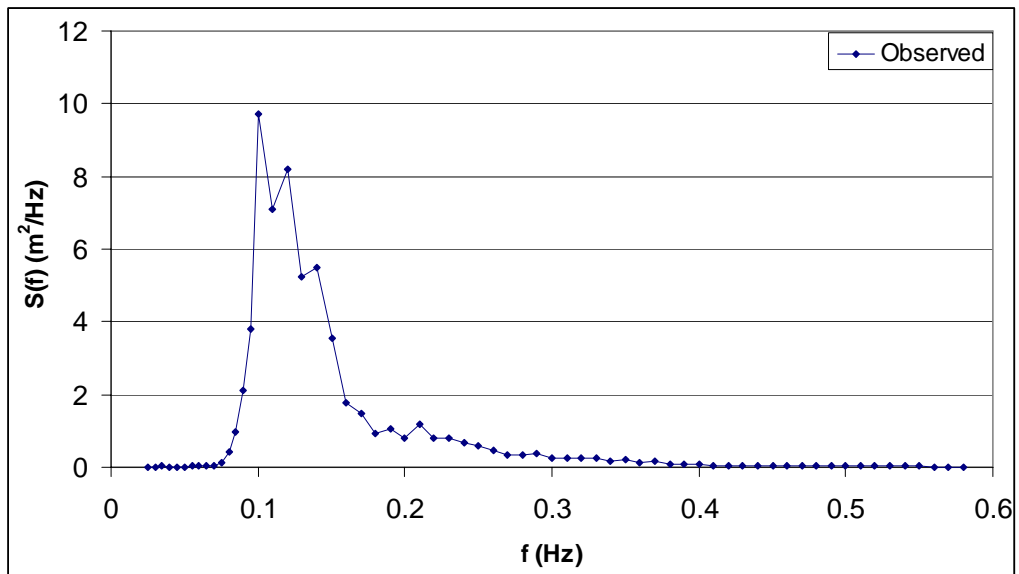


Figure 3.5 An example of observed and fitted spectrum (11141928.SPT, Sinop at 1994)

measurements for which γ parameter was estimated less than 1.5 were separated from the data set for belonging to the fully arisen sea records. The remaining data sets were considered as developing sea records. 235 out of 1432, 372 out of 4128 and 828 out of 5180 measurements were separated at Sinop, Hopa and Gelendzhik respectively. The parameters of PM spectrum were found for these records.

The mean values and standard deviations for the JONSWAP parameters, α , γ and f_p of the spectra identified as developing sea (having a γ value equal to or greater than 1.5) were computed for different sea states. Tables 3.13 to 3.15 provide these results for three stations.

As it is seen from the tables, mean α value decreases with decreasing significant wave height at all three stations. In case of γ values, however, the dependence on the sea state is less sensitive. The peak frequency increases with decreasing significant wave height.

It is also observed from the tables that among the three stations, Hopa has the smallest mean α values for each sea state as well as for the overall data. On the contrary, γ values are the highest for Hopa records. Both parameters, α and γ have higher values at Gelendzhik than at Sinop, except the α values for the highest sea state. In the case of peak frequency, Hopa records give lower values than those of Sinop and Gelendzhik for all sea states.

At all three stations, the mean γ values are smaller than the value of 3.3 which was obtained from the original JONSWAP data belonging to the North Sea.

Table 3.13 Parameters of JONSWAP spectrum obtained from the modified fitting method of Acar at Sinop.

| SINOP | | α | γ | f_p (Hz) | SI |
|----------------------------|------------|----------------|-------------|--------------|---------------|
| $H_s \geq 3.0$ m. | Mean | 0.00884 | 2.74 | 0.120 | 0.0597 |
| | Stand.Dev. | 0.00304 | 0.85 | 0.009 | 0.0388 |
| 3.0 m. > $H_s \geq 2.0$ m. | Mean | 0.00622 | 2.34 | 0.127 | 0.0316 |
| | Stand.Dev. | 0.00310 | 0.75 | 0.014 | 0.0270 |
| 2.0 m. > $H_s \geq 1.0$ m. | Mean | 0.00507 | 2.57 | 0.162 | 0.0148 |
| | Stand.Dev. | 0.00301 | 0.87 | 0.027 | 0.0151 |
| 1.0 m. > $H_s \geq 0.5$ m. | Mean | 0.00347 | 2.75 | 0.194 | 0.0136 |
| | Stand.Dev. | 0.00331 | 1.02 | 0.037 | 0.0118 |
| ALL $H_s \geq 0.5$ m. | Mean | 0.00455 | 2.63 | 0.172 | 0.0174 |
| | Stand.Dev. | 0.00340 | 0.94 | 0.039 | 0.0191 |
| ALL $H_s \geq 1.0$ m. | Mean | 0.00552 | 2.53 | 0.153 | 0.0208 |
| | Stand.Dev. | 0.00317 | 0.85 | 0.029 | 0.0232 |

Table 3.14 Parameters of JONSWAP spectrum obtained from the modified fitting method of Acar at Hopa.

| HOPA | | α | γ | f_p (Hz) | SI |
|----------------------------|------------|----------------|-------------|--------------|---------------|
| $H_s \geq 3.0$ m. | Mean | 0.00511 | 2.97 | 0.102 | 0.0438 |
| | Stand.Dev. | 0.00182 | 1.07 | 0.010 | 0.0507 |
| 3.0 m. > $H_s \geq 2.0$ m. | Mean | 0.00443 | 2.96 | 0.119 | 0.0174 |
| | Stand.Dev. | 0.00226 | 1.16 | 0.015 | 0.0189 |
| 2.0 m. > $H_s \geq 1.0$ m. | Mean | 0.00319 | 3.01 | 0.140 | 0.0089 |
| | Stand.Dev. | 0.00216 | 1.14 | 0.022 | 0.0115 |
| 1.0 m. > $H_s \geq 0.5$ m. | Mean | 0.00226 | 3.18 | 0.177 | 0.0081 |
| | Stand.Dev. | 0.00297 | 1.39 | 0.044 | 0.0103 |
| ALL $H_s \geq 0.5$ m. | Mean | 0.00292 | 3.09 | 0.155 | 0.0103 |
| | Stand.Dev. | 0.00270 | 1.28 | 0.041 | 0.0153 |
| ALL $H_s \geq 1.0$ m. | Mean | 0.00355 | 3.00 | 0.134 | 0.0123 |
| | Stand.Dev. | 0.00225 | 1.14 | 0.023 | 0.0187 |

Table 3.15 Parameters of JONSWAP spectrum obtained from the modified fitting method of Acar at Gelendzhik.

| GELENDZHIK | | α | γ | f_p (Hz) | SI |
|---------------------------|------------|----------------|-------------|--------------|---------------|
| $H_s \geq 3.0$ m. | Mean | 0.00730 | 3.06 | 0.110 | 0.0238 |
| | Stand.Dev. | 0.00340 | 1.20 | 0.016 | 0.0284 |
| 3.0 m. $>H_s \geq 2.0$ m. | Mean | 0.00707 | 2.80 | 0.133 | 0.0122 |
| | Stand.Dev. | 0.00351 | 1.13 | 0.019 | 0.0157 |
| 2.0 m. $>H_s \geq 1.0$ m. | Mean | 0.00589 | 2.73 | 0.157 | 0.0078 |
| | Stand.Dev. | 0.00399 | 1.03 | 0.029 | 0.0099 |
| 1.0 m. $>H_s \geq 0.5$ m. | Mean | 0.00553 | 2.99 | 0.217 | 0.0100 |
| | Stand.Dev. | 0.00554 | 1.24 | 0.066 | 0.0137 |
| ALL $H_s \geq 0.5$ m. | Mean | 0.00613 | 2.84 | 0.166 | 0.0104 |
| | Stand.Dev. | 0.00440 | 1.13 | 0.053 | 0.0147 |
| ALL $H_s \geq 1.0$ m. | Mean | 0.00636 | 2.78 | 0.146 | 0.0105 |
| | Stand.Dev. | 0.00385 | 1.08 | 0.030 | 0.0150 |

The standard deviations are observed to be quite high except for the peak frequency. Especially, the standard deviation of α is very high. This result indicates the high variability of the α parameter. As it was mentioned in Chapter 2, α was found to be dependent on fetch distance and wind speed during JONSWAP project and also at later studies. JONSWAP spectrum and the later modifications provided relationships of α with fetch distance and wind speed, or sometimes with wave age. Therefore, this high variability with α is rather natural.

The wave records separated as belonging to fully developed waves were analyzed and the PM spectrum was fitted to the observed spectra. Two parameters, α and f_p were estimated on the basis of the least square error between the model spectrum and the measurements. Similar to the

procedure used earlier for JONSWAP spectrum, α values were determined as to give the least square difference in the frequency range between $1.35f_p$ and $2.0 f_p$. Mean and standard deviation of the parameters of PM spectrum for three locations are given in Table 3.16. Similar to the results obtained for the JONSWAP spectrum, the α parameter obtained from the Hopa records is the lowest among three locations. Standard deviation of α is again high. At all stations, α is less than 0.0081 which is the mean value proposed for PM spectrum.

Table 3.16 Parameters of PM spectrum

| PM Spectrum | | α | | f_p (Hz) | | SI | |
|------------------|------------|----------|------------|------------|------------|--------|------------|
| | | mean | stand.dev. | mean | stand.dev. | mean | stand.dev. |
| $H_s \geq 0.5$ m | SINOP | 0.00532 | 0.00338 | 0.170 | 0.039 | 0.0370 | 0.0631 |
| | HOPA | 0.00337 | 0.00232 | 0.152 | 0.033 | 0.0277 | 0.0626 |
| | GELENDZHIK | 0.00651 | 0.00357 | 0.154 | 0.035 | 0.0215 | 0.0456 |
| $H_s \geq 1.0$ m | SINOP | 0.00647 | 0.00299 | 0.149 | 0.024 | 0.0539 | 0.0727 |
| | HOPA | 0.00420 | 0.00212 | 0.131 | 0.020 | 0.0473 | 0.0774 |
| | GELENDZHIK | 0.00725 | 0.00325 | 0.144 | 0.025 | 0.0271 | 0.0507 |

3.4 Fetch Dependencies of the JONSWAP Spectrum Parameters at Sinop, Hopa and Gelendzhik

It was presented in Chapter 2 that fetch dependencies of spectral parameters have been studied since 1960s by a number of researchers in various parts of the world. For the present study, in order to examine the probable fetch dependencies of the JONSWAP spectrum parameters at three stations, modified (enhanced) ECMWF analysis wind fields obtained from NATO TU-WAVES Project were utilized. The data are available with 6 hours time interval for a period of 8 years between 01 September 1991 and 31 July 1999, and with a spatial resolution of 0.3° in longitudinal direction and 0.25° in latitudinal direction covering whole Black Sea basin (608 points).

A mesh consistent with this spatial resolution of ECMWF wind fields was prepared for the analysis. Due to shape of the earth, while the distance between two longitudes at the northmost latitude of the mesh is 22.86 km, it is 25.18 km at the southmost one. In order to cope with this variability the average value of 24.02 km was used as a constant distance between longitudes. Distance between the latitudes is constant all over the mesh and equals to 27.8 km. Thus, scaled in accordance with these distances, the mesh for the Black Sea basin was formed to be used in determining the corresponding wind and fetch information for the wave records.

The nearest grid points to the buoy locations are $42.00^\circ\text{N}-35.00^\circ\text{E}$, $41.50^\circ\text{N}-41.00^\circ\text{E}$ and $44.50^\circ\text{N}-37.70^\circ\text{E}$ at Sinop, Hopa and Gelendzhik respectively. Grid points at these coordinates were marked as the buoy locations on the mesh. Lines with intervals of 22.5° were drawn from each location to represent the wind directions within $\pm 11.25^\circ$ of alignment of each line. Grid points on these lines were utilized in order to determine the wind speed,

storm direction and the fetch length. One and two grid points at right and left, and at up and down around each station were also marked on the mesh. Wind information of these grid points were averaged to decide on the wind speed and the direction for the considered location as the first step of analysis. Figures C1, C2 and C3 of Appendix C show the prepared mesh and three measurement locations with the lines representing the directions and with the areas around them.

In order to study the fetch dependencies of spectral parameters, following criteria were tested and applied to select the records belonging to stable wind conditions:

- Average wind speed at the grid points at the area around each station should be greater than or equal to 5 m/s. This ensures the existence of large-scale atmospheric circulation systems and thus homogeneity of wind field over the region.
- Whenever the difference between wave and wind directions is greater than 45° , that measurement is to be discarded.
- To ensure stationarity of wind, a rather rigid criteria were applied. Only the records with stable winds along the fetch length in the limits of $\pm 10\%$ of wind speed and $\pm 11.25^\circ$ (This was decided after comparing with $\pm 22.5^\circ$) of wind direction were selected.
- A minimum fetch of 100 km was required for any directions. (Although ECMWF analysis wind fields utilized in this study was enhanced to overcome the two basic problems of ECMWF analysis wind fields (the treatment of the land-boundary in the ECMWF meteorological model and the underestimation by the ECMWF wind speeds over enclosed basins), this criterion was set considering that the land-boundary might still not be entirely correct.)

According to these criteria, in order to analyze the dataset that was isolated from multi peaked and fully developed sea spectra in the previous sections, a FORTRAN program was prepared. The program reads the date of the record from a list and searches for the time series of ECMWF analysis winds to determine the wind speed and direction corresponding to that date at the grid points around the considered station. Then, the program computes the average wind speed and wind direction at these grids. If the average wind speed is less than 5 m/s, that record is directly discarded and the program returns to the beginning to investigate the wind condition of the next measurement in the list. When the average wind speed computed is greater than or equal to 5 m/s, the program continues with checking the difference between the average wind direction and the measured wave direction. If the difference is more than 45° , that record is also discarded and the analysis continues with the next record. If both criteria are satisfied (e.g. wind speed is greater than or equal to 5 m/s and the directional difference between wind and wave is less than 45°), the program continues with the analysis of wind to determine the wind speed and fetch of the corresponding storm.

In the next step, the grid points along the line which is representing the determined wind direction are investigated one by one. Beginning from the nearest grid to the station area, firstly wind direction is checked. If the wind direction at that grid is still inside the limits of the direction range, then averages of the wind speed and wind direction of all previous grid points on the line are recomputed.

Then, the following two conditions are checked for either continuing with the analysis by including the next grid point on the line or ending the analysis of that record by setting the average wind speed and wind direction computed for the previous grid point as the finalized wind speed and wind

direction and the distance between the station and the grid point as the finalized fetch length for the analyzed record:

- If the average wind speed is greater than or equal to 5 m/s,
- If the wind speed change along the line is within 10 %,

By applying these steps, the dataset is further refined to include only the spectra belonging to the wind waves generated by relatively stable wind speed and direction. Undoubtedly, this procedure excluded the single peak swell as well.

In this analysis, two questionable points arise from comparison of results with those of previous studies. In order to decide on which directional interval (22.5° or 45°) and which area around the station (one or two grid points) to use, the program were run for all four alternatives. Then, the regression lines of each relationship obtained from these four alternatives were drawn together with the upper and lower envelop of previous results (Figures 3.6 to 3.14). The relationships of Sinop records are given in Figures 3.6 to 3.8, of Hopa in Figures 3.9 to 3.11 and of Gelendzhik in Figures 3.12 to 3.14.

In these figures, the results obtained for the larger area (two grid points) around the stations were denoted by capital letter 'A'. For the relationship between \tilde{E} and \tilde{X} , the results of Kahma (1981) and theoretical study of Zakharov and Zaslavskii in 1983 (Shokurov and Efimov, 1999) were excluded, and results by Evans and Kibblewhite (1990) and Shokurov and Efimov (1999) were given as the lower and upper limits of previous studies. While for \tilde{f}_m and \tilde{X} relationship JONSWAP (1973) and Donelan et al. (1985) results formed the envelop, the results of Evans and Kibblewhite (1990) and Shokurov and Efimov (1999) were the envelops for the \tilde{E} and \tilde{f}_m relationship similar to the relationship between \tilde{E} and \tilde{X} .

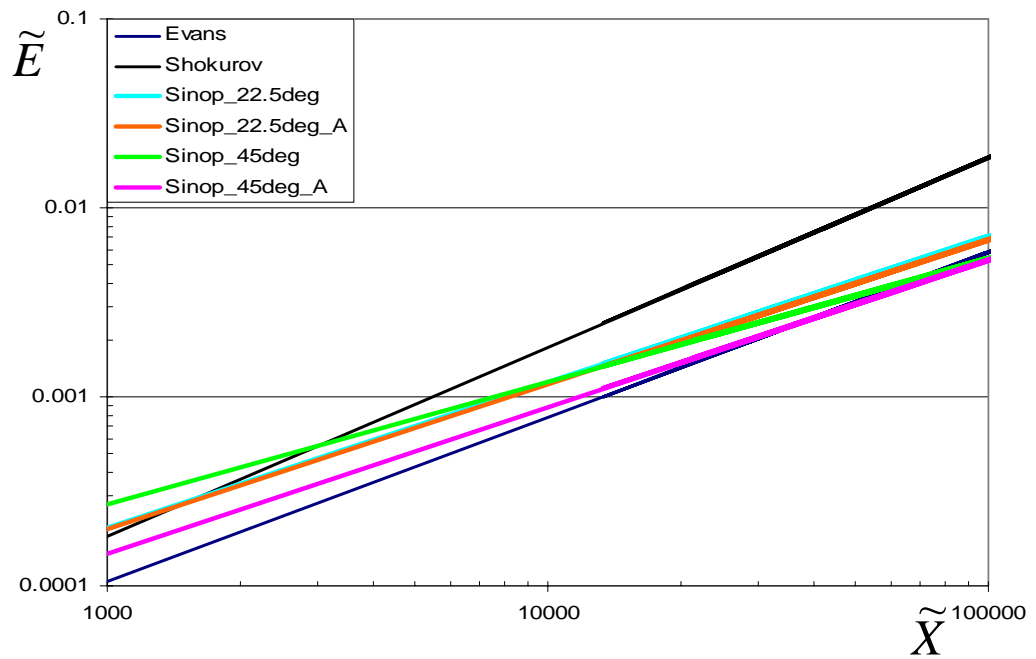


Figure 3.6 Relations between the dimensionless fetch and energy obtained for four alternatives at Sinop.

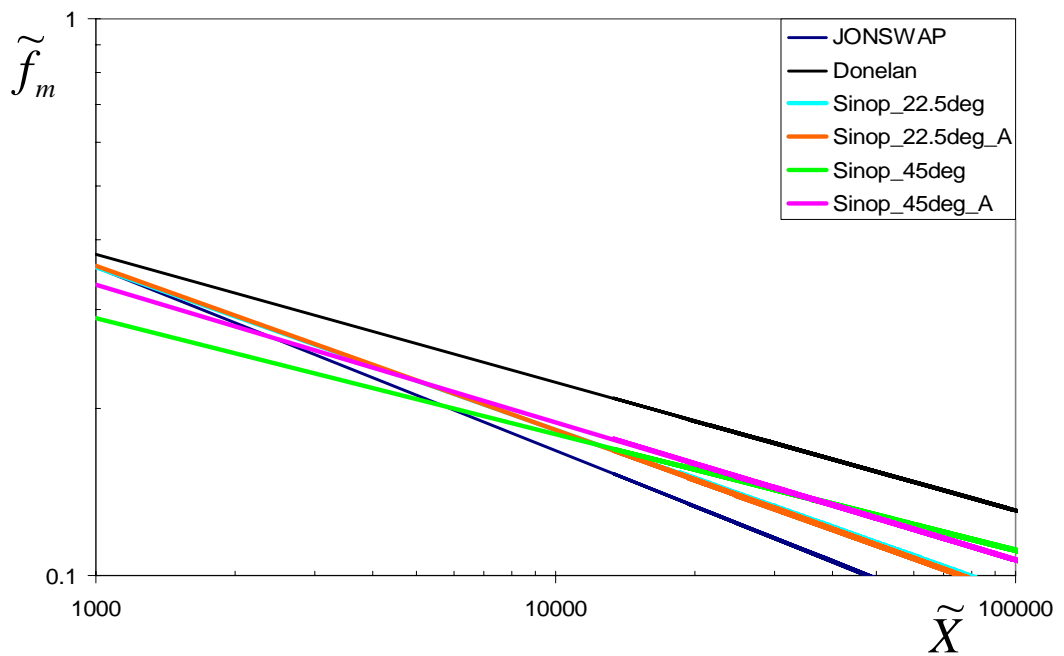


Figure 3.7 Relations between the dimensionless fetch and peak frequency obtained for four alternatives at Sinop.

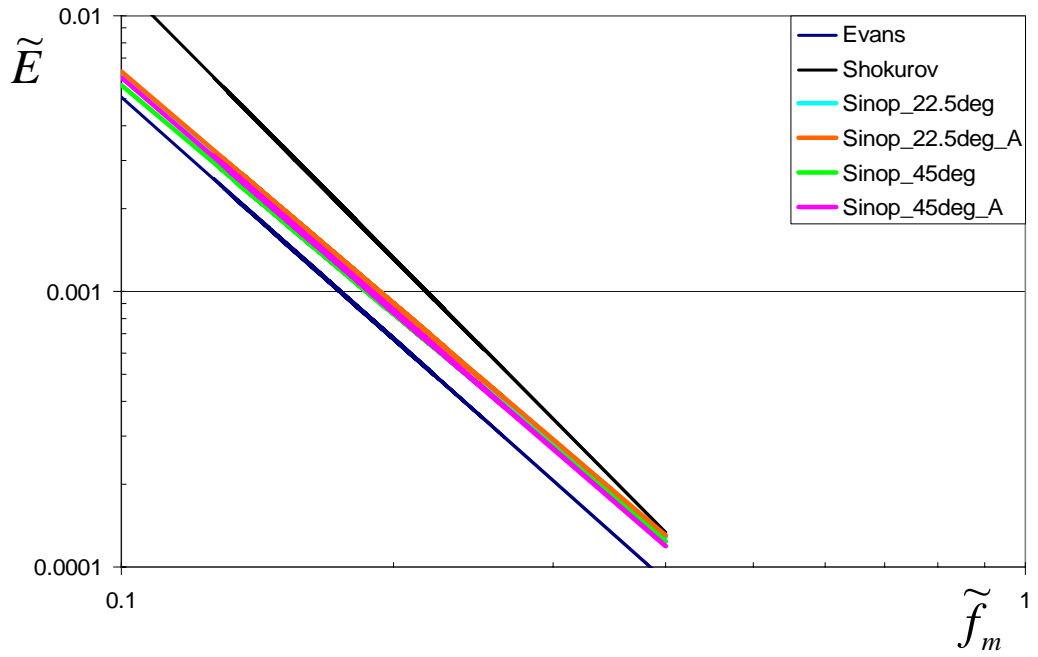


Figure 3.8 Relations between the dimensionless peak frequency and energy obtained for four alternatives at Sinop.

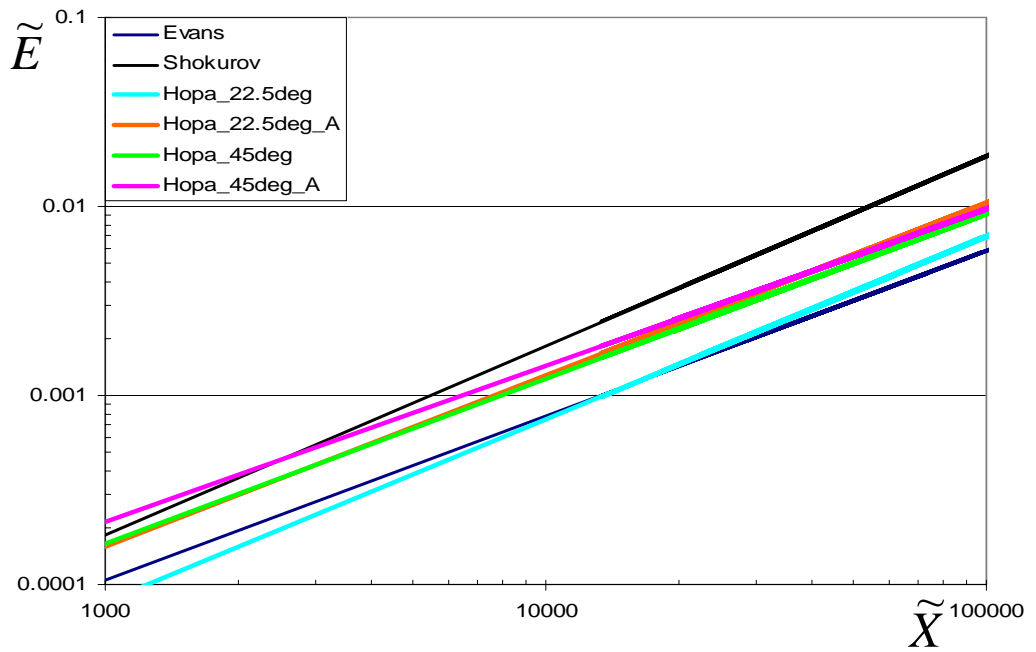


Figure 3.9 Relations between the dimensionless fetch and energy obtained for four alternatives at Hopa.

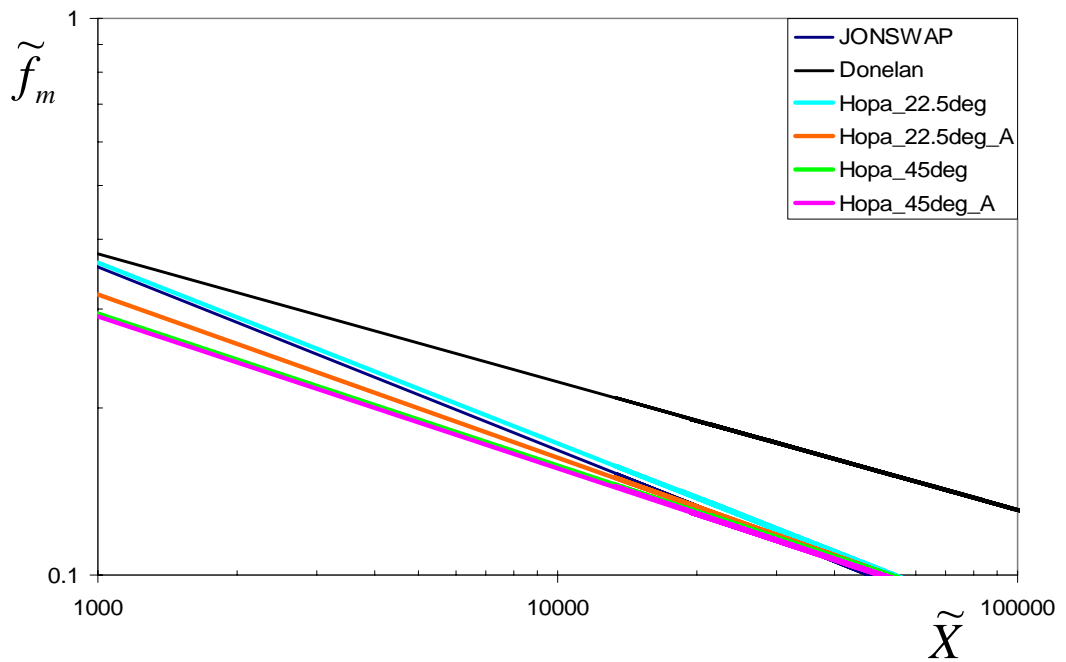


Figure 3.10 Relations between the dimensionless fetch and peak frequency obtained for four alternatives at Hopa.

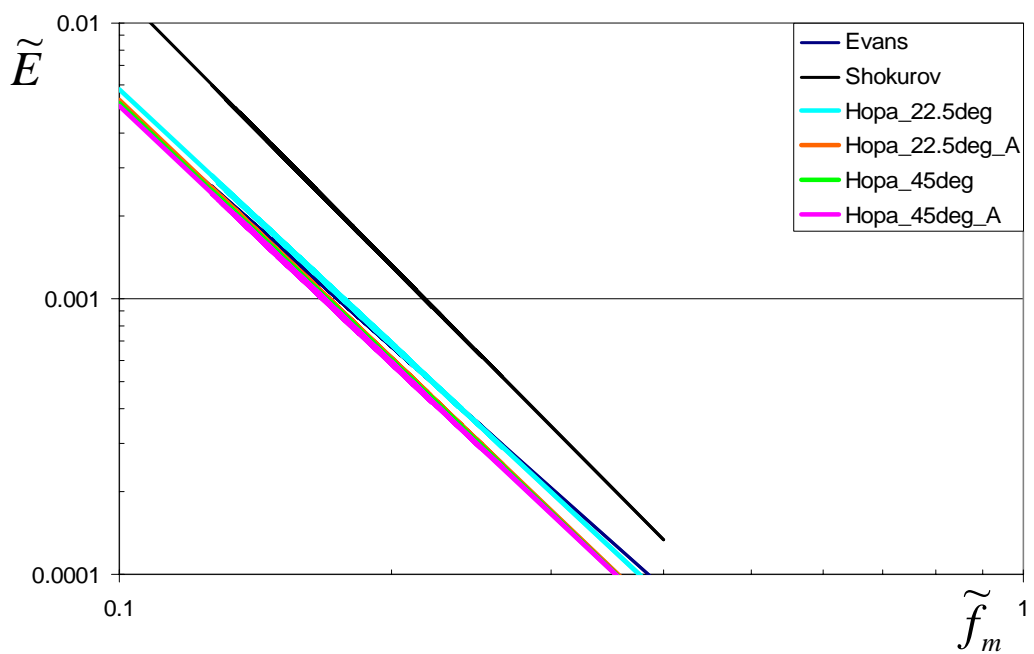


Figure 3.11 Relations between the dimensionless peak frequency and energy obtained for four alternatives at Hopa.

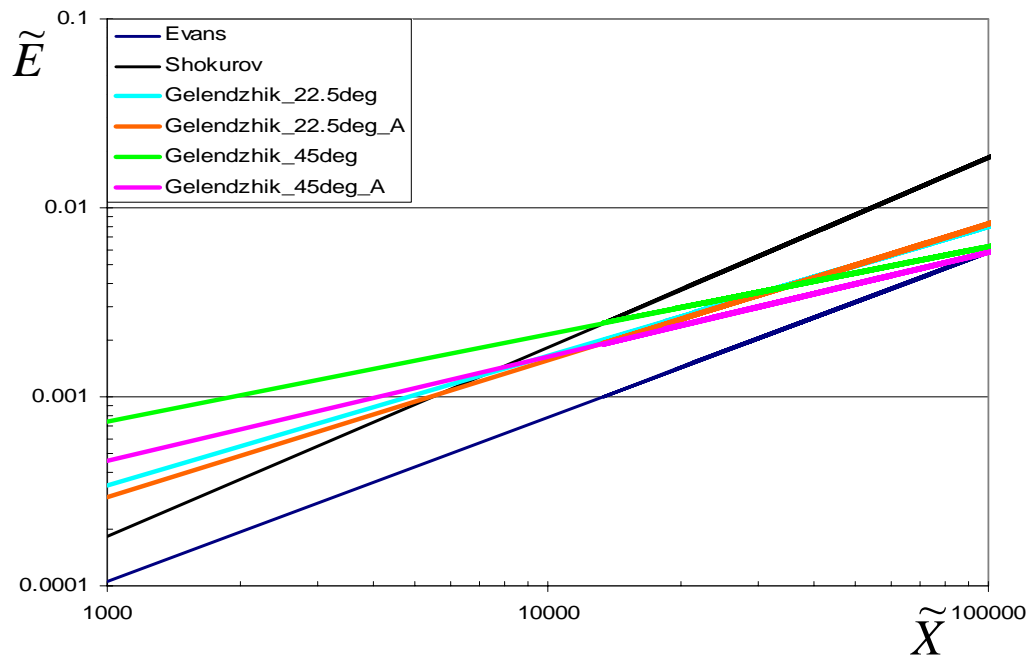


Figure 3.12 Relations between the dimensionless fetch and energy obtained for four alternatives at Gelendzhik.

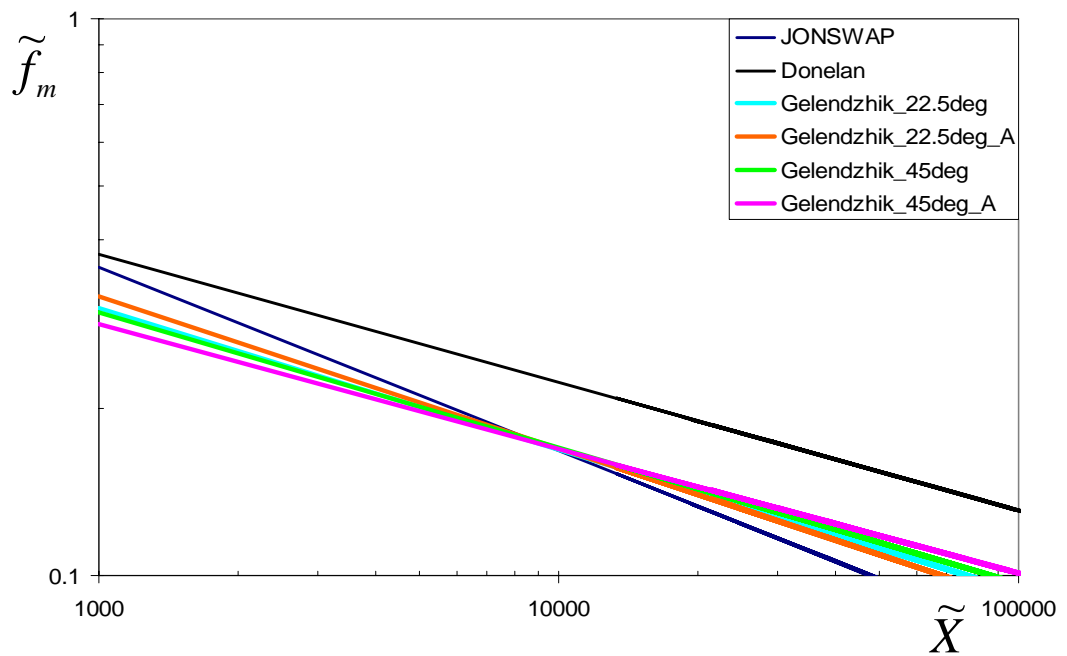


Figure 3.13 Relations between the dimensionless fetch and peak frequency obtained for four alternatives at Gelendzhik.

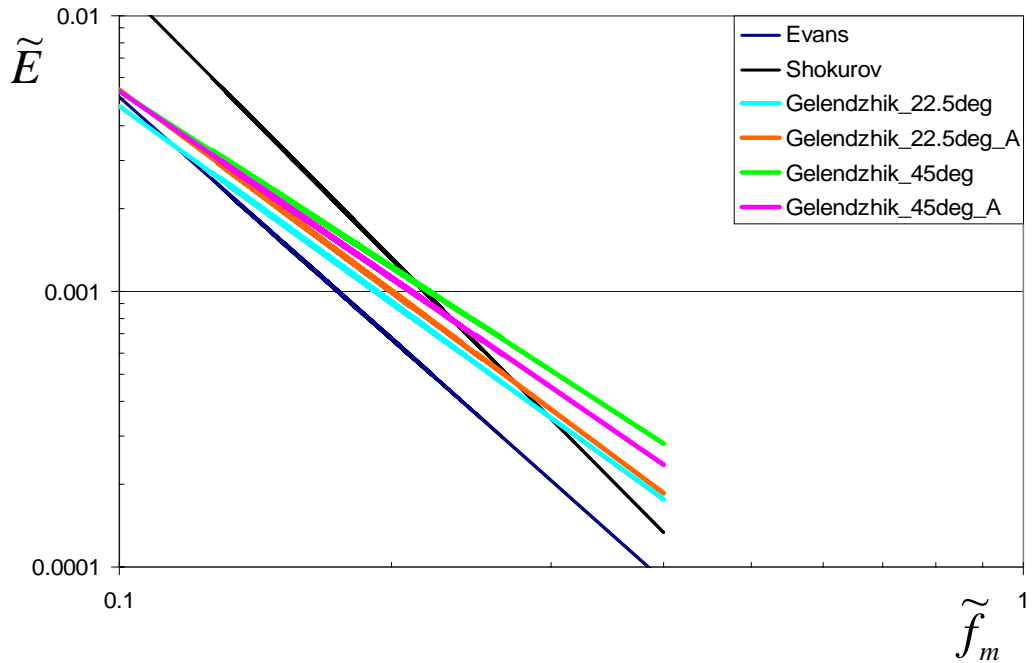


Figure 3.14 Relations between the dimensionless peak frequency and energy obtained for four alternatives at Gelendzhik.

It is observed in Figure 3.6 that increasing the area around the station at Sinop does not affect the relationship between \tilde{E} and \tilde{X} when 22.5° interval is used to represent the directions. However, if 45° interval is used, increase in area causes a change in the slope of the best fit lines and a downward shift of the line representing the use of greater area. Except the line obtained by applying 45° interval and the smaller area, other three alternatives appears to give reasonable results when compared to the envelop of the previous studies. A similar conclusion is also reached by investigating the relationship between \tilde{f}_m and \tilde{X} (Figure 3.7). When 22.5° interval is applied, there is almost no change between increasing the area or not. However the use of 45° interval leads to changes. For the relation between \tilde{E} and \tilde{f}_m (Figure 3.8), all four approaches seem to give almost the same results and they stay inside the limits of previous studies. Thus, in case of Sinop, it was

decided that, except the use of 45° interval and the smaller area, other three alternatives give results consistent with the previous studies.

From the figures showing the relationships derived from the Hopa records, different results are observed compared to Sinop. In Figure 3.9, it is seen that the use of 22.5° interval (not the 45° interval) gives different results in relation to the use of the smaller or larger area for the relationship between \tilde{E} and \tilde{X} . While the regression line obtained by using 22.5° interval and the smaller area is near the lower limit of previous results, it shifts upward to the center of the envelop almost with the same slope when the larger area is utilized. In the case of using 45° interval, it seems that although there is a difference in the slopes of regression lines corresponding to the smaller or larger area, the difference is not too pronounced. Except the relationship obtained for 22.5° interval with smaller area, other three alternatives give similar relationships between \tilde{E} and \tilde{X} . It is also observed in Figure 3.10 that these three alternatives give close results also for \tilde{f}_m and \tilde{X} relationship, but they are below the lower envelop especially at smaller \tilde{X} values. The line for 22.5° interval and the larger area approach is the closest to the result of JONSWAP. In this case, only the relationship obtained by using 22.5° interval and the smaller area falls inside the envelop and follows closely the JONSWAP line. If the relationship between \tilde{E} and \tilde{f}_m in Figure 3.11 is examined, all four approaches seem to give similar results gathered near the lower envelop. However, similar to \tilde{f}_m and \tilde{X} relationship, the regression line obtained using 22.5° interval with the smaller area has the best agreement with the lower envelop of Evans and Kibblewhite (1990).

Unlike the results for Sinop and Hopa, all four relationships obtained from Gelendzhik wave records show significant differences with the envelops

from the previous studies. The worst agreement is observed when the 45° interval is used. This is clearly seen in Figure 3.12 which shows the \tilde{E} and \tilde{X} relationship. When the direction interval of 45° is used for the analysis of Gelendzhik records, slopes of the regression lines for both smaller and larger areas are significantly different from the results of previous studies and have much flatter slopes. The energy is rather high at small fetches, but its increase with fetch is milder. The use of 22.5° interval gives relatively more reasonable regression lines compared to the use of 45° interval.

As observed from Figures 3.6 to 3.14, it is difficult to drive definite conclusions as to the best choice among four possibilities to be used in the analysis of records from three stations. It should be noted that most of the previous studies were performed under relatively controlled special conditions such as selecting the study area, location of the recorder, etc. to work mainly on the theory of fetch dependencies of fetch limited waves. Even so, they show considerable differences. In the present study, the aim of this section was to deduce the relations of estimated spectral parameters with fetch and wind speed by using the available ECMWF analysis wind fields, and to find out the fetch dependencies of measured wind waves which were isolated for belonging to developing sea ($\gamma \geq 1.5$) at three locations. It was decided that the use of 22.5° increment for the directional variability together with the larger area for averaging around the stations gave the most appropriate results among four alternatives. The results for the selected alternative are given for Sinop, Hopa and Gelendzhik in Figures 3.15 to 3.17. It is seen that variation of \tilde{E} with \tilde{X} is the highest at Hopa followed by Sinop and Gelendzhik. However, for a larger ranges of \tilde{X} , Gelendzhik is found to have higher \tilde{E} values compared to Sinop and Hopa.

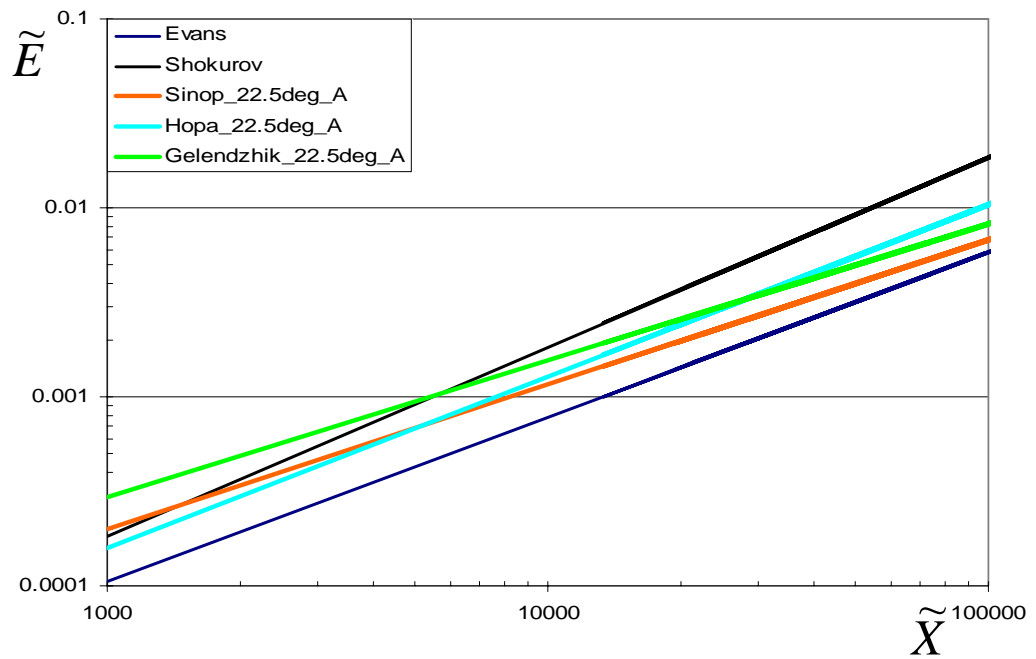


Figure 3.15 Relations between dimensionless fetch and energy obtained for 22.5° angle and the larger area around the stations.

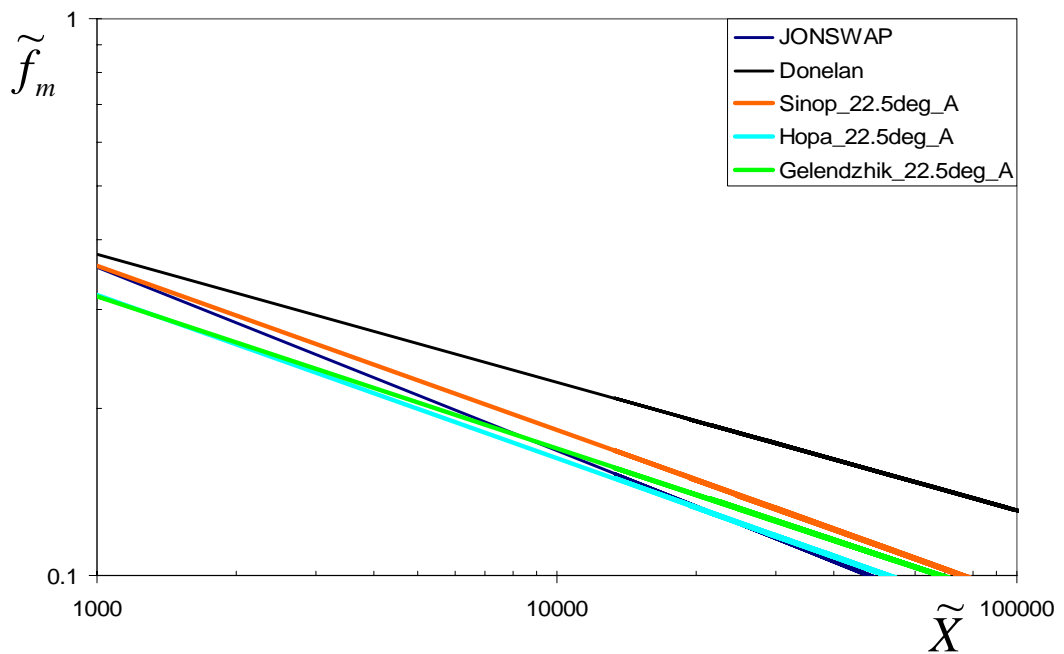


Figure 3.16 Relations between dimensionless fetch and peak frequency obtained for 22.5° angle and the larger area around the stations.

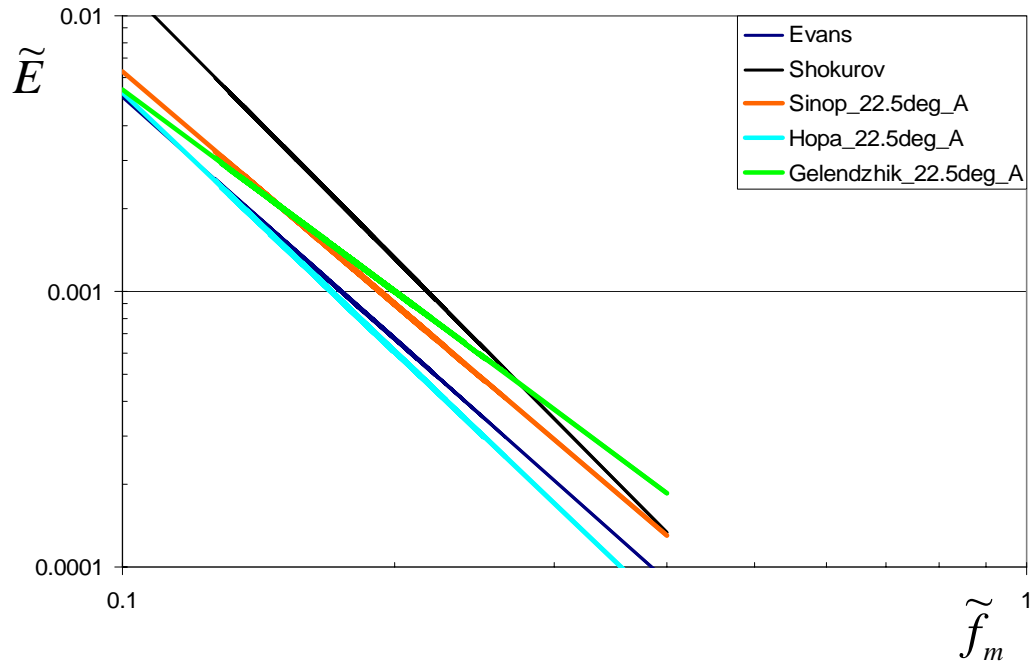


Figure 3.17 Relations between dimensionless peak frequency and energy obtained for 22.5° angle and the larger area around the stations.

The final identified data sets after the described selection procedure was assumed to be for developing seas of stable wind conditions without any swell presence. The scatter plots for the relationships of dimensionless spectral parameters and mean α parameter with dimensionless fetch are given in Figures 3.18, 3.19 and 3.20 together with the regression lines and corresponding equations. Numbers of data used are respectively 155, 181 and 197 for Sinop, Hopa and Gelendzhik. Consistent with the previous studies, \tilde{E} is found to increase with \tilde{X} while \tilde{f}_m and α decrease at three locations. Scatter of data points for α and \tilde{E} is high. It is relatively lower for \tilde{f}_m .

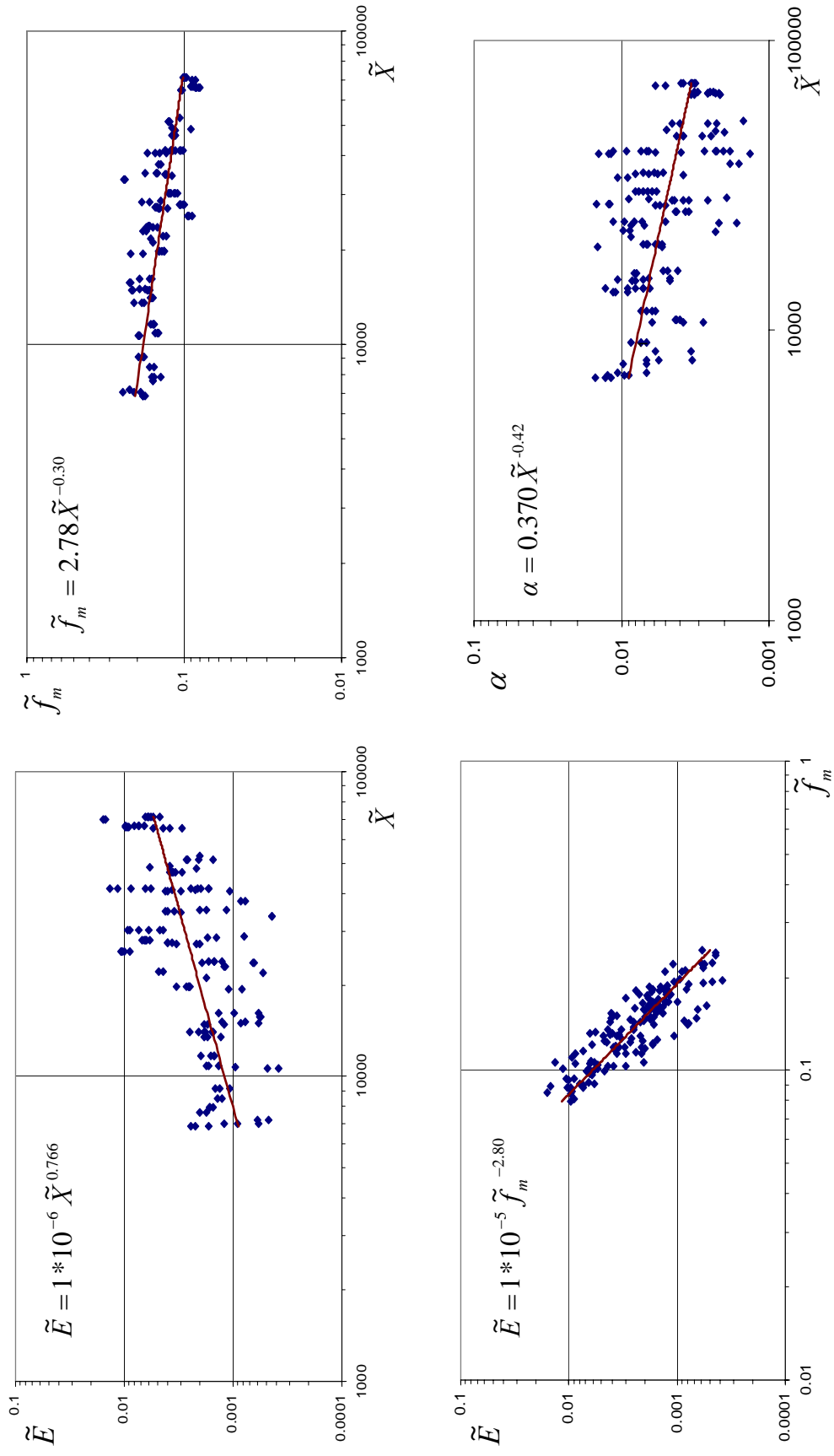


Figure 3.18 Relations between dimensionless spectral parameters and dimensionless fetch at Sinop.

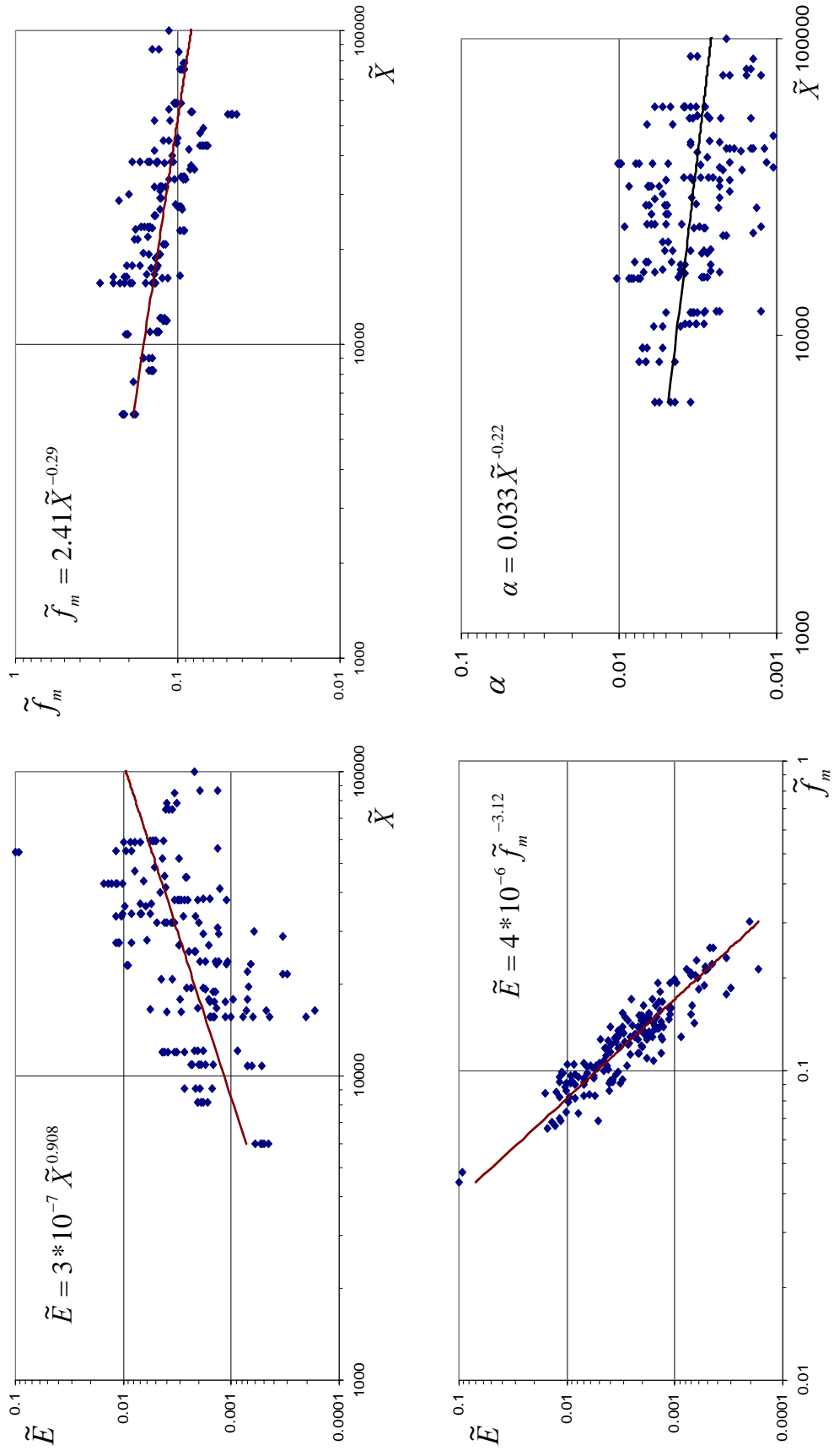


Figure 3.19 Relations between dimensionless spectral parameters and dimensionless fetch at Hoppa.

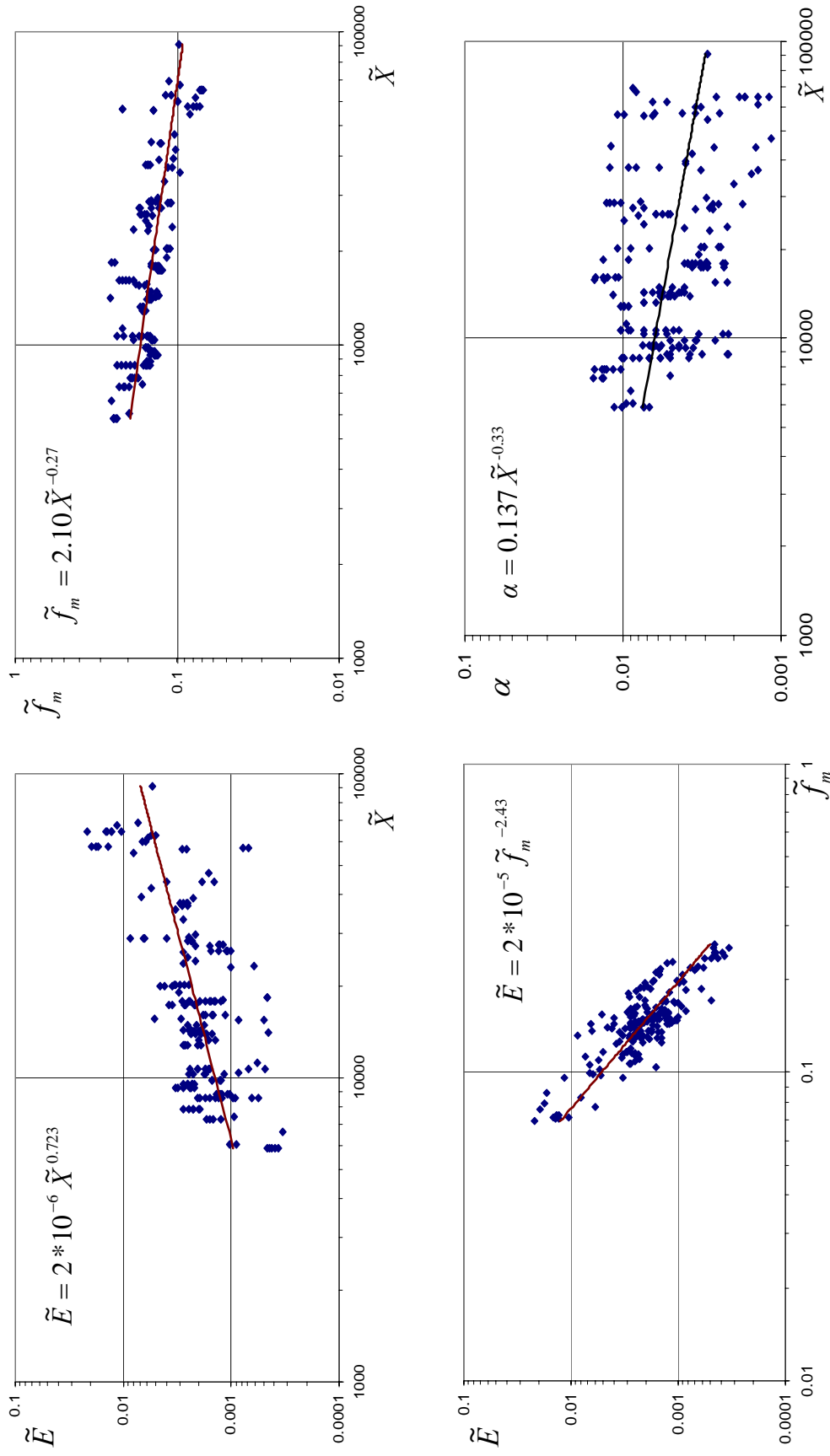


Figure 3.20 Relations between dimensionless spectral parameters and dimensionless fetch at Gelendzhik.

The mean values and standard deviations for the JONSWAP parameters, α , γ and f_p obtained from the observed spectra of wind waves identified as belonging to developing sea of stable wind conditions were recomputed. The results are given in Table 3.17. It is seen that when compared to the values obtained in Section 3.3 (Tables 3.13, 3.14 and 3.15), the mean α increases, while the mean γ and f_p decrease for this data sub-set at Sinop and Hopa. However, for Gelendzhik records the change in mean α is negligible. In case of mean γ and f_p however, slight decreases are observed similar to Sinop and Hopa data.

The observed spectra for wind waves identified as belonging to developing sea of stable wind conditions, were converted to the dimensionless form by dividing the energy densities with $g^2 f_p^{-5}$ and the frequencies with f_p . Envelops obtained for the non-dimensional spectra of Sinop, Hopa and Gelendzhik together with the JONSWAP spectrum obtained by using the mean values of α , γ and f_p (the mean JONSWAP spectrum) are given in Figures 3.21, 3.22 and 3.23 respectively. Figure 3.24 compares the non-dimensional mean JONSWAP spectra at three locations. JONSWAP spectrum was rewritten to be dimensionless in the following form:

$$\frac{S(f)}{g^2 f_p^{-5}} = \alpha (2\pi)^{-4} \left(\frac{f}{f_p} \right)^{-5} \exp \left[-\frac{5}{4} \left(\frac{f}{f_p} \right)^{-4} \right] \gamma \exp \left[\frac{1}{2\sigma^2} \left(\frac{f}{f_p} - 1 \right)^2 \right] \quad (3.2)$$

It is observed from Figures 3.21, 3.22 and 3.23 that mean spectral shapes (the mean JONSWAP spectrum) do not satisfactorily represent the individual spectra. Mean spectra are exceeded significantly at all three locations. From the comparison of the non-dimensional mean JONSWAP spectrum (Figure 3.24), it is seen that Hopa has the mildest spectral shape, whereas Gelendzhik has a more peaked shape.

Table 3.17 Mean parameters of JONSWAP spectrum recomputed for the data set identified as belonging to developing sea of stable wind conditions at Sinop, Hopa and Gelendzhik.

| | Alpha | | Gamma | | Fpeak (Hz) | | |
|-----------------|------------|------------|---------|------------|------------|------------|-------|
| | mean | stand.dev. | mean | stand.dev. | mean | stand.dev. | |
| 0.5 m <Hs<1.0 m | SINOP | 0.00363 | 0.00225 | 2.65 | 0.75 | 0.192 | 0.026 |
| | HOPA | 0.00289 | 0.00192 | 2.83 | 0.92 | 0.182 | 0.030 |
| | GELENDZHIK | 0.00530 | 0.00339 | 2.18 | 0.83 | 0.209 | 0.044 |
| 1.0 m <Hs<2.0 m | SINOP | 0.00582 | 0.00288 | 2.50 | 0.71 | 0.165 | 0.024 |
| | HOPA | 0.00366 | 0.00189 | 2.71 | 0.76 | 0.138 | 0.020 |
| | GELENDZHIK | 0.00536 | 0.00342 | 2.55 | 0.92 | 0.153 | 0.025 |
| 2.0 m <Hs<3.0 m | SINOP | 0.00759 | 0.00325 | 2.08 | 0.46 | 0.134 | 0.014 |
| | HOPA | 0.00530 | 0.00194 | 2.89 | 0.96 | 0.127 | 0.010 |
| | GELENDZHIK | 0.00743 | 0.00355 | 3.06 | 1.20 | 0.137 | 0.018 |
| 3.0 m <Hs | SINOP | 0.00874 | 0.00307 | 2.94 | 0.86 | 0.120 | 0.008 |
| | HOPA | 0.00267 | 0.00078 | 3.83 | 0.81 | 0.086 | 0.003 |
| | GELENDZHIK | 0.00649 | 0.00262 | 2.86 | 0.75 | 0.108 | 0.013 |
| ALL DATA | SINOP | 0.00605 | 0.00321 | 2.48 | 0.73 | 0.160 | 0.030 |
| | HOPA | 0.00404 | 0.00210 | 2.82 | 0.88 | 0.140 | 0.028 |
| | GELENDZHIK | 0.00622 | 0.00351 | 2.73 | 1.05 | 0.148 | 0.035 |
| Hs ≥ 1.0 m | SINOP | 0.00650 | 0.00316 | 2.45 | 0.72 | 0.154 | 0.027 |
| | HOPA | 0.00425 | 0.00206 | 2.82 | 0.87 | 0.132 | 0.020 |
| | GELENDZHIK | 0.00634 | 0.00351 | 2.79 | 1.05 | 0.140 | 0.026 |

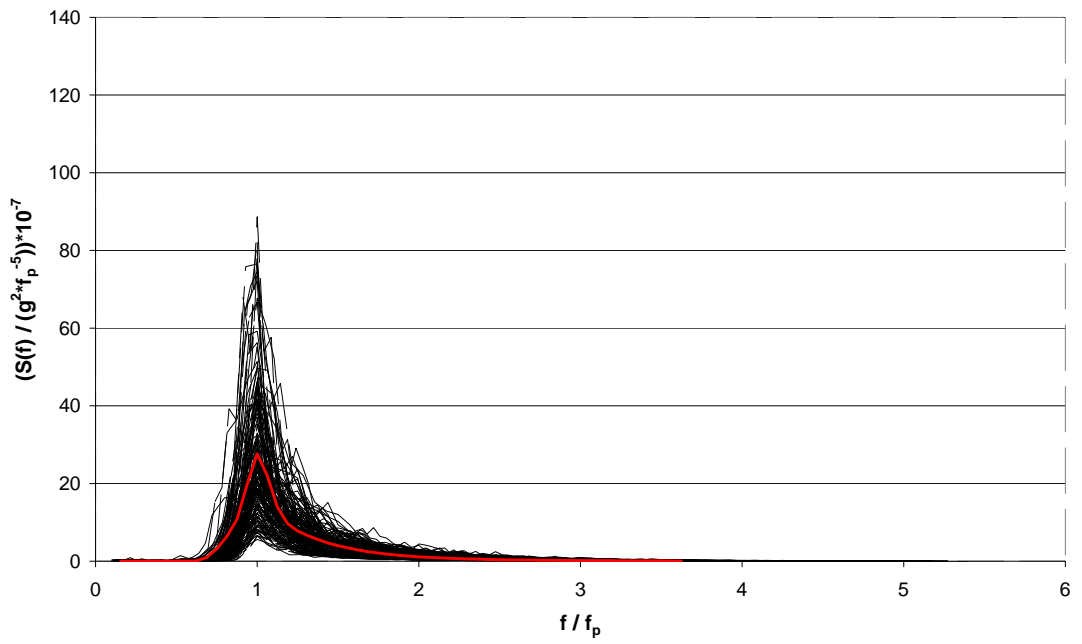


Figure 3.21 Cluster of dimensionless spectra together with the mean JONSWAP spectrum (red line) at Sinop.

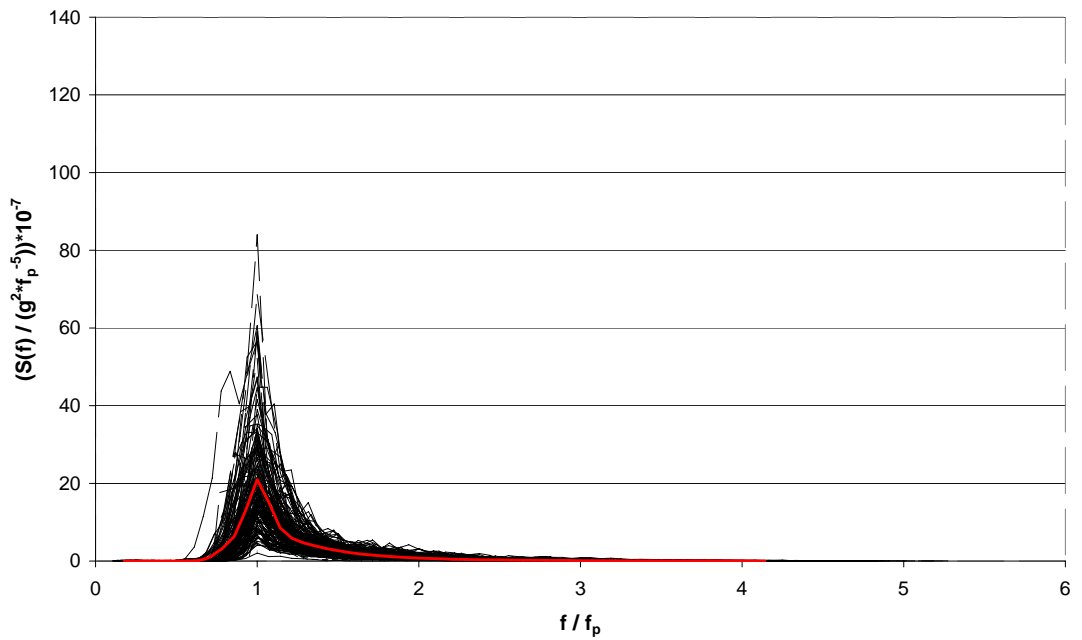


Figure 3.22 Cluster of dimensionless spectra together with the mean JONSWAP spectrum (red line) at Hopa.

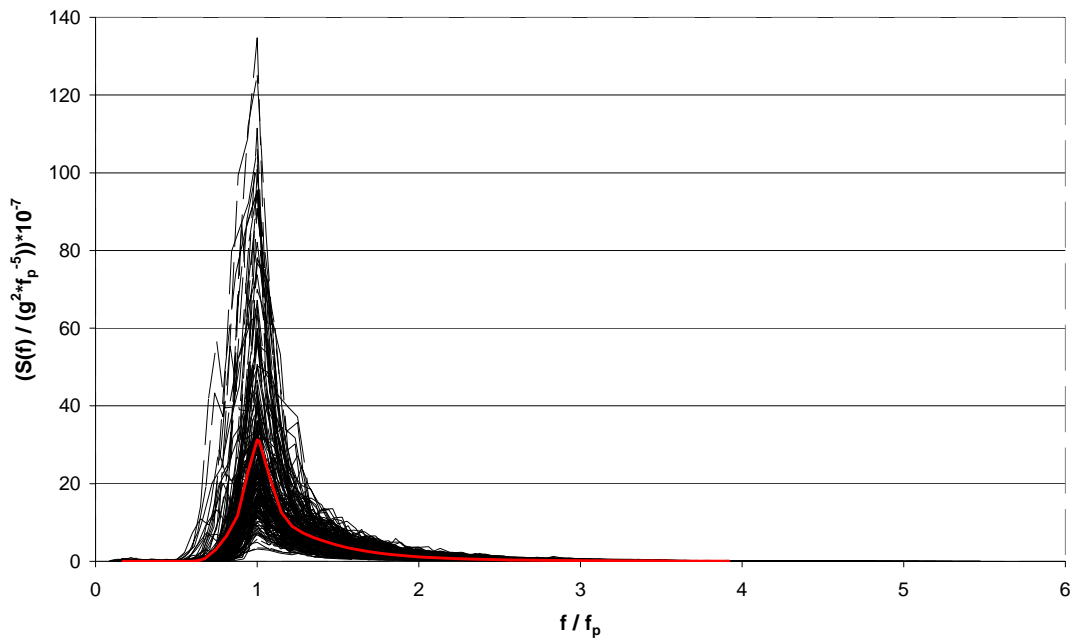


Figure 3.23 Cluster of dimensionless spectra together with the mean JONSWAP spectrum (red line) at Gelendzhik.

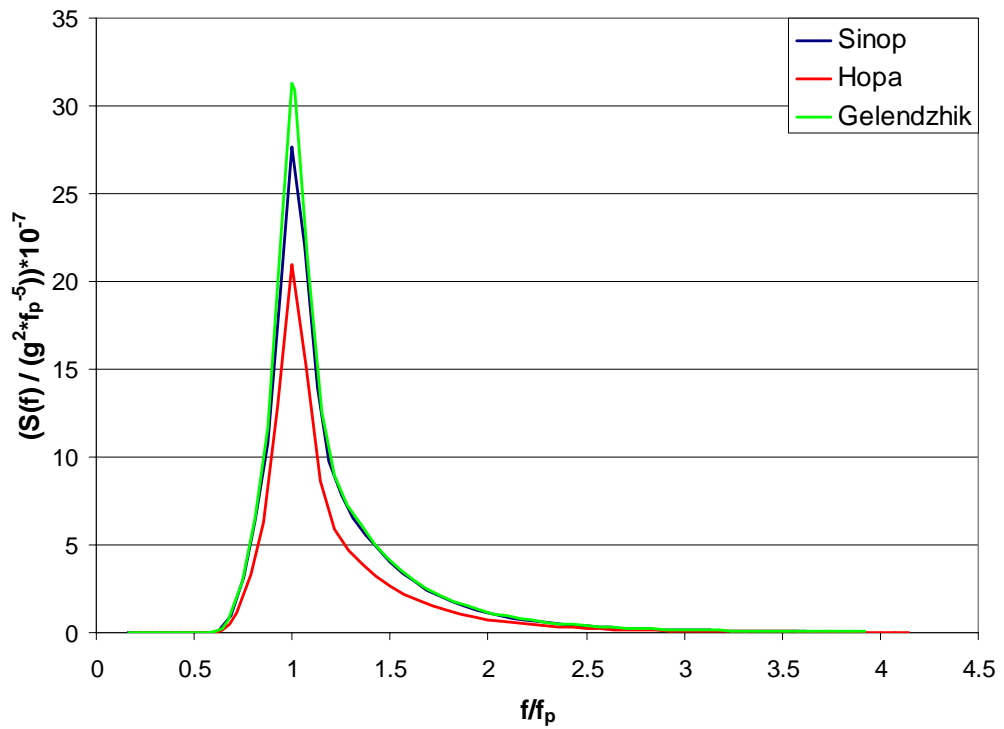


Figure 3.24 Non-dimensional mean JONSWAP spectra at Sinop, Hopa and Gelendzhik.

CHAPTER 4

SUMMARY AND CONCLUSIONS

For investigating the characteristics of wind-wave spectra of the eastern Black Sea, long-term wave measurements obtained by directional buoys deployed offshore Sinop and Hopa in Turkey and Gelendzhik in Russia were utilized. Respectively, 2450, 5538 and 8284 observed frequency spectra at Sinop, Hopa and Gelendzhik were analyzed. The wave records were grouped into sea states defined by significant wave height limits of 0.5 m, 1.0 m, 2.0 m and 3.0 m. Results obtained throughout the study were generally given for these different sea states.

Analysis of the records was carried out in three steps. Firstly, the number of spectral peaks of each record were identified. Occurrences of spectral peaks were computed at each sea state as well as overall data. Secondly, the single peaked spectra, which were determined in the first step, were fitted to the JONSWAP model spectrum. Spectra for which γ parameter was less than 1.5 were separated as belonging to the fully arisen sea state. These records were reanalyzed to estimate the spectral parameters of the corresponding PM model spectrum. The remaining data (records with γ parameter greater than or equal to 1.5) were considered as developing sea records. In the third step, these developing sea records were further investigated for identifying the data that belonged to developing sea, which was generated by a stable wind field. Rather rigid criteria were applied for the identification process.

Fetch dependencies of dimensionless spectral variables, mean parameters of JONSWAP model spectrum and the envelop of dimensionless spectra were determined for this data sub-set.

The followings are the main results and conclusions of this thesis study:

- Percent occurrences of the multi-peaked spectra decrease with increasing significant wave height. For all sea states and for overall data, occurrence of the multi-peaked spectra was higher at Sinop and Gelendzhik compared to Hopa. There was no significant seasonal variability for occurrence of multi peaked spectra at any of the locations.

- Percent occurrences of the double-peaked spectra for the data recorded at Sinop and Gelendzhik were computed in the order of 20-25%, while at Hopa it was considerably less (around 10-15%).

- For the uni-modal spectra which were identified as developing sea, JONSWAP spectrum parameters were estimated. In general, mean α values decreased with decreasing significant wave height at all three locations. However, for γ values, the dependency on the sea state is less sensitive. The peak frequency increases with decreasing significant wave height.

- Hopa has the smallest mean α values for each sea state as well as for the overall data. On the contrary, γ values are the highest for Hopa records. Both α and γ have higher values at Gelendzhik than at Sinop, except the α value for the highest sea state (e.g. $H_s \geq 3.0$ m). In the case of peak frequency Hopa records give lower values than those of Sinop and Gelendzhik. Generally, standard deviation of α is rather large, indicating the high variability with

this parameter. At all three stations, the mean γ values are smaller than the value of 3.3 which was obtained for the original JONSWAP data of the North Sea.

- For the uni-modal spectra which were identified as fully arisen sea, the PM spectrum parameters were estimated. The α parameter obtained from the Hopa records is the lowest among three locations. Standard deviation of α is again high. At all stations, α is less than 0.0081 which is the mean value for the original PM spectrum.

- Only a very small sub-set of the records were identified for belonging to developing sea state generated by rather stable winds from thousands of data at three locations.

- Consistent with the previous studies, dimensionless energy is found to increase with dimensionless fetch while dimensionless peak frequency and α decrease at three locations. Scatter in the values of α and energy is high but it is relatively low for peak frequency.

- Compared to the mean spectral parameters estimated for all single peaked spectra, the mean α increases, while the mean γ and f_p decrease for the records identified as belonging to developing seas generated by stable winds at Sinop and Hopa. However, for Gelendzhik records the change in the mean α is negligible. In case of mean γ and f_p , a slight decrease is observed similar to Sinop and Hopa data.

- Clusters of the dimensionless spectra show that mean spectral shapes (the mean JONSWAP spectrum) do not satisfactorily represent the individual

spectra. Mean spectra are exceeded significantly at all three locations. Hopa has the mildest spectral shape, whereas Gelendzhik has a more peaked shape.

The following two subjects are recommended for further studies.

In the scope of the present research, only the frequency spectra were studied. However, wave records utilized were obtained from directional buoys. So, directional spectra can also be computed from these records. Directional spectra can be analyzed to provide information on directional distribution of wave energy as well. Besides, the use of directional spectra could be important in multi-modal spectra identification. For example, spectra composing of mixed wave systems coming from different directions but have very close peak frequencies can not be identified by analyzing the frequency spectra alone. This type of spectra can only be identified by investigating the directional spectra. Therefore, it would be useful to make the analysis by utilizing the directional spectra and compare its results with the ones obtained in this study.

Secondly, records exhibiting more than one spectral peak were identified in this study and the percent occurrences of these multi-modal spectra were computed without any further investigation on these records. Since the bimodal sea states can have significant impacts on the design and operability of fixed and floating offshore platforms, and in other ocean engineering applications, it will be valuable to investigate the characteristics of bimodal spectra in the eastern Black Sea.

REFERENCES

- Abdalla, S. (1991), 'Development of a Third Generation Wind Wave Model Applicable to Finite Depths', Ph.D. Thesis, Middle East Technical University, Ankara, Turkey.
- Acar, S. O. (1983), Statistical Analysis of Wind Waves at Ordu and Akkuyu (Mersin), Master's thesis, Middle East Technical University, 112 pages.
- Araujo, C. E. S., Franco, D., Melo, E. and Pimenta, F. (2003), 'Wave Regime Characteristics of the Southern Brazilian Coast', Proceedings of the Sixth International Conference on Coastal and Port Engineering in Developing Countries, COPEDEC VI, Colombo, Sri Lanka, Paper No. 097, pp. 15.
- Arikan, E.Ş. (1998), 'Comparison of Two Different Sources of Wind Data for Wave Prediction in the Black Sea', MS Thesis, Middle East Technical University, Ankara, Turkey.
- Borgman, L.E. (1972), 'Confidence intervals for ocean wave spectra', Proceedings of the 13th Coastal Engineering Conference, ASCE, pp. 167–195.
- CEM (2006), 'Coastal Engineering Manual', Coastal Engineering Research Center, Dept. of Army Corps of Engineers, US, Chapter I, Part 2.

- Donelan, M. A., Hamilton, J. and Hui, W. H. (1985), 'Directional spectra of wind waves', *Phil. Trans. R. Soc. Lond., Ser. A*, 315, pp. 509-562.
- Ewans, K.C. and Kibblewhite, A.C. (1990), 'An Examination of Fetch-Limited Wave Growth off the West Coast of New Zealand by a Comparison with the JONSWAP Results ', *Journal of Physical Oceanography*, 20, pp. 1278-1296.
- Feld, G. and Mørk, G. (2004), 'A Comparison of Hindcast and Measured Wave Spectra', 8th International Workshop on Wave Hindcasting and Forecasting, November 14-19, 2004, North Shore, Oahu, Hawaii, USA.
- Gerling, T. (1992), 'Partitioning sequences and arrays of directional ocean wave spectra into component wave systems', *J. Atmos. Oceanic Technol.*, 9, pp. 444-458.
- Goda, Y. (1998), 'An Overview of Coastal Engineering With Emphasis On Random Wave Approach', *Coastal Engineering Journal*, Vol.40, No:1, pp. 1- 21, World Scientific Pub. and JSCE.
- Goda, Y. (1999), 'A Comparative Review on the Functional Forms of Directional Wave Spectrum', *Coastal Engineering Journal*, Vol. 41, No. 1, pp. 1-20.
- Goda, Y. (2000), *Random Seas and Design of Maritime Structures*, World Scientific, Advanced Series on Ocean Engineering – Volume 15, 443 pages.

- Guedes Soares, C. (1984), 'Representation of double-peaked sea wave spectra', *Ocean Engineering*, Vol. 11, pp. 185–207.
- Guedes Soares, C. (1991), 'On the occurrence of double peaked wave spectra', *Ocean Engineering*, Vol.18, pp.167–71.
- Guedes Soares, C. and Nolasco, M. C. (1992) 'Spectral Modeling of Sea States with Multiple Wave Systems', *J. Offshore Mech. Arct. Eng.*, 114, pp. 278–284.
- Guedes Soares, C. and Henriques, A.C. (1996), 'Statistical uncertainty in long-term distributions of significant wave height', *Journal of Offshore Mechanics and Arctic Engineering*, 11, pp. 284–91.
- Hasselmann, K., Barnett, T.P., Bouws, E., Carlson, H., Cartwright, D.E., Enke, K. et al. (1973), 'Measurements of wind-wave growth and swell decay during the Joint North Sea Wave Project (JONSWAP)', *Deutsche Hydr Zeit*, A 8(12), 95 pp.
- Hasselmann, S., Bruning, C., Hasselmann, K. and Heimbach, P. (1996), 'An improved algorithm for the retrieval of ocean wave spectra from Synthetic Aperture Radar image spectra', *J. Geophys. Res.*, Vol. 101, No: C7, pp. 16,615–16,629.
- Houmb, O.G. and Due, E. (1978), 'On the occurrence of wave spectra with more than one peak', Report, Division of Port and Ocean Eng., Norwegian Institute of Technology, Trondheim.

- Kahma, K. K. (1981), 'A study of the growth of the wave spectrum with fetch', *Journal of Physical Oceanography*, Vol. 11, pp. 1503-1515.
- Kahma, K. K. and Calkoen C. J. (1992), 'Reconciling discrepancies in the observed growth of wind-generated waves', *Journal of Physical Oceanography*, Vol. 22, pp. 1389-1405.
- Liu, P. C. (2000), 'Is the wind wave frequency spectrum outdated', *Technical note, Ocean Engineering*, Vol. 27, pp. 577-588.
- Miles, J.W., (1957), 'On the Generation of Surface Waves by Shear Flows', *Journal of Fluid Mechanics*, 3, pp. 185-204.
- Moon, I.J. and Oh, I.S. (1998), 'A study of the characteristics of wave spectra over the seas around Korea by using a parametric spectrum method', *Acta Oceanographica Taiwanica (AOT)*, Vol. 37, No.1, June 1998, ISSN: 0379-7481, pp. 31-46.
- Ochi, M. K. and Hubble, E. N. (1976), 'Six-Parameter Wave Spectra', *Proceedings of the 15th Coastal Engineering Conference*, pp. 301-328.
- Özhan, E. (1981), 'Rüzgar dalgalarının kısa dönem istatistiksel özellikleri, enerji spektrumu ve dalga tahminleri', *METU-KLARE, Special Report*, METU, Ankara.
- Özhan, E., Abdalla, S., Seziş-Papila, S. and Turhan, M. (1995), 'Measurements and modeling of wind waves along the Turkish Mediterranean Coasts and the Black Sea.', *Proc. 2nd International Conference on the Mediterranean Coastal Environment*,

MEDCOAST'95, E. Özhan (ed.), MEDCOAST Publications, Ankara, Turkey, pp.1899-1910.

Philips, O.M., (1957), 'On the Generation of Waves by Turbulent Wind', *Journal of Fluid Mechanics*, Vol. 2, pp. 417-445.

Phillips, O. M. (1958), 'The Equilibrium Range in the Spectrum of Wind-Generated Waves', *Journal of Fluid Mechanics*, Vol. 4, pp. 426-434.

Rodriguez, G. R. and Guedes Soares, C. (1999), 'A Criterion for the Automatic Identification of Multimodal Sea Wave Spectra', *Appl. Ocean. Res.*, 21, pp. 329–333.

Shokurov, M.V. and Efimov, V.V. (1999), 'Integral Wind Wave Parameters for Fetch Limited Conditions in the Black Sea', *The Proc. of the International MEDCOAST Conference on Wind and Wave Climate of the Mediterranean and the Black Sea* (Eds. S. Abdalla & E. Özhan), pp. 49-58, MEDCOAST Secretariat, Ankara, Turkey.

Violante-Carvalho, N., Parente, C.E., Robinson, I.S. and Nunes, L.M.P. (2002), 'On the Growth of Wind Generated Waves in a Swell Dominated Region in the South Atlantic', *J. Offshore Mech. Arctic Engng.*, Vol. 124, pp.14–21.

Violante-Carvalho, N., Ocampo-Torres, F.J. and Robinson, I.S. (2004), 'Buoy observations of the influence of swell on wind waves in the open ocean', *Applied Ocean Research*, 26, pp. 49–60.

WMO (1988), 'Guide to Wave Analysis and Forecasting', Secretariat of the World Meteorological Organization, Geneva, Switzerland.

Yilmaz, N. (2000). 'Extremal wind and wave climatology of the Aegean and the Mediterranean coast of Turkey' MSc Thesis, Middle East Technical University, Ankara, Turkey.

Yilmaz, N., Ozhan, E. and Abdalla, S. (2003), 'Comparison of wave hindcasting with measurements in the Eastern Black Sea', Proceedings of the Sixth International Conference on the Mediterranean Coastal Environment, MEDCOAST 03, E. Özhan, (ed.), Ravenna, Italy, MEDCOAST Publications, Ankara, Turkey, vol.3, pp.1905-1916.

Young, I.R. and Verhagen, L.A. (1996), 'The growth of fetch limited waves in water of finite depth. Part 1. Total energy and peak frequency', Coastal Engineering, 29, pp. 47–78.

APPENDIX A

CONTENT OF THE SPECTRA FILES

Spectra files used as the source of this study were provided directly by the Datawell Waverider buoys. The data is automatically assembled and processed by means of a spectral analysis system provided by Datawell. The results of this analysis are saved in a Datawell pre-defined file, which have a 'SPT' extension. They are named corresponding to the time they represent as 'MMDDHHmm.SPT'. 'MM' stands for 'month', 'DD' for 'day', 'HH' for hour and 'mm' for minute. The files contain the energy density, mean direction and directional spreading for each frequency band from which other general parameters can be calculated.

A sample page with explanations added for each value is given in the next page.

'01260014.SPT' (Name of the file)

| 7 | : Current transmission number | | | | |
|----------------|---|-------------------------------|-----------------------------------|----------|----------|
| 423 | : Significant height (cm) ($4\sqrt{m_0}$) | | | | |
| 8.510638 | : Mean period (sec) ($\sqrt{(m_0/m_2)}$) | | | | |
| 46.62763 | : Maximum spectral density (m^2/Hz) | | | | |
| 25.3 | : Sea surface temperature ($^{\circ}C$) | | | | |
| 9.8 | : Reference (dummy) temperature ($^{\circ}C$) | | | | |
| 7 | : Battery condition (7=full, 0=empty) | | | | |
| -0.14875 | : Vertical accelerometer offset (m/sec^2) | | | | |
| -0.42375 | : X accelerometer offset (m/sec^2) | | | | |
| 0.115 | : Y accelerometer offset (m/sec^2) | | | | |
| 310.7813 | : Compass heading ($^{\circ}$) | | | | |
| 59.0625 | : Magnetic field inclination ($^{\circ}$) | | | | |
| Frequency (Hz) | Normalised spectral density | Mean direction ($^{\circ}$) | Directional spread ($^{\circ}$) | Skewness | Curtosis |
| 0.025 | 0.000396 | 291.575 | 70.27681 | 3.399935 | 2.417151 |
| 0.03 | 0.00093 | 277.5125 | 57.29575 | -2.51416 | 3.71875 |
| 0.035 | 0.001159 | 288.7625 | 45.20992 | -3.45568 | 5.295888 |
| 0.04 | 0.001416 | 285.95 | 40.28607 | 1.662612 | 6.74838 |
| 0.045 | 0.001114 | 284.5438 | 53.71476 | 0.955116 | 3.054301 |
| : | : | : | : | : | : |
| : | : | : | : | : | : |
| : | : | : | : | : | : |
| 0.09 | 1 | 281.7313 | 17.90492 | 8 | 34.4064 |
| 0.095 | 0.612626 | 285.95 | 26.40976 | 6 | 13.28853 |
| 0.1 | 0.499075 | 281.7313 | 23.2764 | -2.63137 | 17.92654 |
| 0.11 | 0.267135 | 284.5438 | 27.305 | 1.221766 | 13.37147 |
| 0.12 | 0.113608 | 281.7313 | 24.17164 | 1.824712 | 9.156328 |
| 0.13 | 0.098274 | 281.7313 | 21.03828 | 0.870321 | 9.898194 |
| 0.14 | 0.077305 | 287.3563 | 20.59066 | -1 | 15.98348 |
| 0.15 | 0.060205 | 288.7625 | 20.59066 | -0.77277 | 13.17319 |
| 0.16 | 0.031905 | 278.9188 | 29.54312 | 1.295878 | 8.855686 |
| 0.17 | 0.027187 | 281.7313 | 31.78123 | 1.390882 | 7.223699 |
| : | : | : | : | : | : |
| : | : | : | : | : | : |
| : | : | : | : | : | : |
| : | : | : | : | : | : |
| : | : | : | : | : | : |
| : | : | : | : | : | : |
| : | : | : | : | : | : |
| 0.53 | 0.00024 | 247.9812 | 59.53386 | 0.410506 | 2.284015 |
| 0.54 | 0.000277 | 252.2 | 55.95288 | 0.646747 | 1.909381 |
| 0.55 | 0.000296 | 250.7937 | 57.29575 | 0.454004 | 1.84375 |
| 0.56 | 0.000268 | 240.95 | 52.81952 | 0.745917 | 2.262079 |
| 0.57 | 0.000264 | 270.4813 | 57.29575 | -0.93556 | 2.171875 |
| 0.58 | 0.000235 | 274.7 | 58.63861 | 0.394411 | 2.124079 |

APPENDIX B

NUMBER OF SEASONAL DATA

Table B1 Number of Winter measurements in each significant wave height range.

| | SINOP | HOPA | GELENDZHIK |
|----------------------|-------|------|------------|
| Hs ≥ 6.0 m. | 0 | 0 | 5 |
| 5.0 m. ≤ Hs < 6.0 m. | 0 | 1 | 2 |
| 4.0 m. ≤ Hs < 5.0 m. | 2 | 6 | 36 |
| 3.0 m. ≤ Hs < 4.0 m. | 24 | 31 | 134 |
| 2.0 m. ≤ Hs < 3.0 m. | 81 | 224 | 656 |
| 1.0 m. ≤ Hs < 2.0 m. | 408 | 551 | 1329 |
| 0.5 m. ≤ Hs < 1.0 m. | 610 | 777 | 835 |
| Hs < 0.5 m. | 210 | 1727 | 777 |
| TOTAL # | 1335 | 3317 | 3774 |

Table B2 Number of Spring measurements in each significant wave height range.

| | SINOP | HOPA | GELENDZHIK |
|----------------------|-------|------|------------|
| Hs ≥ 6.0 m. | 0 | 0 | 0 |
| 5.0 m. ≤ Hs < 6.0 m. | 0 | 0 | 6 |
| 4.0 m. ≤ Hs < 5.0 m. | 0 | 0 | 17 |
| 3.0 m. ≤ Hs < 4.0 m. | 4 | 0 | 41 |
| 2.0 m. ≤ Hs < 3.0 m. | 47 | 53 | 196 |
| 1.0 m. ≤ Hs < 2.0 m. | 322 | 441 | 556 |
| 0.5 m. ≤ Hs < 1.0 m. | 601 | 782 | 486 |
| Hs < 0.5 m. | 541 | 2087 | 914 |
| TOTAL # | 1515 | 3363 | 2216 |

Table B3 Number of Summer measurements in each significant wave height range.

| | SINOP | HOPA | GELENDZHIK |
|----------------------|-------|------|------------|
| Hs ≥ 6.0 m. | 0 | 0 | 0 |
| 5.0 m. ≤ Hs < 6.0 m. | 0 | 0 | 0 |
| 4.0 m. ≤ Hs < 5.0 m. | 0 | 0 | 0 |
| 3.0 m. ≤ Hs < 4.0 m. | 0 | 3 | 29 |
| 2.0 m. ≤ Hs < 3.0 m. | 1 | 42 | 93 |
| 1.0 m. ≤ Hs < 2.0 m. | 75 | 331 | 457 |
| 0.5 m. ≤ Hs < 1.0 m. | 54 | 885 | 965 |
| Hs < 0.5 m. | 101 | 2276 | 2447 |
| TOTAL # | 231 | 3537 | 3991 |

Table B4 Number of Autumn measurements in each significant wave height range.

| | SINOP | HOPA | GELENDZHIK |
|----------------------|-------|------|------------|
| Hs ≥ 6.0 m. | 0 | 0 | 0 |
| 5.0 m. ≤ Hs < 6.0 m. | 0 | 0 | 1 |
| 4.0 m. ≤ Hs < 5.0 m. | 1 | 6 | 4 |
| 3.0 m. ≤ Hs < 4.0 m. | 12 | 46 | 57 |
| 2.0 m. ≤ Hs < 3.0 m. | 65 | 182 | 395 |
| 1.0 m. ≤ Hs < 2.0 m. | 87 | 535 | 1026 |
| 0.5 m. ≤ Hs < 1.0 m. | 56 | 642 | 958 |
| Hs < 0.5 m. | 111 | 1595 | 1838 |
| TOTAL # | 332 | 3006 | 4279 |

APPENDIX C

MESH OVER THE BLACK SEA

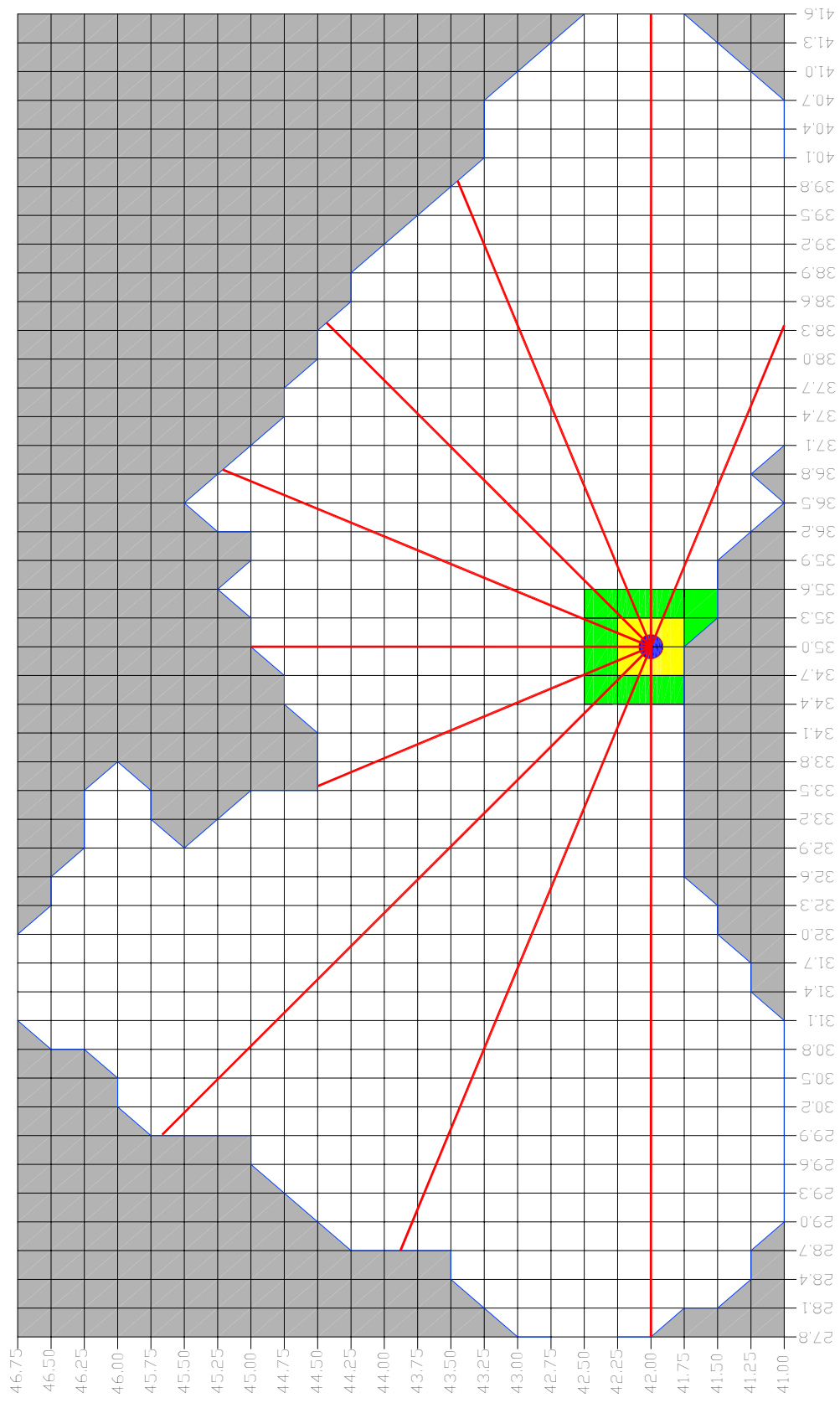


Figure C1 Location of Sinop on the mesh and alignments of directions considered in the analysis.

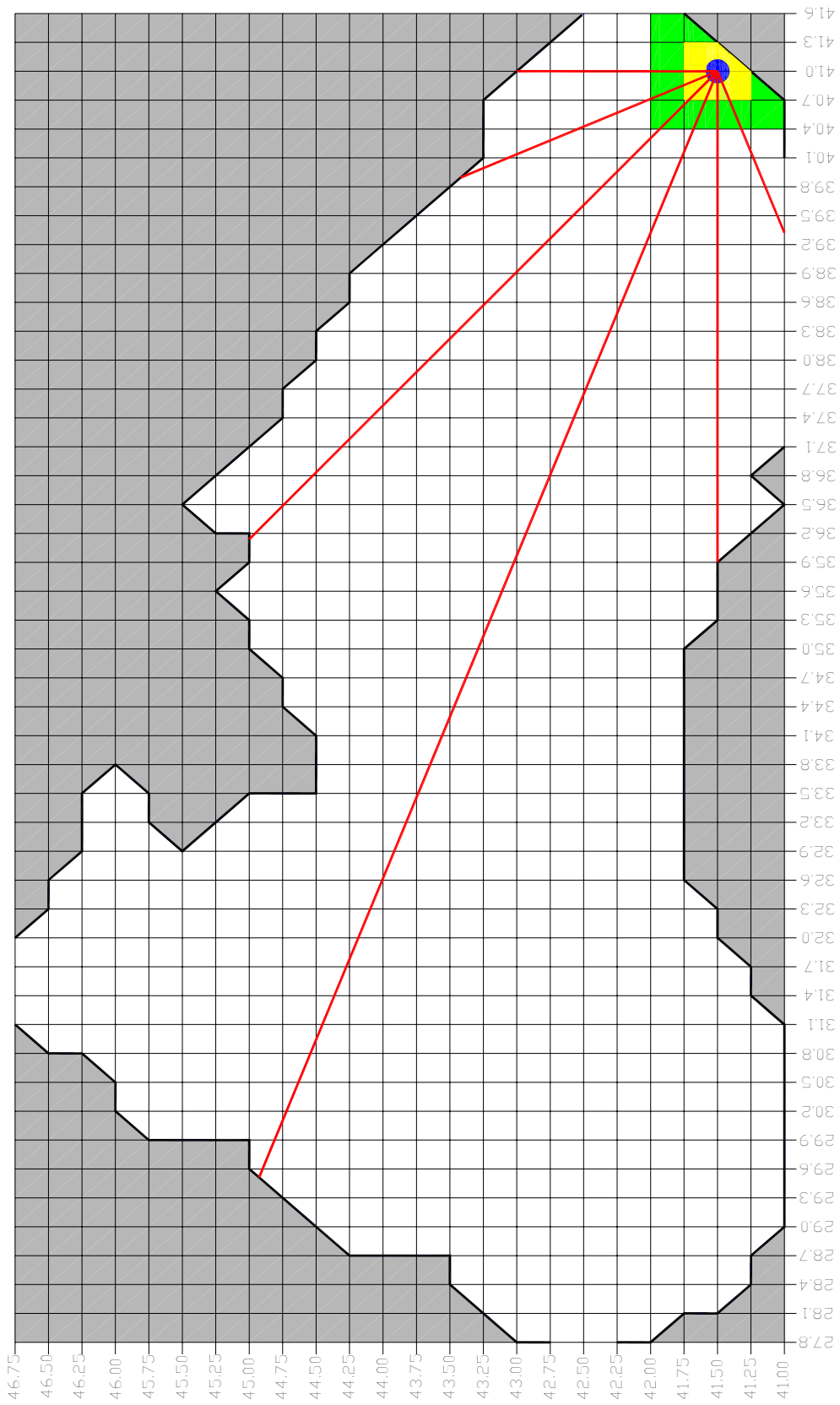


Figure C2 Location of Hopa on the mesh and alignments of directions considered in the analysis.

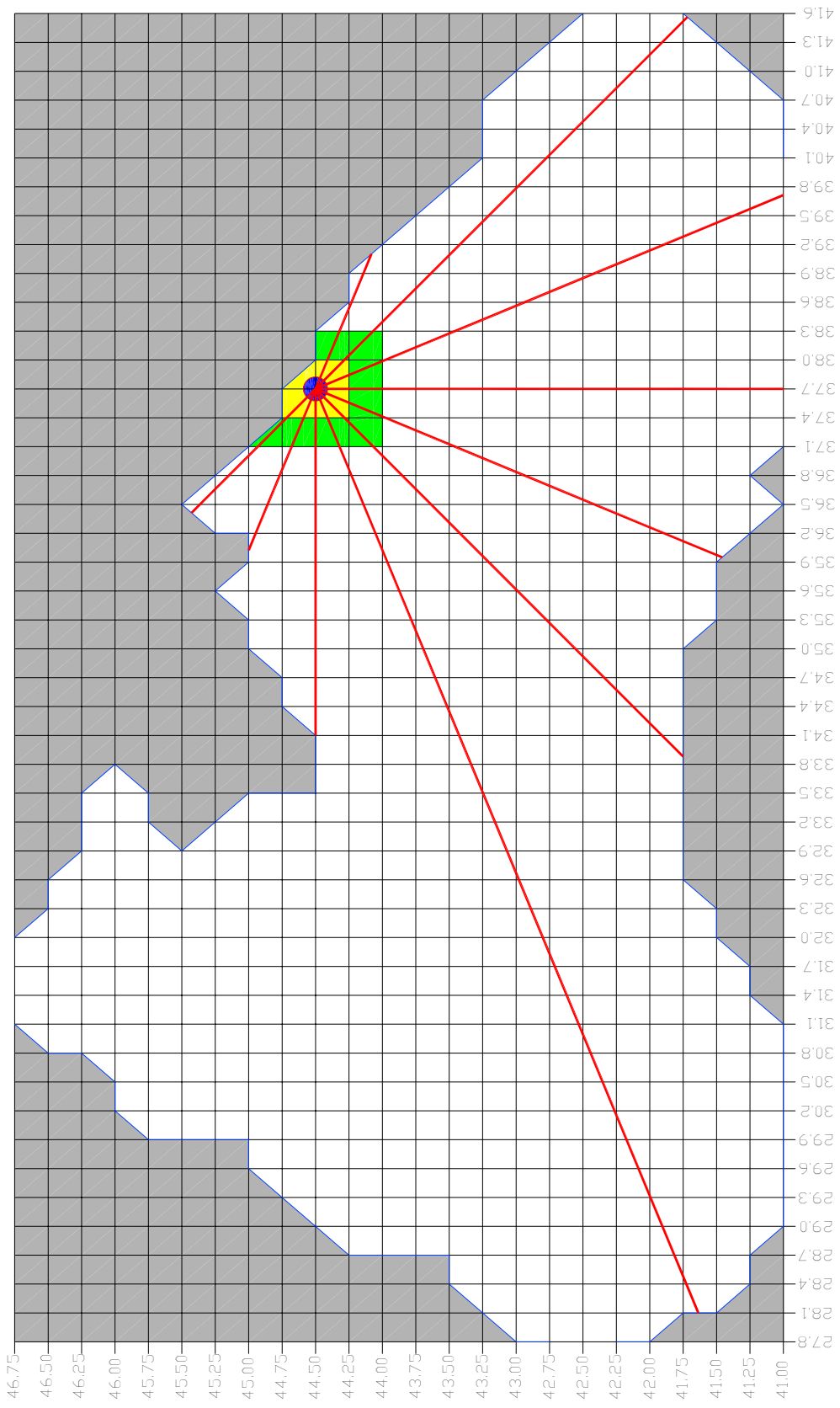


Figure C3 Location of Gelendzhik on the mesh and alignments of directions considered in the analysis.

VITA

Nihal Yılmaz was born in Ankara on July 4, 1975. She graduated from the Civil Engineering Department of the Middle East Technical University in June 1997. She received her M.Sc. degree in Civil Engineering from the Middle East Technical University in September 2000 with her study on extreme wind and wave climate of the Aegean and the Mediterranean coast of Turkey. She was a research assistant in the Civil Engineering Department, Coastal and Harbor Engineering Laboratory of the Middle East Technical University between December 1997 and April 2005. Since May 2005, she is working as a research assistant in the Civil Engineering Department of Muğla University. Her main interest has been statistics of wind waves.